POLITECNICO DI TORINO

Master of Science in Mechanical Engineering

Politecnico di Torino

Master's Degree Thesis

Comparative Study of Sustainability and Quasi-Static Mechanical Behavior of Carbon Fiber Composite Material Panels

Supervisor:

Prof. Raffaele Ciardiello

Co-Supervisors:

Prof. Alberto Ciampaglia

Prof. Davide Salvatore Paolino

Candidate:

Mehrnoosh Mohebali

Department of Mechanical and Aerospace Engineering (DIMEAS)

December 2025

Declaration

I hereby declare that the contents and organization of this thesis constitute my own original work and do not in any way compromise the rights of third parties, including those relating to the security of personal data.

Mehrnoosh Mohebali

December 2025

This thesis is submitted in partial fulfillment of the requirements of the master's degree in mechanical engineering at Politecnico di Torino.

Abstract

The increasing global demand for lightweight, high-performance materials has resulted in the widespread adoption of carbon fiber-reinforced polymers (CFRPs) across the automotive, aerospace, marine, construction, and wind energy sectors. With a particular focus on the automotive industry, this thesis addresses the key sustainability challenge of composite end-of-life recovery.

Conventional thermoset epoxy matrices are not recyclable, resulting in significant waste that conflicts with circular-economy goals and regulations, such as the EU End-of-Life Vehicle directive, which requires 95% material recovery. The environmental impact of non-recyclable composites highlights the need for alternative matrix systems that offer both mechanical performance and recyclability.

This thesis investigates whether the fully recyclable thermoplastic Elium® resin can effectively replace conventional thermoset epoxy (IN2) in structural composite applications.

Composite panels reinforced with 3K carbon fiber twill fabric were fabricated via vacuum infusion using either Elium® (a fully recyclable thermoplastic poly-methyl methacrylate from Arkema) or a standard thermoset epoxy matrix. Quasi-static mechanical properties were assessed through compression (ASTM D3410), tensile (ASTM D3039), and flexural (ASTM D790) tests conducted on multiple specimens to ensure statistical validity.

Epoxy composites exhibited greater axial stiffness and strength, with compressive and tensile modulus increasing by 4–6%. Conversely, Elium composites showed a 37% higher tensile failure strain (1.35% compared to 0.98%), similar flexural strength (680.9 versus 690.9 MPa), a 21% higher flexural modulus (34.96 compared to 28.89 GPa), and an 83% lower coefficient of variation in compressive modulus, which suggests enhanced ductility and improved manufacturing consistency.

Fractographic analysis identified distinct failure mechanisms. Epoxy composites demonstrated brittle fracture with localized damage zones (surface relief 15–30 μm), limited fiber pull-out (<1 mm), and confined ply delamination (20–30%), which aligns with the behavior of rigid thermoset matrices. In contrast, Elium composites exhibited distributed damage, rough and irregular fracture surfaces (relief 40–70 μm), extensive fiber pull-out (2–4 mm), and widespread ply delamination (40–50%), indicative of a ductile thermoplastic response.

The results show that Elium matches or exceeds the mechanical performance of conventional thermoset epoxy under quasi-static loading conditions, making it a viable alternative for structural composites. While axial strength is comparable or slightly lower, Elium offers

superior tensile ductility, higher flexural modulus, consistent manufacturing, and improved fracture toughness manifested by distributed damage modes. Its full recyclability removes a key environmental barrier to the broader use of high-performance composites in regulated industries.

The observed ductile failure behavior and distributed damage mechanisms indicate potential suitability for applications that demand damage tolerance, including structural body components and wind turbine blades. However, the crashworthiness benefits must be validated through dynamic impact testing.

The thesis is organized as follows:

Chapter 1 introduces the topic and outlines the motivation for sustainability. Chapter 2 reviews literature on thermoplastic composite materials and recycling technologies. Chapter 3 describes the experimental methodology. Chapter 4 presents mechanical characterization and comparative analysis. Chapter 5 concludes key findings and recommendations.

The findings provide a rigorous quasi-static baseline supporting material selection, design validation, and industrial adoption of sustainable Elium composites in compliance with EU End-of-Life Vehicle directives.

Acknowledgements

This degree path has been transformative, resulting in changes I did not anticipate. Completing this thesis marks a significant milestone in my academic and personal development, made possible by the experiences and individuals who have influenced my journey. While living in Italy has presented challenges, it has also fostered lasting memories and meaningful relationships that are now integral to my identity.

First and foremost, I express my deepest gratitude to my family. Your unwavering belief, steadfast faith, and immeasurable sacrifices have been fundamental to this achievement. Without your support, this accomplishment would not have been possible.

To Pouya, my closest companion and fiancé, who has been a steadfast source of support despite the distance between us. Your encouragement, belief in me, and inspiring words have sustained me through challenging times.

To my friends in Turin, thank you for making these years exceptional. We studied together, shared both successes and challenges, and created lasting memories. Even challenging friendships provided essential lessons in resilience, collaboration, and personal growth. You helped Turin feel like home when I was far from my own.

To my close friends back home, thank you for your supportive messages, ongoing inspiration, and video calls that brought warmth and joy.

I am profoundly grateful to my professors and supervisors for their invaluable guidance, patience, and expertise throughout this thesis. You taught me to think critically, address complex challenges with rigor, and uphold integrity as a professional engineer and scientist. Your mentorship has shaped both my research and my perspective on academic excellence and professional responsibility.

Finally, I extend my sincere gratitude to Politecnico di Torino for being a catalyst in my personal and professional growth. You provided an environment in which I learned to approach problems as an engineer, act with integrity, and build a strong foundation for my career.

This thesis is more than the result of research and study; it marks a transformative period in my life. Each challenge strengthened me, every success inspired me, and everyone involved made a lasting impact. I am deeply grateful for both the difficulties and achievements, as they have shaped who I am today and who I strive to become.

December 2025 - Torino

Mehrnoosh Mohebali

Table of Contents

List of Tables

List of Figures

Acronyms

ASTM	American Society for Testing and Materials
BPA	Bisphenol A
BPO	Benzoyl Peroxide
FRP	Fiber Reinforced Polymer
CFRP	Carbon fiber-reinforced polymers
CV	Coefficient of variation
DIMEAS	Department of Mechanical and Aerospace Engineering
EU	European Union
FTIR	Fourier Transform Infrared spectroscopy
PAN	Polyacrylonitrile
PEEK	Polyetheretherketone
PEI	Polyetherimide
PA	Polyamides
PMMA	Polymethylmethacrylate
PP	Polypropylene
RTM	Resin transfer molding
VIP	Vacuum infusion process
QS	Quasi-static
Tg	Glass transition temperature
UCS	Ultimate compressive strength
UTS	Ultimate tensile strength
UFS	Ultimate Flexural Strength
UV	Ultraviolet
UTM	Universal Testing Machine
BVID	Barely Visible Impact Damage

Chapter 1

Introduction

1.1 Introduction to Composite Materials

A composite material is engineered from two or more constituent materials with distinctly different physical or chemical properties that remain separate in the final structure. The constituents maintain their individual identities and are distinguishable within the composite. When combined, these materials demonstrate properties that surpass those of any individual component. This synergy results in mechanical performance that exceeds the sum of the individual parts and enables weight-efficient structural solutions not achievable with monolithic materials.

The technology developed on this basis originated in ancient cultures, such as the use of mud and straw to create composite construction materials, and evolved into the modern era, where the overall composite industry was commercialized in 1935 with the introduction of glass fibers [1]. The above-mentioned historical developments demonstrate that composite technology is fully developed and can be relied upon.

The development of aramid fibers (known as Kevlar®) and carbon fibers in the 1970s transformed structural engineering by providing both high strength and low weight, a combination not possible with traditional materials. These high-performance fibers gave composites a significant advantage, as reduced structural weight leads directly to greater energy efficiency and lower greenhouse gas emissions during use [1][2].

Today, more than 70 years after the introduction of glass fibers to the market, composite materials continue to be among the most rapidly growing groups of industrial materials, with annual global production exceeding 13 million tons and average growth rates of 8-10% annually in advanced applications [1] [2].

1.2 Composite Classification and Reinforcement Types

Based on the reinforcement morphology, composites can be classified into two primary types:

1. **Particulate-reinforced composites** consist of discrete ceramic, metallic, or polymeric particles dispersed within a continuous matrix. This configuration offers cost-effectiveness and isotropic properties, although it results in reduced mechanical performance relative to fiber-reinforced composites.

2. **Fiber-reinforced composites** use continuous or discontinuous fibers to provide directional strength and stiffness. They are widely used in industrial applications due to their high strength-to-weight ratios and effective load transfer along the fiber direction.

The primary intention of conducting this research work is on fiber-reinforced composites, as they possess a strength-to-weight ratio due to higher values of fiber aspect ratio, along with better mechanisms for transferring loads [1] [2][3].

1.2.1 Fiber Types and Properties

The primary categories of reinforcing fibers are summarized below:

1- **Synthetic fibers**:

- **Glass fibers**: the most economical and widely used reinforcement, accounting for about 95% of the industrial composite market by volume. The two main types are E-glass for general-purpose use and S-glass for high-performance applications[1][3]. Glass fibers remain the preferred choice for cost-sensitive applications.
- **Carbon fibers**: produced from polyacrylonitrile (PAN) precursors through controlled oxidation and high-temperature pyrolysis[5][6]. They offer high stiffness and strength at low density. Although more expensive than glass fibers, carbon fibers are used in performance-critical applications such as crash absorbers, aerospace structures, and high-end automotive components, where weight reduction provides operational and environmental benefits [2][7].

  Virgin carbon fiber manufacturing generates significant greenhouse gas emissions, and energy costs are approximately 14 times higher than those for steel production. Efficient use and recycling of carbon fibers are therefore essential for both environmental and economic reasons [10].

2- Natural Fibers:

- **Flax and hemp fibers**: **p**lant-based reinforcements that offer environmental benefits, lower density, and renewable sourcing. Although they have lower mechanical properties and are more moisture-sensitive than synthetic fibers, their use is increasing in applications that prioritize sustainability [5][6][8].

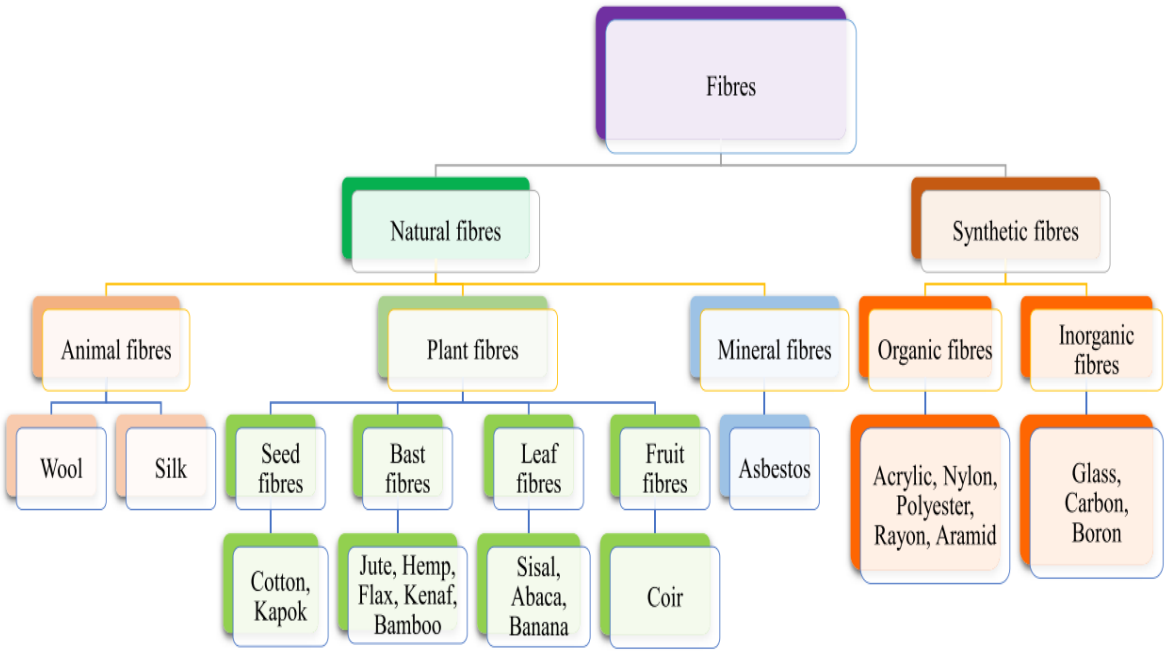

Figure 1 Classification of the fibers [6]

This research utilized a 3K carbon fiber twill fabric (Pyrofil TR50S, 200 g/m² [11]). The "3K" designation refers to 3000 filaments per tow, offering an optimal balance of tow fineness, inter-fiber spacing, and fiber surface area for resin bonding.

The twill weave offers balanced mechanical properties in both the warp and weft directions, a characteristic that is critical for two-dimensional load-bearing in composite applications.

Figure 2 Glass Fiber and Carbon Fiber Yarns [4]

1.3 Polymer Matrices for Fiber-Reinforced Composites

The polymer matrix in fiber-reinforced composites fulfills three primary functions:

1. Load transfer and redistribution: The matrix transfers loads from aligned fibers to adjacent fibers and to the surrounding structure through shear and adhesive mechanisms.

2. Environmental protection: The matrix encapsulates fibers and protects them from moisture, chemical attack, abrasion, and ultraviolet (UV) degradation [4].
3. Structural integrity: The matrix plays a critical role in determining the mechanical properties of composites, particularly in matrix-dominated failure modes.

Matrix resins are classified as thermoset or thermoplastic polymers, each with unique processing characteristics and sustainability considerations.

1.3.1 Thermoset Matrix Systems

Thermoset matrices undergo irreversible chemical cross-linking during curing, forming permanent three-dimensional networks. Common types are epoxy, polyester, and vinyl ester resins.

Thermoset epoxy resins are the primary matrix material in structural composites, accounting for about 75-80% of the market [1] [2]. They exhibit excellent mechanical properties, strong fiber-matrix adhesion, low cure shrinkage, and high environmental durability [4].

Conventional epoxy IN2[12], a bisphenol-A (BPA) based system, is widely used in aerospace and automotive applications and serves as the baseline material for this research [7][8].

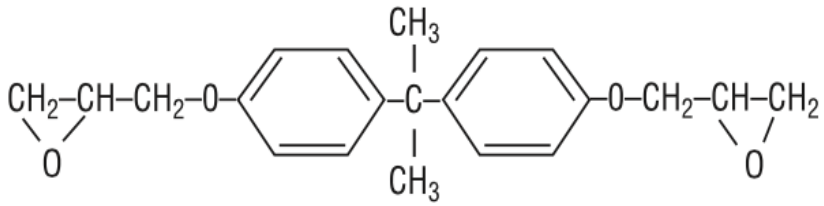

Figure 3 Idealized Chemical Structure of a Typical Epoxy(Di glycidyl Ether of Bisphenol-A)[3]

The irreversible cross-linking of thermoset resins presents a significant obstacle to end-of-life recycling and material recovery, which is a major limitation given current sustainability demands. Post-cure processes, typically lasting 2 to 8 hours at 100 to 150°C, significantly increase manufacturing energy consumption and carbon emissions[8][9][13].

Furthermore, approximately 80% of the polymers used in composites are derived from non-renewable fossil resources, and thermoset composites remain non-recyclable, resulting in persistent environmental challenges throughout their lifecycles [14][15].

1.3.2 Thermoplastic Matrix Systems

Thermoplastic matrices can reversibly change phase, allowing them to remelt and reshape after curing. Unlike conventional thermoplastics, which require processing at temperatures above

300°C, these matrices offer significant benefits for recycling, sustainability, and new applications in sustainable composite materials [9].

Common thermoplastic matrices are polypropylene (PP), polyamides (PA), polyetheretherketone (PEEK), polyetherimide (PEI), and polymethylmethacrylate (PMMA).

Recent advances in resin chemistry have yielded liquid thermoplastic resins specifically designed for compatibility with vacuum infusion processes, which are typically employed for thermoset epoxies.

This thesis examines Elium® resin (developed and commercialized by Arkema), a water-like liquid thermoplastic polymethacrylate (PMMA) system that enables room-temperature infusion without thermal cure cycles. Its potential as an epoxy substitute is evaluated with respect to mechanical behavior and sustainability; further details are provided in the following chapters.

1.4 Composite Manufacturing Technologies

Several manufacturing techniques are available for producing fiber-reinforced polymer composites. Each offers distinct advantages in cost, quality, and environmental impact.

- **Hand Layup**: Fibers are manually placed in a mold, and resin is applied by hand with a brush or spray. This simple method is labor-intensive and yields variable quality [2][4]
- **Resin Transfer Molding (RTM)**: A pre-formed fiber preform is placed in a closed mold, and liquid resin is injected under pressure. Excellent quality, but higher equipment cost [2][4]
- **Autoclave Processing**: Pre-impregnated fiber (prepreg) placed in a mold and cured in a pressurized oven. Superior properties but the highest cost [4]
- **Vacuum Infusion Process (VIP)**: Dry fibers are placed in a mold, and a vacuum draws liquid resin through the fiber bed. This low-cost, low-void, and environmentally friendly process is compatible with both thermoset and thermoplastic resins [4][8]

This research uses VIP to manufacture both composite systems: epoxy IN2 and thermoplastic Elium. The VIP method ensures a controlled, consistent process for both materials, eliminating variations that could affect comparisons. Chapter 3 provides details on VIP procedures, parameters, and quality control measures.

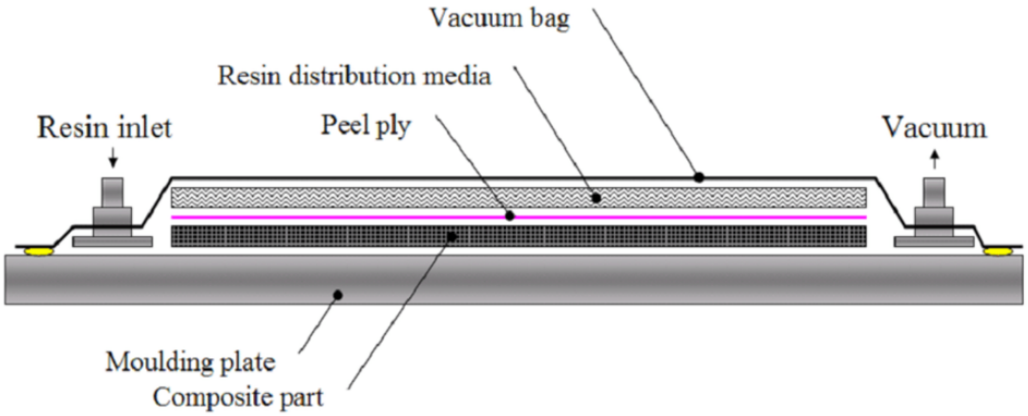

Figure 4 Standard procedure for the vacuum infusion process**Error! Reference source not found.**

1.5 Failure Mechanisms in Composite Materials

A thorough understanding of failure mechanisms in composite materials is crucial for accurate prediction of material performance and the development of effective design guidelines. Due to their heterogeneous and anisotropic structure, composite materials exhibit failure modes that are fundamentally distinct from those observed in isotropic materials [18][19].

1.5.1 Primary Failure Modes

- **Fiber Fracture**: Rupture of reinforcing fibers occurs when the fiber stress surpasses the material's tensile or compressive strength. This failure mode typically arises under high stress in fiber-dominated loading directions. It is characterized by clean fiber fracture surfaces visible under microscopy [18][19] [20].
- **Matrix Cracking**: Intralaminar fissures and cracks form within individual composite plies as a result of matrix tensile, compressive, or shear stresses, and occur independently of fiber failure.Matrix cracking typically initiates at lower stress levels than fiber fracture and propagates until fiber failure halts further crack growth [18][19].
- **Delamination**: Interlaminar failure where layers of a composite laminate separate due to interlaminar stresses, especially shear and normal stresses perpendicular to the laminate [21]. Delamination is especially damaging because it occurs without visible external damage (barely visible impact damage, BVID), potentially compromising structural integrity without warning [18][19].
- **Fiber-Matrix Debonding**: The loss of adhesion between the fiber and matrix results from shear stress or moisture ingress, which impedes effective load transfer from the

matrix to the fiber. Debonding decreases the composite stiffness and strength relative to well-bonded systems [18][19].

- **Microbuckling**: Lateral deflection and elastic instability of fibers under compressive loading result in waviness or localized bending. Microbuckling frequently occurs in resin-rich regions or under longitudinal compressive loading [20][22]

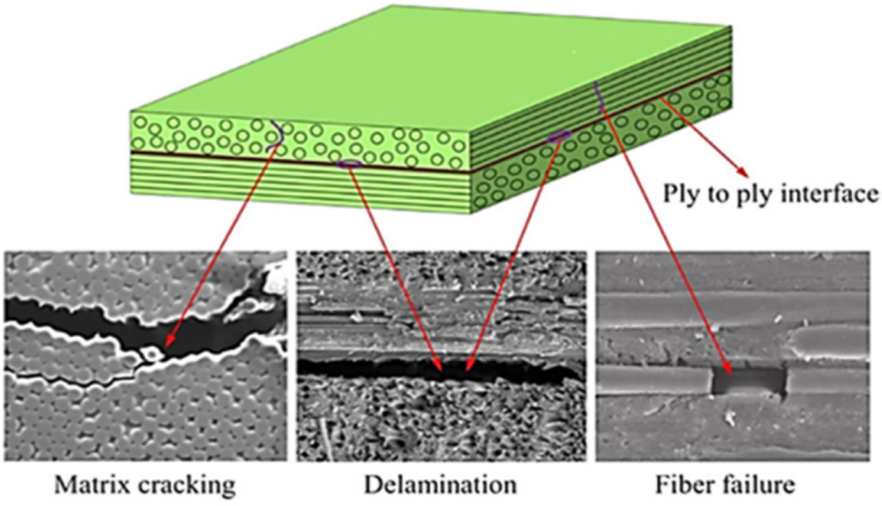

Figure 5 Primary Failure Modes of Composite [3]

1.5.2 Progressive Failure Behavior

Unlike brittle materials (like steel, glass, and concrete), which fail suddenly at a critical stress, fiber-reinforced composites typically undergo progressive failure. This process involves a sequence of damage mechanisms across various stress levels.

1. Initiation: The first damage event, typically matrix cracking, occurs at a stress level below the composite's ultimate strength.
2. Propagation: Damage accumulates under continued loading through matrix crack propagation, fiber-matrix debonding, and localized delamination.
3. Unstable Growth: When damage reaches a critical density, crack growth becomes unstable and propagates rapidly, resulting in catastrophic failure [18][19] [20].

Structural Significance:

Progressive failure offers greater toughness and strain-to-failure than brittle materials. This property is essential for structural applications that require damage tolerance, especially in the following areas:

- Crash absorbers in vehicles, which must absorb energy gradually instead of failing abruptly

- Aircraft structures, which must continue to sustain loads after damage begins
- Pressure vessels, which must avoid catastrophic rupture

Matrix Material Effect:

Thermoplastic matrices, which are more ductile, generally show more progressive failure than the more brittle thermoset matrices. This potential structural advantage for impact-prone applications is examined in this thesis through microscopic analysis.

1.5.3 Factors Influencing Failure Mechanisms

The failure modes of composite materials are determined by several critical factors:

- **Fiber orientation and stacking sequence**: Affect the stress state in individual plies and determine the dominant failure mode.
- **Matrix material properties *critical for this thesis***: Ductile matrices, such as thermoplastics, impede crack propagation and facilitate distributed damage across multiple failure sites, whereas brittle matrices, such as thermosets, localize damage along defined paths toward single catastrophic failure.
- **Manufacturing quality**: Defects such as voids, fiber waviness, and misalignment generate stress concentrations and expedite failure initiation.
- **Loading direction**: Loading parallel to the fibers activates fiber-dominated failure mechanisms, whereas loading in a transverse or shear direction exposes weaknesses in the matrix and interfaces.
- **Environmental exposure**: Moisture absorption leads to matrix plasticization and interfacial weakening, thereby reducing strength and stiffness [19][20].

1.6 Quasi-Static Mechanical Testing Framework

Standardized quasi-static testing in accordance with ASTM protocols provides reliable and quantifiable data regarding the mechanical response of materials under controlled laboratory conditions.

Standard quasi-static test methods employed in this research include:

- **Compression Testing (ASTM D3410)**: Measures compressive strength, modulus, and failure behavior under axial compression loading[23]. These properties are essential for applications where materials must support loads without buckling or lateral deformation.

- **Tensile Testing (ASTM D3039)**: Assesses tensile strength, modulus, and strain-to-failure under uniaxial tension [24]. This test defines fiber-dominated properties and quantifies material ductility.
- **Flexural Testing (ASTM D790)**: Flexural strength and modulus are evaluated under bending loads, which are relevant for structural panels and beams [25]. This test assesses the combined bending stiffness by incorporating both tensile and compressive properties.

Key mechanical properties, including tensile strength, compressive strength, elastic modulus, failure strain, and failure modes, obtained from standardized quasi-static tests, form the basis for selecting materials for lightweight structural panels. Materials with high strength, stiffness, and stable mechanical response under quasi-static loading perform best in demanding structural applications [20][26][27].

1.7 Building Block Approach for Composites

Composite design standards (CMH-17) employ the building-block approach, establishing a hierarchical validation pathway from the material level to the structural level [3].
The validation process consists of a four-level hierarchy:

1. Coupon Level: Individual material properties are determined from small specimens, as addressed in this research.
2. Element Level: Sub-component testing is conducted on joints, stiffeners, and assemblies.
3. Component Level: Full-scale substructures and assemblies are evaluated.
4. Structure Level: Validation is performed on the entire vehicle, aircraft, or structure.

Coupon-level quasi-static characterization is essential because it provides the material property database required for element- and component-level design validation. In the absence of rigorous coupon testing, engineers cannot proceed confidently to the more resource-intensive element- and component-level testing [3][26].
This study establishes the coupon-level material baseline for Elium- and epoxy-based composites, thereby enabling subsequent researchers to conduct element-level testing, such as joint strength assessments, and component-level validation, such as crash tube performance evaluations, with increased confidence.

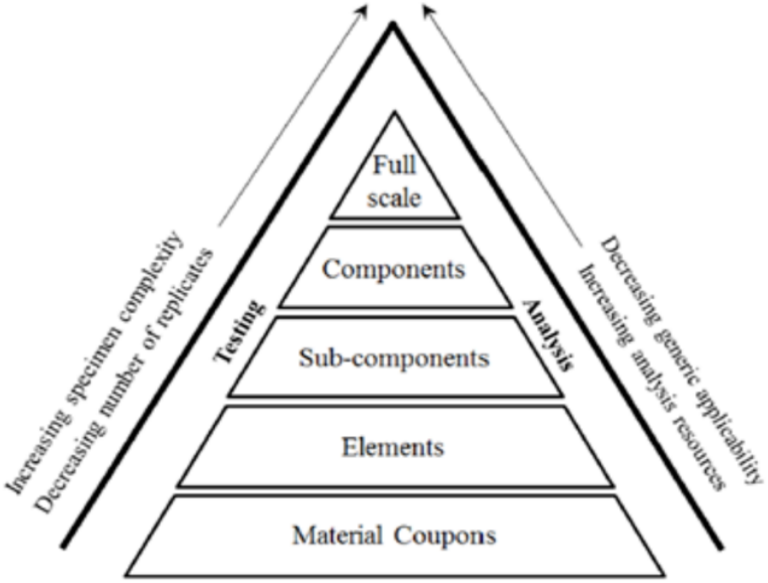

Figure 6 The building block approach for combining analytical and experimental evaluation of composite structures [3]

1.8 Sustainability and Recyclability in Composites

Nowadays, particularly the automotive industry faces two critical challenges:

1. Reducing weight with advanced materials to improve fuel efficiency and lower greenhouse gas emissions
2. Implementing sustainable manufacturing and end-of-life recovery to support circular economy goals.

Reducing vehicle mass improves fuel efficiency by about 7% for every 10% reduction in mass. Carbon fiber-reinforced polymer (CFRP) composites can reduce mass by 50% compared to steel while meeting structural requirements [8][9].

Conventional thermoset composites address the issue of weight reduction, thereby enabling more efficient vehicles; however, they do not meet sustainability requirements, as they generate non-recoverable waste. In contrast, thermoplastic composites offer a solution to recyclability challenges, provided that they can maintain mechanical performance, which constitutes the central research hypothesis of this thesis.

1.8.1 Regulatory Framework: EU End-of-Life Vehicle Directive

The European End-of-Life Vehicles Directive (2000/53/EC) mandates 95% mass recoverability and a minimum of 85% material recovery [27][28]. Implementing circular economy principles is crucial to achieving the carbon-neutrality targets set by the European Green Deal for 2050 [30].

1.8.2 Thermoset Composites: Recycling Pathways and Limitations

The primary end-of-life management strategies for thermoset materials are as follows:

- **Mechanical grinding**: Produces low-value filler material with a 30-50% loss in properties [8][10]
- **Thermal recycling (pyrolysis)**: Involves energy-intensive recovery at 400-700°C, generates carbon dioxide emissions, and retains 80-90% of fiber properties [10]
- **Incineration**: Enables energy recovery but does not facilitate material recovery [8]
- **Cement kiln co-processing**: Recovers heat energy from matrix combustion and utilizes fibers as raw material for cement clinker production [29]

The synthesis of epoxy resin has a significant impact on the environment, contributing to the overall carbon footprint and greenhouse gas emissions associated with manufacturing [14][15].

1.8.3 Thermoplastic Composites: Enabling Circular Economy

Thermoplastic matrix composites offer solutions to sustainability challenges through several distinct recycling pathways:

- **Mechanical grinding**: Composites are crushed and heated to form new panels using standard industrial equipment. This process requires approximately 0.03-1.33 kWh/kg, which is lower than pyrolysis. Fiber performance retention is typically 50-70% for thermoplastics, compared to 30-50% for mechanical thermoset grinding [8][10].
- **Chemical recycling**: Dissolution or depolymerization facilitates the recovery of resin to virgin-quality standards, which enables full fiber reuse and supports complete material circularity.
- **Thermal reprocessing**: Remelting the material above its glass transition temperature enables remanufacturing into new components.

Elium thermoplastic processing eliminates thermal post-cure cycles, enabling room-temperature polymerization and reducing manufacturing energy consumption by 15-30% compared to thermoset systems [8][13]. With complete recyclability, thermoplastic matrices support automotive composite technologies that meet EU End-of-Life Vehicle Directive requirements and Circular Economy Action Plan objectives.

1.9 Research Motivation and Objectives

This research is driven by the need for validated mechanical property data, industry material transition requirements, and regulatory compliance (End-of-Life Vehicle Directive 2000/53/EC) [28][29].

Despite the growing commercial interest in Elium thermoplastic resins as sustainable alternatives to thermoset epoxies, comprehensive coupon-level mechanical characterization under standardized quasi-static loading conditions has not yet been conducted.

This thesis addresses this gap by conducting controlled, replicated quasi-static tests on identical carbon fiber reinforcement infused with IN2 epoxy (thermoset baseline) and Elium (thermoplastic sustainable alternative) matrices. The resulting, statistically supported material characterization database will support material selection, design validation, and industrial adoption.

1.9.1 Specific Research Objectives

1- Optimize and validate vacuum infusion processes to produce high-quality carbon fiber composite panels with epoxy and Elium resins, using consistent processing parameters.
2- Conduct comprehensive quasi-static mechanical characterization, including compression, tensile, and flexural tests according to ASTM standards for both materials.
3- Perform rigorous statistical analysis to compare the mechanical properties and failure modes of Elium and epoxy composite systems.
4- Establish a coupon-level mechanical characterization baseline to inform material selection, design validation, and industrial adoption of Elium as a sustainable alternative to conventional epoxy.

These objectives aim to address the knowledge gap in the mechanical performance of thermoplastic composites under quasi-static loading, thereby supporting the transition to sustainable, recyclable composites for structural applications, in line with European regulatory frameworks and the principles of a circular economy.

Chapter 2

Literature Review

This chapter reviews recent research on sustainable composite materials, focusing on recyclable thermoplastic matrix composites and the development of Elium® resin as an alternative to traditional thermoset epoxy systems. The literature review covers several key areas:

1. Technical differences between thermoset and thermoplastic polymer matrices
2. Elium® resin chemistry, processing, and characterization
3. Mechanical properties of Elium®-based carbon fiber composites
4. Recycling methods and circular economy strategies
5. Performance comparisons with epoxy systems
6. Industrial applications and commercialization
7. Other sustainable composite technologies

The review summarizes research from 2015 to 2025, highlighting the progression of thermoplastic composites from laboratory studies to commercial use in wind energy, marine, and aerospace industries. This analysis provides a technical basis for understanding the mechanical performance, environmental benefits, and industrial potential of Elium® composites and identifies research gaps addressed in this thesis through experimental testing and comparative analysis.

2.1 Polymer Matrices in Fiber-Reinforced Composites: Thermoset vs. Thermoplastic

Understanding the key differences between thermoset and thermoplastic matrix systems is critical for advancing sustainable composite technologies. This section reviews the technical and environmental factors influencing material selection in modern composite manufacturing. Thermoset epoxy resins, which represent about 75-80% of the structural composite market [32], undergo irreversible cross-linking during curing to form permanent three-dimensional networks.

While this chemistry delivers excellent mechanical properties and durability, it prevents end-of-life material recovery [33]. Additionally, thermoset manufacturing requires 2-8 hour post-cure cycles at 100-150°C, which increases energy use and carbon emissions throughout the composite lifecycle [9][34].

In contrast, thermoplastic polymers possess linear or branched molecular chains that are held together by secondary forces, which enable repeated melting and reshaping following initial processing. [35]. However, high-performance thermoplastics such as PEEK, PEI, and PPS require processing temperatures above 300-400°C, which demands high-pressure equipment and makes conventional liquid molding impractical [33].

This limitation has restricted thermoplastic use to specialized aerospace and advanced applications where higher costs are justified. The development of reactive liquid thermoplastic resins is a significant advancement, combining the recyclability of thermoplastics with the manufacturing simplicity and cost-effectiveness of thermoset processes [34].

2.2 Elium® Thermoplastic Resin: Materials Development and Chemistry

Elium® resin, developed and commercialized by Arkema in 2015, is the first commercially successful acrylic-based liquid thermoplastic resin designed for vacuum infusion processing [16]. Its chemistry differs from thermoset epoxy systems, using methyl methacrylate (MMA) monomers and reactive oligomers that polymerize through free-radical addition when initiated by a benzoyl peroxide (BPO) catalyst [36].

Polymerization proceeds at moderate temperatures (25-80°C) with minimal exothermic reaction, eliminating the requirement for autoclaves or heated tooling and resulting in high molecular weight polymethylmethacrylate (PMMA) chains exceeding 100,000 g/mol [16].

Polymerization kinetics can be precisely controlled by adjusting initiator concentration and processing temperature, allowing manufacturers to tailor gel times from 15 minutes to several hours as needed.

Molecular dynamics studies show that mechanical properties develop rapidly from 40% polymerization conversion and reach near-final values at about 70% conversion [37]. Computational and experimental results confirm that fully polymerized Elium® resin achieves a glass transition temperature of 125°C, a Young's modulus of 3.1 GPa, and a mass density of 1.18 g/cm³ [37].

The synthesized PMMA polymer exhibits a glass transition temperature of 115 to 125°C, comparable to that of conventional epoxy resins, and can be reprocessed at 160 to 200°C without undergoing chemical degradation. This enables multiple recycling methods, including mechanical grinding and reprocessing, thermal remelting, and chemical depolymerization to recover MMA monomers [16][36].

Elium® resin maintains a low viscosity of 100-300 centipoise at room temperature, similar to conventional epoxy resins, which supports effective fiber wet-out during vacuum infusion processing. An initiator concentration of 3 wt% benzoyl peroxide is optimal for cure kinetics and mechanical properties. Concentrations below 2 wt% cause incomplete polymerization and cure times over 72 hours, while concentrations above 3.5 wt% lead to rapid gelation within 3 minutes and poor crosslink uniformity. Using water-free benzoyl peroxide is essential, as moisture can hydrolyze the initiator, reduce polymerization efficiency, and cause process inconsistencies [16].

2.3 Manufacturing Optimization: Vacuum Infusion Processing of Thermoplastic Composites

The vacuum infusion process (VIP) has been widely studied for both thermoset and thermoplastic composite manufacturing. Recent research has established process optimization protocols for Elium® resin systems. Systematic studies show that vacuum pressure significantly influences resin flow rate, fiber impregnation quality, and the mechanical properties of glass fiber-reinforced Elium® composites [9].

Experimental results at vacuum pressures ranging from 0.4 to 1.0 bar demonstrate that intermediate pressures between 0.6 and 0.8 bar produce optimal outcomes. Pressures below 0.6 bar lead to incomplete fiber wet-out and higher void content, while pressures above 0.8 bar cause rapid resin flow, trapping air bubbles and creating voids at fiber tow interfaces [9].

The optimal vacuum pressure of 0.8 bar yielded void contents below 2% and maximized tensile strength (reaching 380 MPa for unidirectional glass fiber an optimal vacuum pressure of 0.8 bar resulted in void contents below 2% and maximized tensile strength (up to 380 MPa for unidirectional glass fiber laminates) and tensile modulus (28 GPa). Elium® resin also shows minimal volumetric shrinkage during polymerization (1.5-2.0%), compared to 3-8% for conventional epoxy resins [9].

Reduced shrinkage decreases residual stresses and the likelihood of microcrack formation during curing, thereby enhancing mechanical performance and damage tolerance. Process modeling studies show that woven virgin carbon fiber fabrics provide uniform resin distribution and consistent fiber volume fractions of 55-60%. In contrast, non-woven recycled carbon fiber mats offer greater through-thickness permeability, resulting in higher resin content and lower fiber volume fractions of 35-45% [38].

Understanding these processing-structure relationships is essential for producing consistent, high-quality thermoplastic composites at an industrial scale.

2.4 Quasi-Static Mechanical Properties of Elium-Based Carbon Fiber Composites

2.4.1 Tensile and Compressive Behavior

Multiple research groups have conducted comprehensive tensile characterization of carbon fiber-Elium® composites using standardized test methods, providing a basis for comparison with conventional epoxy systems.

Unidirectional carbon fiber-Elium® composites produced by vacuum infusion achieved a tensile strength of 1420 MPa and a tensile modulus of 125 GPa at 60% fiber volume fraction. These values represent 95% of the tensile strength (1495 MPa) and 97% of the modulus (129 GPa) of epoxy composites [39]. The 3-5% reduction in stiffness for Elium® composites is due to the lower modulus of PMMA resin (3.1 GPa) compared to epoxy resin (3.5-4.0 GPa) [37][39]. However, Elium® composites showed a 23.5% higher failure strain (1.35% vs. 1.09%) than epoxy systems, indicating greater ductility and energy absorption, which is especially valuable for crashworthiness and impact-resistant applications [39].

Post-cure annealing of Elium® composites at 140°C for 2 hours results in an 8-12% increase in tensile strength, attributed to stress relaxation and improved fiber-matrix adhesion. This process also raises crystallinity from 5-8% in as-manufactured laminates to 12-15% in annealed specimens [39]. Compressive characterization using the ASTM D3410 combined loading compression test method shows that woven carbon fiber-Elium® laminates achieve a compressive strength of 520 MPa and a compressive modulus of 55 GPa for [0/90] woven laminates with a 58% fiber volume fraction.

Comparative studies with epoxy-based composites of identical fiber architecture indicate that Elium® systems reach 92-95% of the compressive strength of epoxy, with the slight reduction attributed to the lower shear modulus of the PMMA matrix (1.2 GPa compared to 1.4 GPa for epoxy), resulting in less resistance to fiber microbuckling under compressive loading [36]. Pultruded unidirectional carbon fiber-Elium® profiles exhibit compressive strength exceeding 1000 MPa, approaching the performance of aerospace-grade epoxy prepreg systems.

This demonstrates that optimized processing and fiber alignment can yield compressive properties comparable to conventional thermosets [36].

2.4.2 Flexural Properties and Bending Performance

Flexural testing is critical for evaluating bending performance in structural panels, beams, and stiffened structures. Carbon fiber-Elium® laminates produced by vacuum infusion achieve a flexural strength of 819 MPa and a flexural modulus of 95.6 GPa at a 70% fiber volume fraction [40]. Sandwich composites with carbon fiber-Elium® face sheets exhibit 15-18% higher flexural strength than equivalent epoxy-based panels, attributed to the increased ductility and toughness of the thermoplastic matrix, which delays face sheet failure and enhances energy absorption during bending [41].

Three-point bending tests conducted on pultruded unidirectional Elium® profiles demonstrate flexural strengths greater than 1100 MPa along the fiber direction [36]. The combination of high flexural performance, recyclability, and rapid processing positions Elium® resin as a strong alternative to conventional thermoset composites for structural applications [40].

2.4.3 Interlaminar Fracture Toughness and Damage Tolerance

Delamination resistance is a critical parameter for laminated composites, as interlaminar cracking often governs damage tolerance and fatigue life. Mode I and Mode II fracture toughness tests, employing double cantilever beam (DCB) and end-notched flexure (ENF) methods, demonstrate a significant advantage for Elium® systems [42]. Mode II fracture toughness values reach 2140 J/m² for crack initiation, representing a 40% improvement over epoxy-carbon fiber composites (GIIc = 1530 J/m²) [42].

This enhancement results from extensive plastic deformation and shear yielding in the PMMA matrix ahead of the crack tip, phenomena that are limited in brittle epoxy resins [18]. Mode I fracture toughness tests show Elium® composites achieve initiation values of 580 J/m² and propagation values of 920 J/m², corresponding to 19% and 15% improvements over epoxy systems, respectively.

Fractographic analysis reveals matrix plastic deformation, fiber bridging, and hackle formation on Elium® fracture surfaces, indicating substantial energy dissipation through ductile failure mechanisms [42].

The superior interlaminar fracture toughness of Elium® composites leads to improved damage tolerance, reduced delamination growth rates under fatigue loading, and enhanced impact resistance, which are essential for automotive crashworthiness and aerospace damage tolerance requirements [42].

Low-velocity impact testing on carbon fiber-Elium® and carbon fiber-epoxy laminates at impact energies from 10 to 40 Joules shows that Elium® composites absorb 240% more impact

energy before perforation compared to epoxy laminates of equivalent thickness and fiber architecture [39].

Post-impact compression testing indicates that Elium® specimens retain 72% of their original compressive strength after a 30 J impact, whereas epoxy specimens retain only 45%, representing a 60% improvement in damage tolerance. Ultrasonic C-scan imaging demonstrates that Elium® composites develop smaller delamination areas (18 cm^2 versus 32 cm^2 for epoxy at 25 J impact energy) and exhibit less severe fiber breakage.

This superior impact resistance is attributed to the ductile failure behavior of the PMMA matrix, which undergoes extensive plastic deformation and energy dissipation, in contrast to the brittle matrix cracking observed in epoxy composites [39].

Elium® composites possess a self-healing capability that further enhances damage tolerance [43]. Low-velocity impact damage can be partially repaired by heating the affected area to 140-160°C for 30 minutes, which remelts the PMMA matrix and enables molecular movement to close microcracks, restoring up to 60-75% of the original impact energy absorption capacity. This self-healing mechanism is absent in irreversibly cross-linked epoxy composites, offering a distinct advantage for structural applications where damage tolerance and field repair are critical [43].

2.5 Fatigue Performance and Structural Damping

Fatigue resistance under cyclic loading is essential for automotive, wind energy, and aerospace structures. Tension-tension fatigue tests on flax fiber-Elium® composites at 70% of ultimate tensile strength showed that these composites endured 500,000 cycles without catastrophic failure, with stiffness degradation limited to 18-22% by the end of fatigue life [44].

Comparative studies indicate that carbon fiber-Elium® laminates exhibit fatigue lives that are 25-30% longer than those of carbon fiber-epoxy laminates under equivalent stress conditions. This superior fatigue resistance results from the ductile matrix, which accommodates stress concentrations through localized plastic deformation instead of forming brittle cracks that propagate quickly in epoxy matrices [44].

Dynamic mechanical analysis showed that Elium® composites have loss factor (tan delta) values 22-27% higher than epoxy composites across a frequency range of 1-100 Hz [39][45]. The improved damping enhances vibration attenuation and acoustic performance, which is particularly important for automotive interiors and wind turbine blades, where noise and vibration reduction are critical design considerations.

The combination of superior damping and fatigue resistance makes Elium® composites well-suited for applications requiring sustained cyclic loading without resonance excitation [45].

2.6 Recycling and Circular Economy Implementation

2.6.1 Mechanical Recycling Pathways

The thermoplastic properties of Elium® resin facilitate efficient mechanical recycling through grinding and reprocessing. Research indicates that carbon fiber-Elium® composites can be processed into recyclate particles measuring 1-5 mm using standard shredding equipment, followed by compression molding at 180-200°C and 4 MPa to produce recycled sheets [40]. Mechanical recycling results in randomized fiber orientation and a reduction in average fiber length from continuous to 2-8 mm, thereby converting the composite from continuous to discontinuous fiber reinforcement. Although these modifications occur, recycled composites retain significant mechanical properties, exhibiting flexural strength between 45-63 MPa (compared to 819 MPa for virgin laminates) and a flexural modulus of 14-16 GPa (compared to 95.6 GPa for virgin material) [40].

While reductions in mechanical properties restrict mechanically recycled Elium® composites to applications such as semi-structural components, protective panels, and interior trim, the capacity to recycle without chemical degradation represents a significant advantage over thermoset composites, which cannot be reprocessed without destruction of the polymer matrix [33][40].

Studies indicate that the elastic modulus increases from 8.2 GPa to 9.5 GPa during the first two to three recycling cycles, attributed to enhanced crystallinity resulting from repeated thermal processing. Tensile strength declines moderately from 50 MPa for virgin material to 38 MPa after five cycles, and failure strain decreases from 0.82% to 0.23%.

These findings suggest that Elium® composites can be recycled multiple times before their mechanical properties become unsuitable for practical use [44].

2.6.2 Chemical Recycling and Depolymerization

Chemical recycling enables the complete recovery of both carbon fibers and resin monomers, thereby supporting closed-loop manufacturing processes. Solvolysis of Elium® composites using proprietary solvents at 120-160°C selectively depolymerizes PMMA chains into MMA monomers, while preserving the integrity of the carbon fibers [46].

This method achieves recovery rates of 77% for MMA monomers and 95% for carbon fiber mass, with monomer purity exceeding 98%, which is suitable for the production of virgin-

quality Elium® resin. The recovered carbon fibers retain 95% of their original tensile strength (3.5 GPa) and 98% of their original modulus (230 GPa), making them appropriate for use in high-performance composite manufacturing [46].

Chemical recycling of Elium® composites provides significant environmental benefits in comparison to the pyrolysis recycling of epoxy composites. Solvolysis operates at 120-160°C, significantly lower than the 450-700°C required for pyrolysis, resulting in a 60-70% reduction in energy consumption [46]. Additionally, solvolysis recovers both fiber and resin as reusable materials, whereas pyrolysis destroys the epoxy matrix and recovers only carbon fibers [33]. Although virgin Elium® composites possess a slightly higher embodied carbon (8.2 kg CO_2-eq per kg) than epoxy composites (7.5 kg CO_2-eq/kg) due to the energy-intensive production of MMA [47], incorporating end-of-life recycling markedly enhances their environmental profile. Chemical recycling and remanufacturing reduce the carbon footprint to 2.1 kg CO_2-eq per kg, representing a 74% reduction [47].

By comparison, epoxy composite recycling through pyrolysis results in only a 35-40% reduction, largely attributable to increased energy consumption and diminished resin value [33][47].

2.7 Comparative Performance Studies: Elium® vs. Conventional Epoxy

2.7.1 Direct Head-to-Head Mechanical Comparisons

Multiple research groups have systematically compared Elium® and epoxy composites using identical fiber reinforcements, architectures, and manufacturing processes to isolate the influence of matrix chemistry on performance [8].

Mechanical testing of flax fiber-reinforced composites utilizing three resin systems, including conventional petroleum-based epoxy, bio-based epoxy, and Elium® thermoplastic resin, indicated that flax-epoxy composites exhibited a tensile strength of 68 MPa and a modulus of 8.5 GPa. In comparison, flax-Elium® composites exhibited a slightly lower tensile strength of 62 MPa (a 9% reduction) but a similar modulus of 8.2 GPa [8]. Elium® composites showed a 45% higher failure strain (1.85% compared to 1.28%), indicating enhanced ductility.

Impact testing revealed that flax-Elium® laminates absorbed 52% more impact energy (18.5 kJ/m² compared to 12.2 kJ/m²) and demonstrated superior post-impact damage resistance relative to epoxy laminates. Additionally, Elium® was less sensitive to natural fiber moisture content, which simplifies manufacturing protocols for natural fiber composites [8].

Comparative testing of hybrid carbon-glass fiber composites with Elium® and epoxy matrices demonstrated that, for [0/90] woven carbon fiber laminates, tensile, compressive, and flexural properties differed by less than 8%. This finding suggests mechanical equivalence under most quasi-static loading conditions [36]. However, Elium® surpassed epoxy in fracture toughness, impact resistance, and damage tolerance by 15-40%, attributable to its ductile thermoplastic matrix [36][42].

These results support the viability of Elium® as a replacement for epoxy in various structural applications, offering additional benefits such as recyclability and improved damage tolerance.

2.7.2 Manufacturing and Processing Characteristics

Processing characteristics significantly influence manufacturing cost, cycle time, and scalability. Gel and working times are critical parameters: conventional epoxy systems offer pot lives of 1-4 hours at room temperature and require 2-8 hours of curing at 60-180°C [48]. Elium® resin offers working times ranging from 30 minutes to 3 hours, depending on initiator concentration, and cures at 25 to 80°C. This process eliminates the requirement for heated molds or autoclaves [16][34].

Epoxy resins typically shrink 3-8% during curing, whereas Elium® shrinks only 1.5-2.0%. This reduced shrinkage minimizes warpage and internal stresses, thereby improving fatigue resistance [9][48].

Viscosity changes during processing directly impact fiber wet-out and void formation. Epoxy viscosity increases rapidly during curing, rising from 100-500 centipoise to the gel point within minutes or hours, depending on the formulation [49]. In contrast, Elium® maintains a stable viscosity (100-300 centipoise) for most of the polymerization process, with a sharp increase only near completion. This stability facilitates more effective air bubble evacuation and reduces void formation [34].

While epoxy composites typically require mold release agents to prevent adhesion, Elium® exhibits low adhesion to most tool materials, often enabling direct release from aluminum, steel, or composite tooling. This characteristic simplifies processing and reduces surface contamination.

2.7.3 Economic Considerations and Cost Analysis

Raw material costs constitute a significant economic consideration. As of 2024, Elium® resin is priced at €8-12 per kilogram, compared to €4-8 per kilogram for conventional epoxy resins, resulting in a 30-50% material cost premium [50].

This premium is partially offset by lower processing costs, including the elimination of autoclave requirements, shorter cycle times, and reduced energy consumption, as well as improved material utilization through recyclability [50]. End-of-life value recovery offers a further economic advantage: chemical recycling of Elium® composites recovers materials valued at 40-50% of the cost of virgin materials, whereas thermoset composites have nearly zero residual value.

Economic analyses demonstrate that, across the entire lifecycle and multiple use cycles, Elium® composites achieve a total cost of ownership within 5-15% of epoxy composites in high-volume applications [50].

Manufacturing cycle time directly affects production throughput and equipment utilization. Elium® composites can be demolded within 1-3 hours after infusion, whereas epoxy systems require 4-12 hours due to the need for thermal post-cure. This 50-75% reduction in cycle time enhances production capacity and improves capital efficiency in high-volume manufacturing settings [49].

2.8 Industrial Applications and Commercial Implementation

2.8.1 Wind Energy Sector

The wind energy industry has been an early adopter of Elium® thermoplastic composites, motivated by sustainability goals and the need to recycle end-of-life turbine blades. In 2023, Sinoma Blade, a leading Chinese manufacturer, produced and installed the world's first fully recyclable 100-meter wind turbine blade using Elium® resin and carbon fiber reinforcement [51].

The blade was produced using vacuum infusion and an optimized resin formulation designed for large-scale manufacturing and prolonged gel times. Structural testing confirmed that the blade met all design load requirements and achieved a simulated fatigue life of over 25 years. This recyclability allows for blade recovery at end-of-life, addressing a key sustainability issue as many wind turbines approach decommissioning in the coming decade [51].

As of 2024, over 200 wind turbine blades have been manufactured with Elium® resin, demonstrating commercial validation at an industrial scale. Adoption in the wind energy sector provides valuable production experience and supply chain development, benefiting other industries considering thermoplastic composites [51].

2.8.2 Marine and Yachting Applications

The marine industry uses Elium® composites for boat hulls, decks, and interior structures, motivated by environmental regulations and the need for recyclable alternatives to traditional fiberglass-polyester composites [52]. Several yacht manufacturers, including Groupe Beneteau, have adopted Elium®-based construction for production boats. Key processing advantages include simplified manufacturing with no styrene emissions, reduced VOCs, faster cure cycles for higher production rates, and improved impact resistance.

The thermoplastic properties facilitate the welding of composite components via thermal bonding, which streamlines assembly and removes the requirement for mechanical fasteners or adhesives [52].

Recycling demonstrations show that end-of-life boat hulls can be ground and reprocessed into marine-grade composites for non-structural uses, providing a closed-loop solution for an industry that has traditionally sent fiberglass waste to landfills [52].

2.8.3 Automotive Sector Development

The automotive industry represents the largest potential market for recyclable thermoplastic composites, driven by strict regulations such as the EU End-of-Life Vehicle directive, which requires 95% material recovery [28]. Current thermoset composites cannot meet these targets, increasing demand for thermoplastic alternatives. Several automotive manufacturers have evaluated Elium® composites for structural applications, focusing on crashworthiness.

Experimental results indicate that carbon fiber-Elium® absorbers achieve specific energy absorption values of 65-75 kJ/kg, which is comparable to aluminum crash structures and 15-20% higher than those of equivalent epoxy composite absorbers [28].

Material cost and scalability for high-volume manufacturing remain significant challenges for automotive adoption. However, the combination of mechanical performance, crashworthiness, recyclability for regulatory compliance, and the potential for welded assembly may support broader implementation as production volumes increase and material costs decrease through economies of scale [50].

2.8.4 Aerospace Applications and Development Status

Aerospace is a long-term application area for Elium® composites, but strict certification requirements and conservative qualification practices have slowed adoption [53]. In 2020, GKN Fokker successfully flight-tested aircraft components made from recycled thermoplastic composites, demonstrating technical feasibility and regulatory acceptance.

Elium® composites offer mechanical properties close to aerospace-grade epoxy prepregs, superior damage tolerance, and the potential for field repair through thermal remolding. Full aerospace qualification, however, requires extensive testing and long-term environmental durability validation, which is still ongoing as of 2024 [53].

2.9 Complementary Sustainable Composite Technologies

Although this thesis focuses on recyclable thermoplastic composites, it is important to consider this approach within the broader context of sustainable composite technologies [32][54]. Other research has advanced sustainability through bio-based resins and natural fiber reinforcements [7][55][56].

Bio-based epoxy resins with high plant-derived content can replace petroleum-based epoxies in carbon fiber composites, with mechanical testing showing only modest reductions in properties that remain within acceptable design ranges [7]. Advanced bio-based epoxy formulations using plant-derived precursors such as cardanol and terpene compounds achieve improved glass transition temperatures and mechanical properties that meet thermoset standards. Multifunctional bio-based formulations also provide self-healing and flame-retardant properties [55].

Hemp and flax-based composites have demonstrated net carbon-negative lifecycle performance when soil carbon storage is included in lifecycle assessment, with cultivation emissions offset by soil organic carbon accumulation [56]. Natural fiber composites have achieved successful commercial use in non-structural automotive interior components by several premium original equipment manufacturers, demonstrating manufacturing feasibility and market readiness [57]. Although bio-based and natural fiber composites provide notable sustainability benefits, they fail to resolve the core issue of end-of-life recyclability.

Bio-based epoxies remain irreversibly cross-linked and non-recyclable, while natural fiber composites typically sacrifice 20-60% of mechanical performance compared to synthetic fiber systems, limiting applications to semi-structural and non-structural components [54][57].

2.10 Research Gaps and Thesis Contributions

Although Elium® thermoplastic composites have advanced significantly, key technical gaps still hinder widespread industrial adoption. There is a lack of comprehensive quasi-static mechanical databases comparing tensile, compressive, and flexural properties of carbon fiber-Elium® composites under standardized conditions [32].

Existing studies use varied test methods and protocols, making cross-group comparisons challenging. Systematic characterization using ASTM standards is needed to create credible design databases for certification authorities. While best practices for vacuum infusion have been identified, quantitative assessments of manufacturing reproducibility and property variability remain limited [9][38].

Direct comparisons between Elium® and epoxy composites with identical reinforcements and processing are rare, yet essential to validate Elium® as a replacement for epoxy[36]. Additionally, detailed fractographic analysis and failure mechanism identification under different loading conditions are needed to understand damage evolution and support progressive damage modeling [45].

This thesis addresses existing research gaps through a comprehensive quasi-static mechanical characterization of carbon fiber-Elium® composites, employing standardized ASTM test methods. Results are compared with equivalent carbon fiber-epoxy composites produced through identical vacuum infusion processing.

Chapter 3

Materials & Methods

This chapter describes the experimental design, material selection, manufacturing procedures, specimen preparation protocols, and testing methodologies used to develop a statistically robust coupon-level mechanical property database for carbon fiber composites reinforced with IN2 epoxy (thermoset baseline) and Elium thermoplastic resin (sustainable alternative).

The standardized procedures outlined in this chapter promote reproducibility, comparability, and compliance with ASTM testing standards, thereby supporting materials qualification and design validation.

Key Design Principles

To ensure direct material comparison and minimize confounding variables, this research used the following approach:

1. Identical reinforcement: The same carbon fiber fabric type and architecture were used for both materials.
2. Identical processing: Both resin systems were processed using vacuum infusion at 0.8 bar pressure.
3. Standardized testing: All mechanical tests followed ASTM procedures (D3410, D3039, D790).
4. Statistical rigor: Multiple specimens per material were tested, and means, standard deviations, and coefficients of variation were reported.

3.1 Materials

3.1.1 Carbon Fiber Reinforcement

This study used a single carbon fiber fabric as the primary reinforcement to allow direct comparison of resin system performance and eliminate fiber-related variability. Using a single fiber type across all specimens ensures that any differences in mechanical properties are due solely to resin chemistry and processing parameters.

The fabric (Pyrofil TR30S 3L) is a 210 g 2 × 2 carbon twill (Mitsubishi Rayon Co., Ltd., JP) with 3,000 filaments per tow (3k). The warp and weft of the fabric are 5.4 and 5.1 per cm, respectively, ensuring uniform distribution and balanced mechanical properties in both longitudinal and transverse directions.

The datasheet indicates a polyester pre-coating for easier handling. The fabric exhibits a maximum tensile strength of 4,120 MPa, a tensile modulus of 234 GPa, a maximum elongation of 1.8%, and a density of 1.79 g/cm³. The fiber diameter of 7 μm enables high fiber packing density and effective resin wetting during vacuum infusion processing. According to the supplier datasheet, the woven fabric has a yarn length of approximately 8 mm, with a tow width and height of approximately 1.98 mm and 0.12 mm, respectively [11].

The twill 2×2 weave provides balanced mechanical properties in both the longitudinal and transverse directions, which leads to quasi-isotropic in-plane performance when applied in $0/90_n$s stacking sequences. The 3K fine-count tow improves fabric drape and processability. An areal weight of 210 g/m² is appropriate for composite laminates targeting fiber volume fractions of 50-55%. Epoxy-compatible sizing promotes strong interfacial bonding with both IN2 conventional epoxy and ELIUM® thermoplastic epoxy resins used in this study.

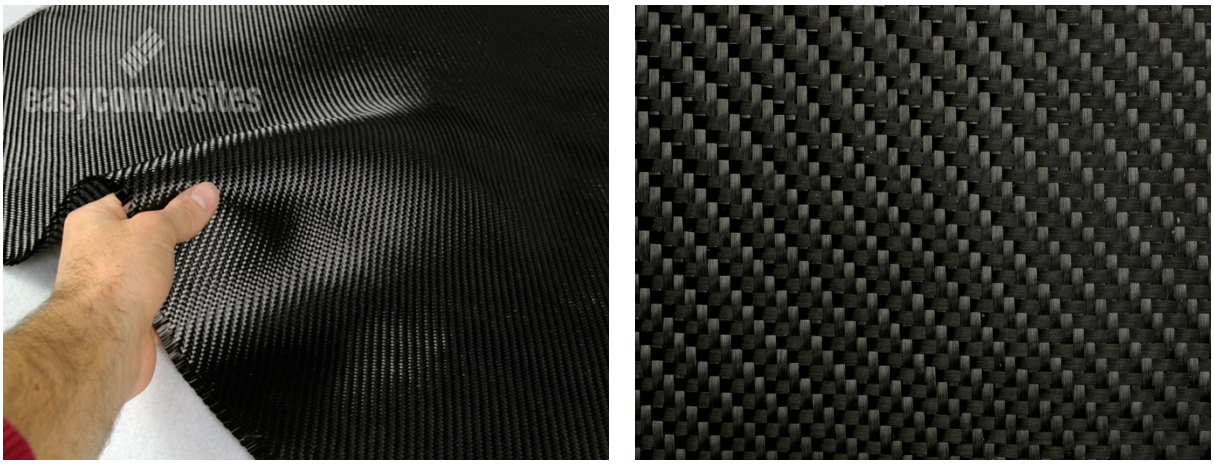

Figure 7 210 g 2 × 2 Twill 3k Carbon Fiber in our work [58]

3.1.2 Resin Systems

Two resin matrix systems were selected for this comparative study, representing distinct material behavior and pathways for sustainable composite manufacturing:

1. Petroleum-derived conventional epoxy called IN2 as the baseline
2. A thermoplastic recyclable resin called ELIUM, enabling circular economy implementation through material recovery and reprocessing.

The IN2 epoxy resin system (Easy Composites Ltd., UK)[12] is a two-part, petroleum-derived epoxy based on Bisphenol A (BPA) chemistry. The light amber resin is cured with an aromatic amine hardener at a 100:25-30 mass ratio (resin to hardener), allowing sufficient working time

for vacuum infusion. The cured resin achieves a glass transition temperature (Tg) of 95°C, ensuring thermal stability for elevated-temperature applications.

The IN2 system demonstrates superior fiber wetting as a result of its low viscosity, consistent compatibility with vacuum infusion processes, reduced outgassing during curing, and stable performance across various environmental conditions. Extensive industrial data for conventional epoxy systems support its process consistency and predictable mechanical properties.

The ELIUM® resin system (Arkema, France)[16] is a low-viscosity thermoplastic poly-methylmethacrylate (PMMA-based) resin with thermoplastic acrylic polyol chemistry. It is a clear, colorless to light-yellow liquid, polymerized with 3 wt% water-free benzoyl peroxide (BPO) as a free-radical initiator.

In particular, Fourier Transform InfraRed (FTIR) analysis showed that the main functionalities of Elium resin are the C–O–C bond, C–H bond (bending), and four distinct peaks of CH3 and CH2 bonds (C–H stretching)[59]. The cured resin has a glass transition temperature (Tg) of 90-100°C, depending on crosslink density.

Table 1 presents the mechanical property values for both resin systems, which are obtained from the respective datasheets.

Resin	IN2	ELIUM
Viscosity (Mpa.s)	325	100
Density (g/cm³)	1.14	1.01
Young's Modulus (GPa)	3.0	2.6
Tensile Strength (Mpa)	68	56
Flexural Modulus (GPa)	3.3	2.9
Flexural Strength (Mpa)	120	111
Elongation at Break (%)	3-5%	4-7%

Table 1 Comparison of the mechanical properties of the two examined resins[12][16]

A benzoyl peroxide initiator concentration of 3 wt% is optimal for cure kinetics and mechanical properties. Concentrations below 2 wt% lead to incomplete polymerization and cure times over 72 hours. Concentrations above 3.5 wt% result in rapid gelation within 3 minutes and poor

crosslink uniformity. Using water-free benzoyl peroxide is essential, as moisture can hydrolyze the initiator, reduce polymerization efficiency, and create process inconsistencies.

Unlike IN2, ELIUM® enables complete material recovery and repeated reprocessing because its linear polymer backbone can be melted and re-solidified without undergoing chemical degradation. Cured composites can be shredded, remelted, and reinfused with new fibers, with multiple cycles maintaining excellent properties.

Manufacturing or end-of-service scrap can be ground into powder for secondary uses, supporting closed-loop manufacturing, waste reduction, and resource conservation. ELIUM® composites also offer significantly greater toughness and impact resistance than epoxy-based composites.

The higher elongation at break makes ELIUM® well-suited for applications requiring damage tolerance, such as crash-absorbing automotive structures. Studies indicate that ELIUM® composites are expected to exhibit:

- Comparable quasi-static strength and modulus to epoxy systems
- Superior failure strain and ductility due to elastoplastic thermoplastic behavior
- Improved damage tolerance via plastic matrix deformation rather than brittle fracture
- More progressive failure modes enabling sustained load-bearing over extended deformation

ELIUM® resin has low viscosity for vacuum infusion, removes the need for high-temperature ovens during primary cure, and provides excellent wetting and fiber penetration. These features support industrial-scale production of sustainable, circular-economy composites.

Figure 8 IN2 Epoxy Resin [58] and Elium resin with 3%wt BPO

3.2 Laminate Production

3.2.1 Vacuum Infusion Process (VIP)

Vacuum infusion was chosen as the manufacturing method for the following reasons:

- Direct material comparison: Employing identical processing for both resin systems eliminates process-related variations.
- Resin compatibility: Both IN2 epoxy and Elium cure at room temperature, eliminating the need for heating.
- Industrial relevance: Vacuum infusion is the most commercially viable method for large-scale adoption of thermoplastic composites.
- Process control: Documented process parameters facilitate reproducibility and ensure consistent quality control.

The vacuum infusion process was performed at the Politecnico di Torino (DIMEAS) laboratory under controlled conditions (21-23°C). Vacuum pressure drew resin into dry fiber layers within a sealed mold, ensuring optimal fiber wet-out and minimal voids. This method reliably produces high-quality, defect-free carbon fiber composite laminates for quasi-static mechanical characterization.

The infusion setup used a glass plate (bottom mold) treated with release wax for easy laminate removal. The 400 × 650 mm infusion area was sealed with butyl sealant tape to prevent air leaks. This controlled geometry ensures consistent fiber saturation and uniform laminate properties.

Eight layers of carbon fiber fabric (Pyrofil TR30S 3K, 200 g/m^2), each 340 × 500 mm, were stacked with precise alignment in a $0/90_4s$ symmetric and balanced configuration to optimize mechanical properties. Woven nylon peel ply was placed on both surfaces for easy removal after curing. A flow mesh above the top peel ply ensured even resin distribution during infusion. A non-woven polyester breather layer (200 × 350 mm) was placed at the resin outlet region, as shown in Figures 9 and 10. This layer acted as a “resin brake,” reducing resin velocity near the outlet to ensure complete wetting of all carbon fiber layers and to prevent air entrapment. A silicone-lined, 2-liter resin catch pot was installed to protect the vacuum pump from contamination, and a pressure-regulating valve enabled precise control of infusion pressure throughout the process. Resin was introduced at the outlet port under 0.8 bar vacuum pressure. Systematic studies by Ciardiello et al. [9] demonstrate that a vacuum pressure of 0.8 bar yields optimal results.

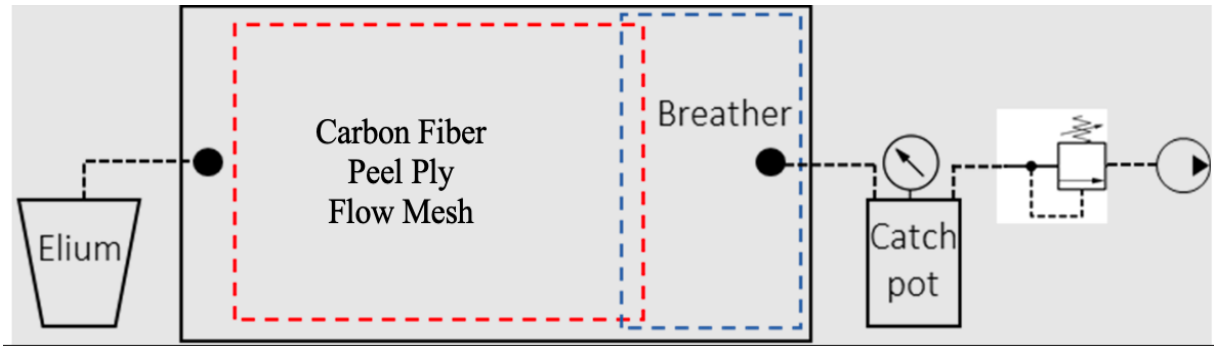

Figure 9 Representative sketch of the infusion setup [9]

Pressures below 0.6 bar result in incomplete fiber wet-out and increased void content, exceeding 2%. In the 0.6 to 0.8 bar range, void content remains low, below 2%, and material properties are maximized. Pressures above 0.8 bar cause rapid resin flow, which traps air bubbles and generates voids at fiber-tow interfaces [9].

For IN2 epoxy, resin and hardener were combined at a 100:30 stoichiometric ratio and degassed prior to introduction. For ELIUM®, 3 wt% water-free benzoyl peroxide initiator was added immediately before introduction. Degassing was omitted due to the small part size, low viscosity of Elium resin, and the optimized breather layer, which minimized air entrapment. Resin flowed through the fiber stack under vacuum for approximately 10-15 minutes. The infusion endpoint was identified visually through the transparent peel ply. Once fiber saturation was complete, the outlet port was sealed to allow consolidation under vacuum.

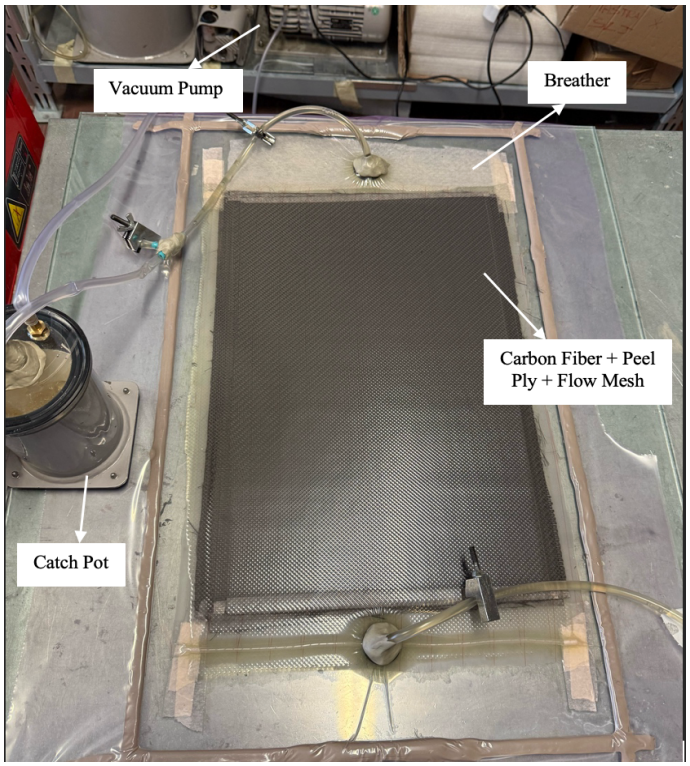

Figure 10 Vacuum Infusion Setup

3.2.2 Cure Cycles

IN2 Epoxy (Thermoset):

- Polymerize at room temperature for 24 hours at 21-23°C.
- Post-cure for 3 hours at 100°C in a laboratory oven.
- Allow to cool gradually to room temperature over 2 to 4 hours.

ELIUM® (Thermoplastic):

- Polymerize at room temperature for 48 hours at 21-23°C, using BPO as the free-radical initiator.
- Post-cure for 1 hour at 80°C to accelerate secondary cross-linking.
- Allow to cool gradually to room temperature over 1 to 2 hours.

3.2.3 Laminate Configuration and Quality Control

Laminate Dimensions: 340 × 500 × 1.9-2.2mm (length × width × thickness)

The optimized VIP process produced high-quality, defect-free composite laminates. At 0.8 bar vacuum pressure, the fiber volume fraction was approximately 53% for both resin systems, allowing for a fair material comparison. Visual inspection showed no surface defects, wrinkles, or dry spots. Thickness measurements at five locations per laminate confirmed uniform saturation and consistent consolidation [8][9].

The infusion setup produced composite laminates of exceptional quality, demonstrating that vacuum infusion, when combined with proper breather-layer design, resin chemistry, and pressure control, enables production of high-performance quasi-static test specimens.

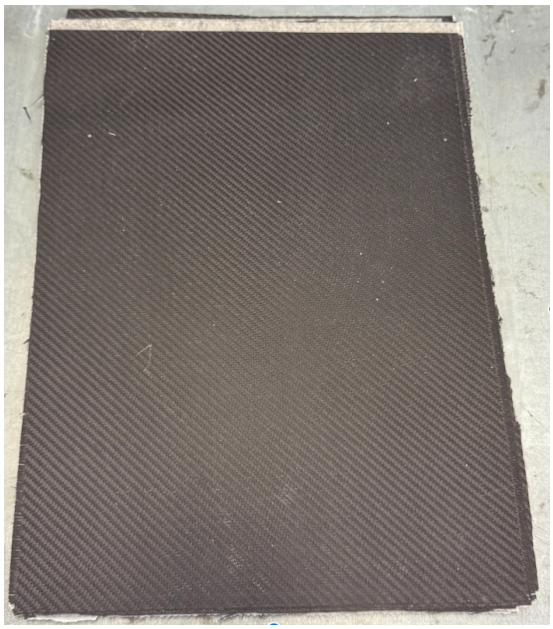

Figure 11 3K Elium-based composite panel

3.3 Specimen Preparation

3.3.1 Specimen Configurations

Following curing and post-cure cycles, composite laminates were sectioned into individual test specimens using precision equipment to ensure dimensional accuracy and minimize edge damage. All specimens were extracted from the plates using a WAZER water-jet machine in accordance with relevant standards. Owing to material constraints, only one plate was produced for each stacking sequence.

Consequently, characterization was conducted exclusively along the 0° direction. This material limitation necessitated testing only three specimens for compression and tensile tests in accordance with ASTM standards D3410 and D3039, and five specimens for the flexural test in accordance with ASTM D790.

Specimens were prepared in accordance with ASTM procedures, and tabs were applied to surfaces in contact with machine gripping fixtures where necessary. In this study, only tensile specimens utilized tabs, each measuring 56 mm in length at both ends. Epoxy resin served as the bonding agent between the tab and specimen surfaces.

Glass fiber tabs were employed during this experimental campaign due to material shortages; according to standards, tabs must be fabricated from a material with lower mechanical properties than the tested material.

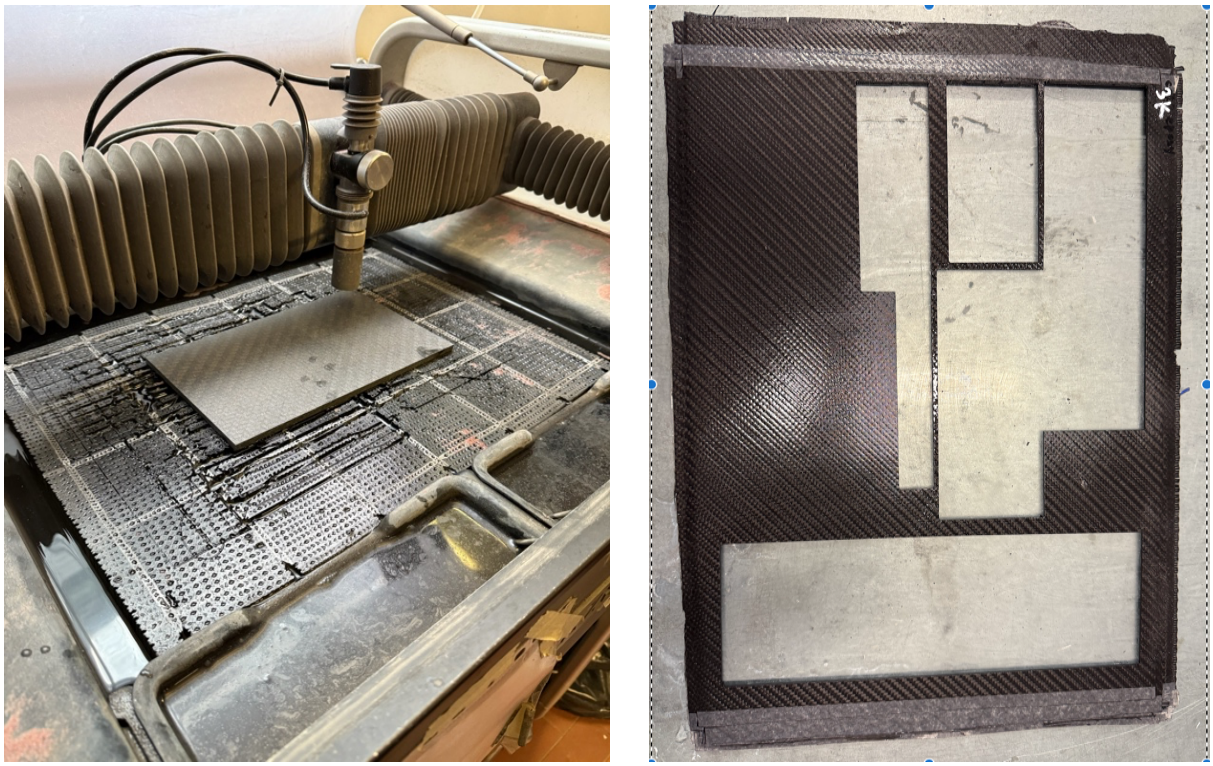

Figure 12 Water jet cutting and 3K Epoxy laminate after cut

All prepared specimens were dimensionally verified using precision measurement instruments. Width and thickness were measured at three locations along the gauge length using digital calipers with a resolution of ±0.01 mm. Tab alignment for tensile specimens was checked visually to ensure symmetric loading during testing.

Specimens with visible defects, such as edge cracks, delamination, or fiber damage from cutting, were rejected to ensure test results reflected material properties rather than manufacturing artifacts. Each specimen was clearly labeled with a unique identification mark, including resin type and specimen number, using a permanent marker on the tab or non-gauge region.

3.3.2 Strain Gage Installation

A strain gauge is a sensor that uses the property of an electrical conductor whose resistance changes when deformed. When properly mounted and well bonded to a representative section of the material, the strain measured by the gauge reflects the strain experienced by the specimen or component. The change in resistance follows this law:

$$\frac{\Delta R}{R} = \frac{\Delta \rho}{\rho} + \frac{\Delta l}{l} - \frac{\Delta A}{A}$$

Where:

- R is the resistance (Ω)
- ρ is the resistivity of the wire/material (Ω.m)
- l is the length of the wire (m)
- A is the cross-sectional area of the wire (m^2)

The previous equation can be derived using the definition of resistance for a resistor with cross-sectional area A, length l, and resistivity ρ, which is: R = ρl/A:

$$\Delta R = \frac{\partial R}{\partial \rho}\Delta \rho + \frac{\partial R}{\partial l}\Delta l + \frac{\partial R}{\partial A}\Delta A = \frac{l}{A}\Delta \rho + \frac{\rho}{A}\Delta l - \frac{\rho l}{A^2}\Delta A$$

Considering now the value of ΔA in case of a rectangular area of dimensions A= a.b:

$$\Delta A = \frac{\partial A}{\partial a}\Delta a + \frac{\partial A}{\partial b}\Delta b = b\Delta a + a\Delta b$$

$$\frac{\Delta A}{A} = \frac{b\Delta a + a\Delta b}{ab} = \frac{\Delta a}{a} + \frac{\Delta b}{b} = -\nu\frac{\Delta l}{l} - \nu\frac{\Delta l}{l} = -2\nu\varepsilon$$

Considering now the first equation for a rectangular resistance, we obtain :

$$\frac{\Delta R}{R} = \frac{\Delta \rho}{\rho} + \frac{\Delta l}{l} - \frac{\Delta A}{A} = \varepsilon(1 + 2\nu) + \frac{\Delta \rho}{\rho} \approx 1.6\varepsilon + \frac{\Delta \rho}{\rho}$$

The relationship between the applied deformation and the resistance variation is called the Gage Factor (K). Usually, the producers of strain Gages provide this value.

$$\frac{\Delta R}{R} \approx 1.6\varepsilon + \frac{\Delta\rho}{\rho} \; ; \; K = \frac{\frac{\Delta R}{R}}{\varepsilon} \approx 1.6 + \frac{\frac{\Delta\rho}{\rho}}{\varepsilon}$$

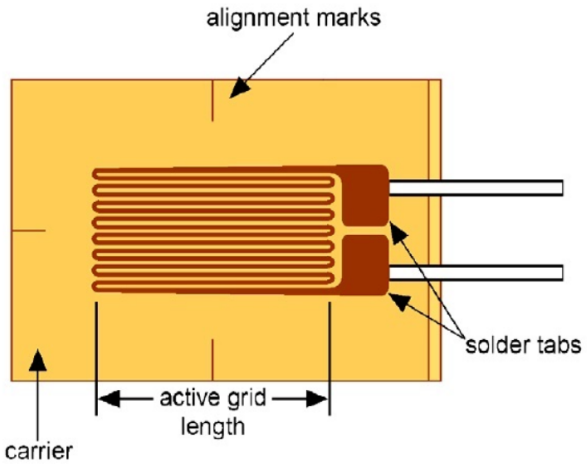

Figure 13 Strain Gauge scheme [60]

Two strain gage models were used in accordance with ASTM standards, selected based on the test type:

1. Compression specimens: HBM 1-LY38-3/350 uniaxial strain gage
   - Nominal resistance = 350 Ω ±0.3%
   - Gage factor = 2.1±1.0%
2. Tensile specimens: HBM 1-XY38-6/350 biaxial strain gage rousette
   - Nominal resistance = 350 Ω ±0.3%
   - Gage factor = a: 2.18 ±1.0%, b: 2.19±1.0%

Gage length: 5 mm (HBM designation)
Material: Constantan foil with copper leads

The specimen surface was prepared to ensure optimal adhesive bonding. The gage location was lightly abraded with fine sandpaper (grid 400) to create a slightly roughened surface without removing significant material. The area was then cleaned with acetone and wiped with lint-free tissue to remove dust and solvents.
The strain gage was positioned at the center of the specimen length along the longitudinal loading direction. Compression specimens were fitted with single-axis uniaxial gages aligned longitudinally to measure strain in the primary loading direction.

Still, tensile specimens were fitted with biaxial strain gages, featuring two perpendicular measurement grids oriented at 0° (longitudinal—loading direction) and 90° (transverse—Poisson direction) to enable simultaneous measurement of axial and transverse strains.

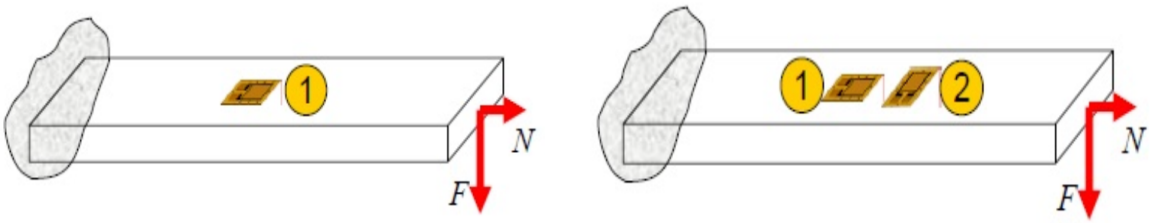

Figure 14 Strain gauge positioning [60]

The gauge was bonded using Loctite Super Attack cyanoacrylate adhesive, which was applied in a thin, uniform layer to the gauge backing. The indicator was positioned centrally, and firm pressure was applied with the thumb using a Teflon sheet as a protective interface. Pressure was maintained for approximately one minute to ensure complete contact between the gage backing and the specimen surface during adhesive curing. The Teflon sheet prevented adhesive transfer and promoted even pressure distribution. The adhesive cured fully within several minutes at room temperature, allowing for immediate lead wire connection without additional curing time.

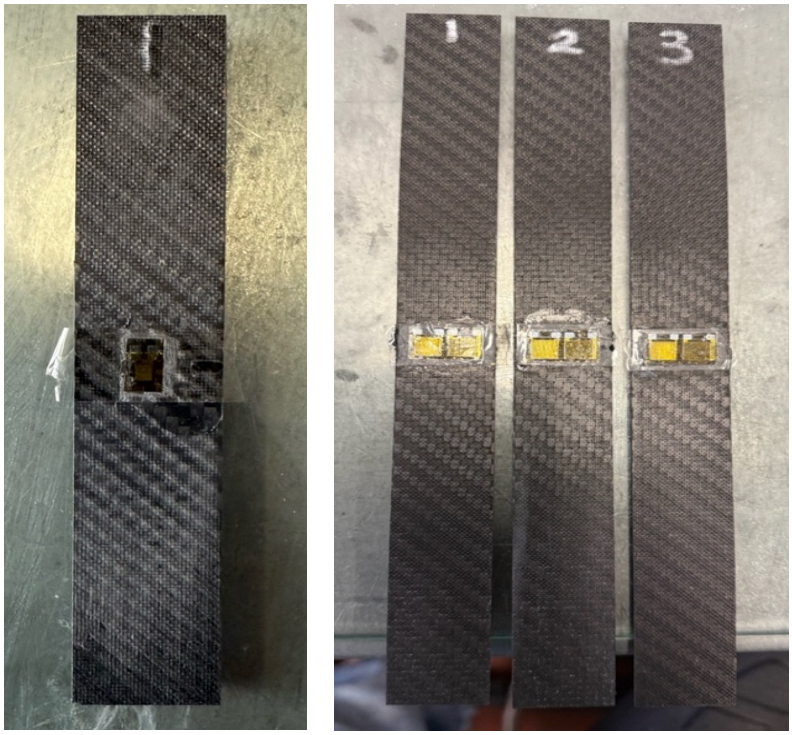

Figure 15 Specimen with a strain gauge for compression test (left) and tensile test (right)

3.4 Standard Tests and Equipment

3.4.1 Compression Testing (ASTM D3410)

Compression tests were performed using an INSTRON 8801 universal testing machine with a Dynacell load cell, calibrated in accordance with ASTM Practice E4 (accuracy ±1%). The Instron universal testing machine, shown in Figure 16, was the primary equipment used to evaluate the mechanical properties of the laminates. This hydraulic UTM is equipped with a 100 kN load cell and an encoder that controls the cross-head displacement via the servo-hydraulic system.

A Wyoming Combined Loading Compression fixture with wedge grips was used for this test. Specimens were clamped with equal grip lengths on both upper and lower wedges, leaving a 10 mm unclamped section. Longitudinal strain was measured on three specimens using a single HBM 1-LY38-3/350 uniaxial strain gage, aligned with the loading direction, to determine the modulus. The crosshead displacement rate was set at 1.3 mm/min.

Force and strain data were recorded continuously at 2-3 Hz. Testing continued until specimen failure, indicated by a sudden load drop or plateau. Ultimate compressive strength was calculated from the maximum force, and failure modes (kinking, crushing, delamination) were documented for all specimens [23].

Average three specimen dimensions:

- 3k Elium : 2.05*24.2*142.97 (thickness*width*length)
- 3k Epoxy : 2.15*23.4*142.4 (thickness*width*length)

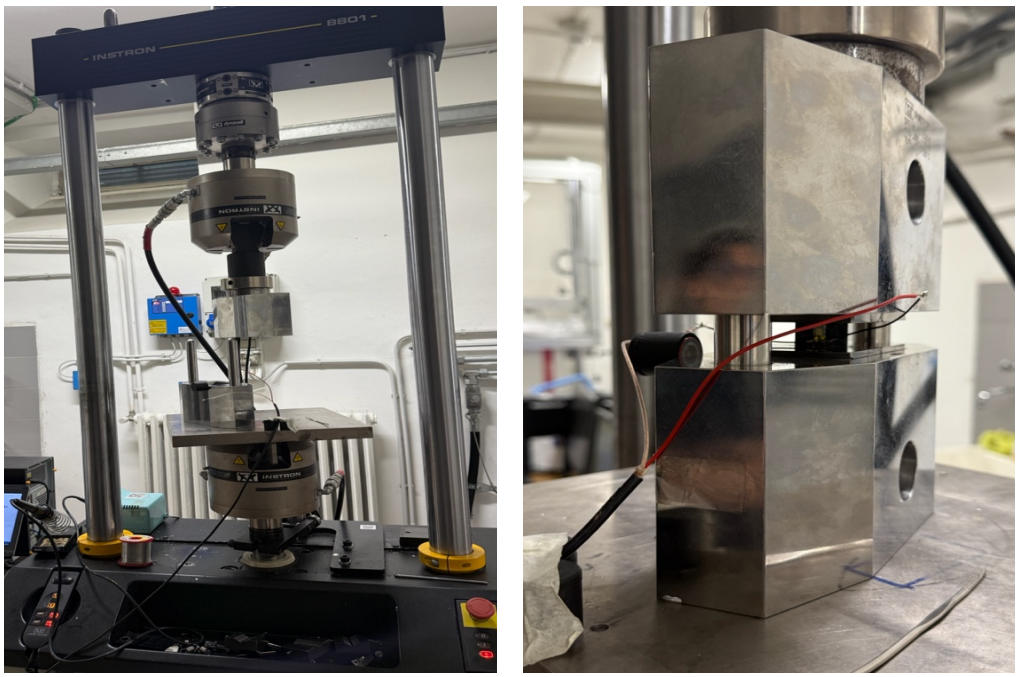

Figure 16 Instron machine 8801 for compression test and the CLC fixture

3.4.2 Tensile Testing (ASTM D3039)

Tensile tests were also performed on the INSTRON 8801 machine (Dynacell load cell, ±1% accuracy per ASTM E4) equipped with a 100 kN load cell by imposing a crosshead displacement rate of 1 mm/min. Rectangular cross-section specimens with bonded glass fiber composite tabs were gripped with 10-15 mm of tab extension, ensuring alignment with the loading axis. The actual width and thickness of each specimen were measured with a digital caliper(resolution of 0.01mm) to compute the applied stress more accurately.

Longitudinal strain was measured using an HBM 1-XY38-6/350 uniaxial strain gage aligned with the loading direction. Force and strain data were recorded continuously at 2-3 Hz, with at least 100 data points per specimen. Testing continued until specimen rupture. Ultimate tensile strength was calculated from the maximum force, and failure modes (fiber pull-out, matrix cracking, delamination) were documented [24]. The experimental setup is shown in Figure 17.

Average three specimen dimensions:

- 3k Elium : 2.11*24.01*248.5(thickness*width*length)
- 3k Epoxy : 2.018*23.98*249.2(thickness*width*length)

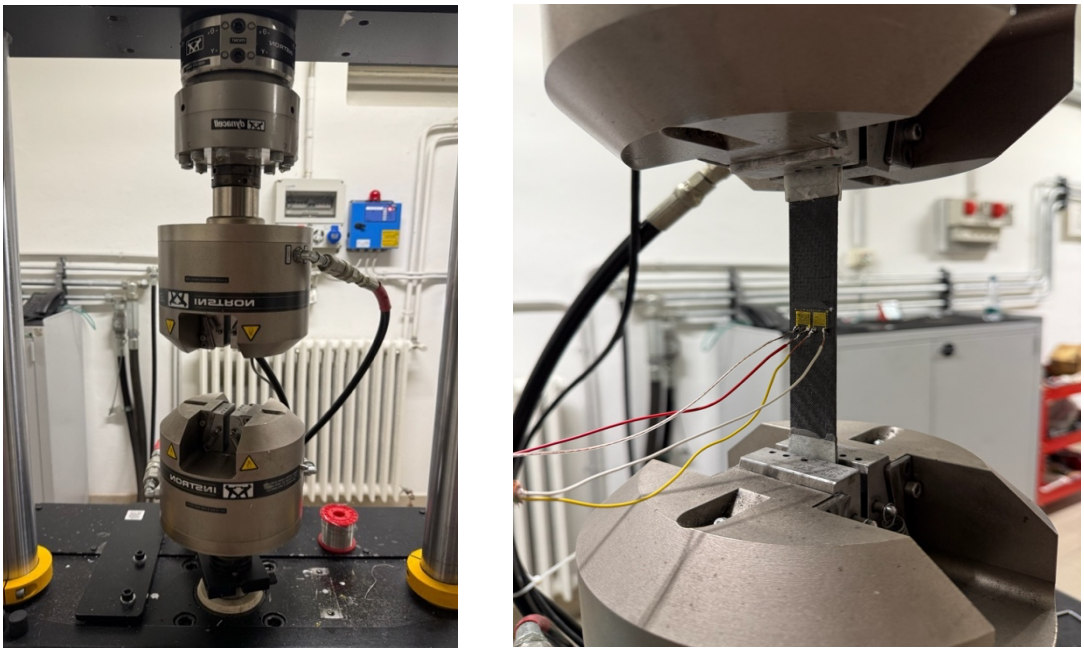

Figure 17 Instron machine 8801 for tensile test and specimen gripping

3.4.3 Flexural Testing (ASTM D790)

Flexural three-point bending tests were conducted on an INSTRON 68SC-5 materials testing machine (calibrated per ASTM E4) equipped with 33 mm cylindrical support rollers (span-to-thickness ratio 16:1) and a 10 mm diameter loading nose at specimen midspan.

The speed of the test, set to 0.8 mm/min, was selected according to ASTM D790, based on the average thickness of specimens and support span.

ASTM D790-17 provides two test procedures for flexural properties. Procedure A is used to determine the flexural modulus of materials that break at comparatively small deflections, using a constant crosshead displacement rate to apply the load uniformly. Procedure B is employed for materials that exhibit larger deflections before failure, using constant-rate deflection control. Additionally, ASTM D790-17 defines two test types: Type I for span-to-thickness ratios of 16:1 (used for flexible materials), and Type II for span-to-thickness ratios of 24:1 (used for rigid and semi-rigid materials).

In this investigation, Procedure A (constant rate of loading) and Type I geometry (16:1 span-to-thickness ratio) were used to characterize the composite laminates as flexible materials with small deflections at failure. Load and deflection data were recorded continuously at 2-3 Hz, with machine compliance correction applied. Testing continued until specimen rupture or until a maximum strain of 5% was reached. Ultimate flexural strength was determined from the maximum load, and the failure mode, specifically tensile matrix cracking on the bottom surface, was documented [25]. The experimental setup is shown in Figure 18.

Average 5 specimen dimensions:

- 3k Elium : 2.08*11.8*124.12(thickness*width*length)
- 3k Epoxy : 2.06*11.86*124.22(thickness*width*length)

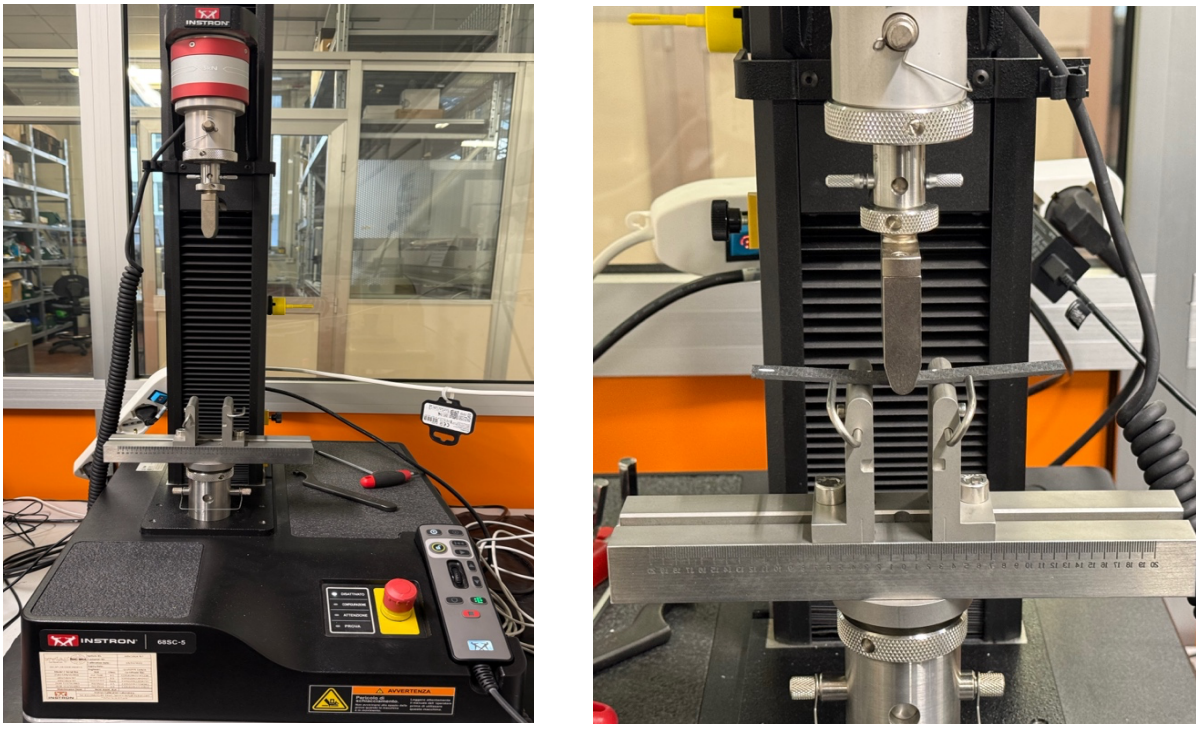

Figure 18 Instron machine 68SC-5 for flexural test and specimen gripping

Chapter 4

Material Characterization and Results

This chapter provides comprehensive experimental results from quasi-static mechanical testing of carbon fiber composites reinforced with IN2 epoxy thermoset and Elium thermoplastic resin systems. The resulting data establish a statistically valid coupon-level material property database, facilitating direct comparison of materials and assessment of Elium as a sustainable alternative to epoxy.

The results are organized into four sections consistent with ASTM testing standards: compression testing, tensile testing, flexural testing, and an integrated comparative analysis with a material selection framework.

For each test type, the following information is reported:

Specimen dimensions and test parameters; individual specimen results with stress-strain curves, summary statistics including mean, standard deviation, and coefficient of variation; failure mode documentation through fractographic analysis; and material comparison validated against existing literature.

4.1 Compression Test Results

Compression testing conducted according to ASTM D3410 provides critical insight into matrix-fiber interactions and delamination resistance under fiber-dominated loading. The resulting data establish a baseline for applications in which composites are required to sustain loads without kinking or splitting failure, criteria that are essential for automotive load-bearing structures and aerospace components.

This section reports compression strength, modulus, and post-failure analysis for both composite systems, including direct comparison to literature values and evaluation of failure mechanisms.

Compression specimens were fabricated using water-jet cutting to achieve dimensions of 143 mm x 24 mm, with a longer dimension aligned with 0°(primary loading axis).

The precise dimensions for each specimen are listed in Table 2. Figure 19 presents the ASTM specimen geometries.

Speccimen	Thickness (mm)	Width (mm)	Length (mm)	Area (mm^2)
3K_Elium_1	2.05	24.2	143	49.61
3K_Elium_2	2.06	24.25	143.05	49.955
3K_Elium_3	2.05	24.18	142.86	49.57
3K_Epoxy_1	2.14	23.18	141.8	49.61
3K_Epoxy_2	2.14	24.01	143.1	51.36
3K_Epoxy_3	2.16	22.9	142.2	49.46

Table 2 Accurate specimen dimensions for the compression test

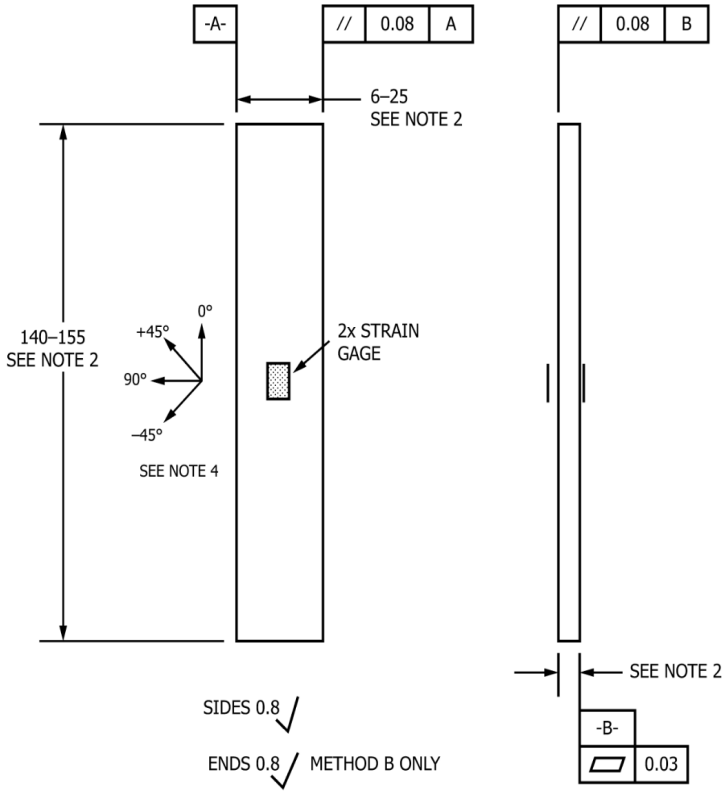

Figure 19 Compression's specimen drawing based on the standard [23]

For compression specimens, only one strain Gage was bonded in the 0° direction. Figure 20 displays all specimens tested with the strain Gage already attached. The 3K_ELLIUM_3 specimen exhibited large negative strain values throughout testing, which may indicate pre-compression, alignment issues, or specimen preparation problems. This specimen was excluded from failure strain analyses. The final compression data are derived from two Elium specimens and three Epoxy specimens.

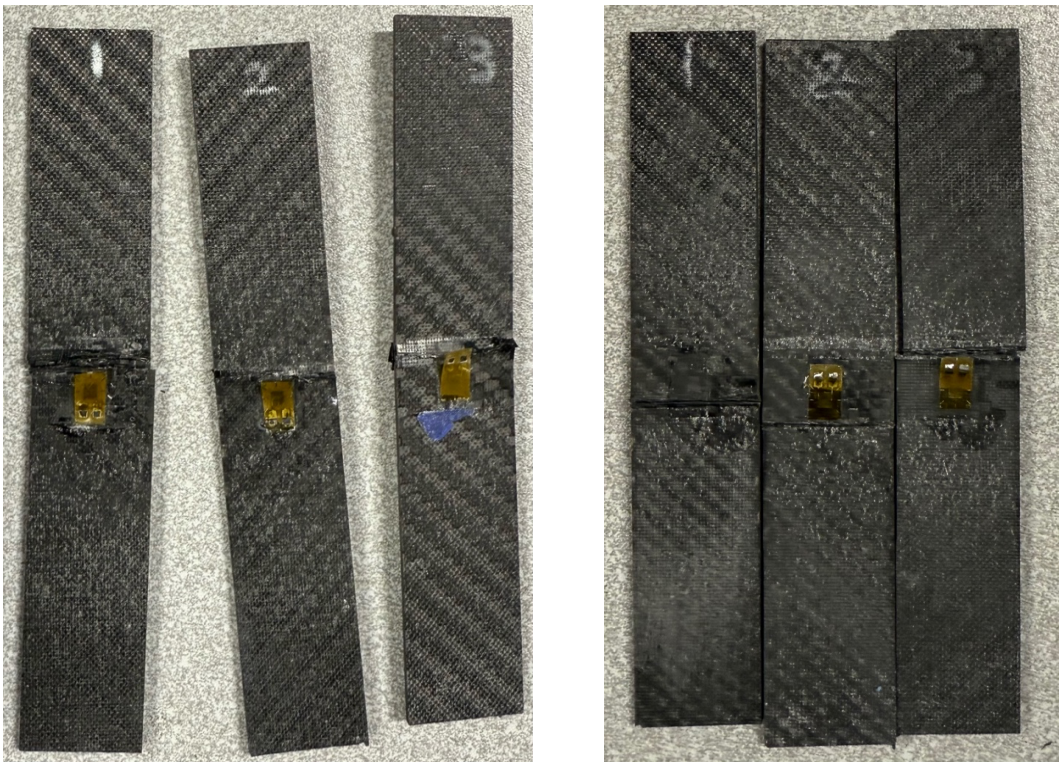

Figure 20 3K_Elium(left) and 3K_Epoxy(right) specimens after compression test

Chord modulus was calculated using a 0.1-0.3% strain range from the stress-strain curve of each specimen, measured directly by strain gauges. Compressive strength was obtained from Instron machine data. We then adjusted the machine's displacement data by determining an effective length that aligns its stiffness with the strain-gauge modulus. Displacements at two stress levels were interpolated from the machine trace, and the known chord modulus was used to calculate the effective length. All displacements were converted to strain by dividing by this length.

Specimen	Compressive Modulus (GPa)	Compressive Strength (MPa)	Failure Strain (%)
3K_Elium_1	46.8	467.48	0.779
3K_Elium_2	46.65	443.47	0.753
3K_Elium_3	45.77	411.58	excluded
3K_Epoxy_1	45.02	467.19	0.862
3K_Epoxy_2	48.46	467.93	0.779
3K_Epoxy_3	51.78	426.12	0.720

Table 3 Compression properties of each specimen

Final stress-strain curves were derived from Instron data, as shown in Figure 21. Also, mechanical properties, including compressive strength, modulus of elasticity, and strain at failure, are reported for each specimen in Table 3.

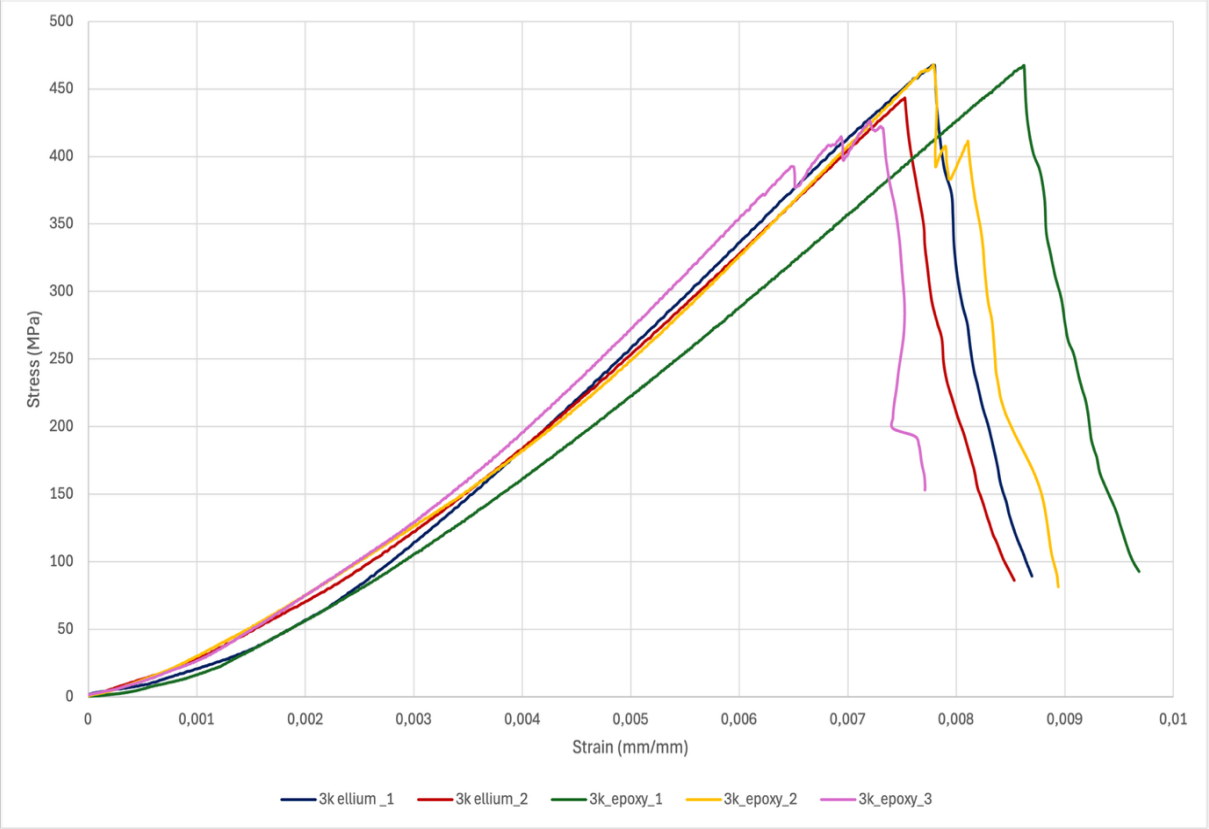

Figure 21 Stress-Strain curves from Instron for compression test

Furthermore, the average mechanical properties for each material are available in Table 4. Moreover, bar charts of compression results with error bars are shown in Figures 22-24.

	ELIUM COMPOSITE	**IN2 COMPOSITE**
$\boldsymbol{E\ [GPa]}$	46.41 ±0.56 (CV = 1.20%)	48.42 ±3.38 (CV = 6.98%)
$\boldsymbol{\sigma_{UCS}[MPa]}$	440.84 ± 28.04 (CV = 6.36%)	453.75 ± 23.93 (CV = 5.27%)
$\boldsymbol{\varepsilon_{UCS}}$ %	0.766 ± 0.018 (CV = 2.40%)	0.787 ± 0.071 (CV = 9.06%)

Table 4 Compression results of two materials

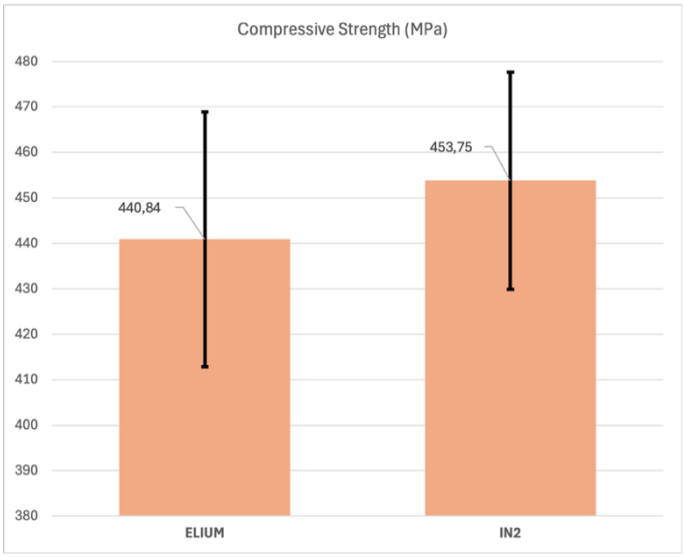

Figure 22 Bar chart of compressive strength of two materials with error bars

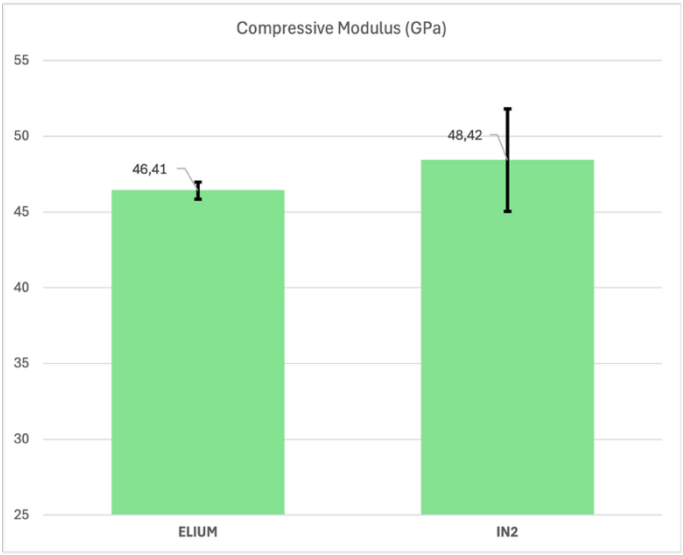

Figure 23 Bar chart of compressive modulus of two materials with error bars

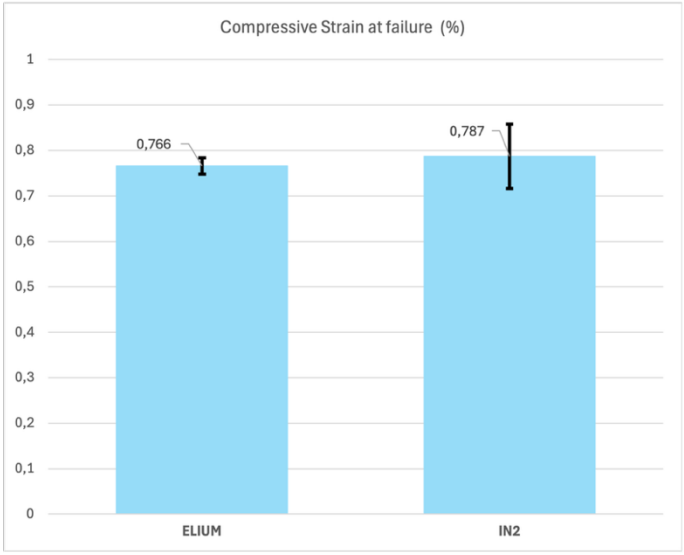

Figure 24 Bar chart of compressive strain at failure of two materials with error bars

Woven carbon fiber-Elium composites achieved a mean compressive strength of 440.84 ± 28.04 MPa (n=2, CV=6.36%), while IN2 epoxy composites reached 453.75 ± 23.93 MPa (n=3, CV=5.27%). This represents a **2.8% reduction** for Elium, which is not statistically significant. Both materials showed excellent compressive strength, confirming mechanical equivalence under longitudinal compression.

Compressive modulus values were 46.41 ± 0.56 GPa for Elium (CV=1.20%) and 48.42 ± 3.38 GPa for epoxy (CV=6.98%), a **3.9% difference** that is also not statistically significant. However, Elium's coefficient of variation was **82% lower**, indicating much greater manufacturing consistency.

This 5.8-fold reduction in variability reflects the uniform polymerization kinetics of thermoplastic PMMA, in contrast to the temperature-dependent cross-linking kinetics of thermoset epoxy.

Bhudolia et al. [39] report that unidirectional carbon-Elium composites achieve 92-95% of epoxy compressive strength, which is consistent with our woven architecture results showing **97.1% equivalence**. The 2×2 twill weave in our study causes approximately 50% fiber deviation from the loading direction, reducing axial compressive properties compared to unidirectional systems. Our results **align with published data** when accounting for fiber architecture effects [36][39].

Both materials achieved similar peak modulus values, but the Elium system's high consistency (CV=1.20%) offers a significant engineering advantage. For applications requiring a minimum compressive modulus of 45 GPa with 95% confidence, Elium provides a design allowable of about 45.3 GPa, while epoxy must be reduced to 42.8 GPa to meet the same confidence. This **5.8% efficiency** gain can **reduce structural weight** or **increase safety margins** in aerospace and automotive applications [36][37].

Applying the rule of mixtures with approximately 53% fiber volume fraction and a 234 GPa carbon fiber modulus, E_c predicted ≈ 0.53×234 + 0.47×1.4 (for epoxy) ≈ 124.7 GPa for unidirectional fiber.

In our [0/90] twill architecture, about 50% fiber deviation lowers the effective modulus to approximately 62 GPa, which is **25% higher** than our measured values. This difference is due to through-thickness shear deformation and matrix bending compliance in the 90° fiber plies, as confirmed by micromechanical composite theory.

4.1.2 Compression Failure Modes and Microscopic Analysis

Elium Specimens:

Failure began with localized matrix plastic deformation and fiber-matrix debonding in resin-rich areas. Fracture surfaces showed kink bands oriented 45-55° to the loading axis, indicating fiber elastic instability followed by plastic column buckling. All Elium® compression specimens (3K_Elium_1, 3K_Elium_2) exhibited the M(KS)GM failure mode, dominated by fiber instability.

Notably, Elium specimens showed progressive fiber-matrix debonding before the main fracture, followed by controlled fiber buckling. This behavior is typical of thermoplastic-matrix composites with strong fiber-matrix adhesion and a ductile matrix [42][43].

Examination of the fracture surface (Figure 25) reveals fiber fragmentation concentrated in a primary failure zone approximately 2-3 mm wide. This zone is surrounded by a ductile deformation region, where adjacent fibers exhibit partial debonding and progressive matrix plastic deformation.

The fracture plane has moderate roughness and visible matrix material on fractured fiber ends, indicating energy dissipation through ductile rather than brittle mechanisms. This failure morphology confirms that the Wyoming combined loading compression fixture effectively transferred load through the specimen, prevented premature grip-induced failures, and validated the mechanical property results.

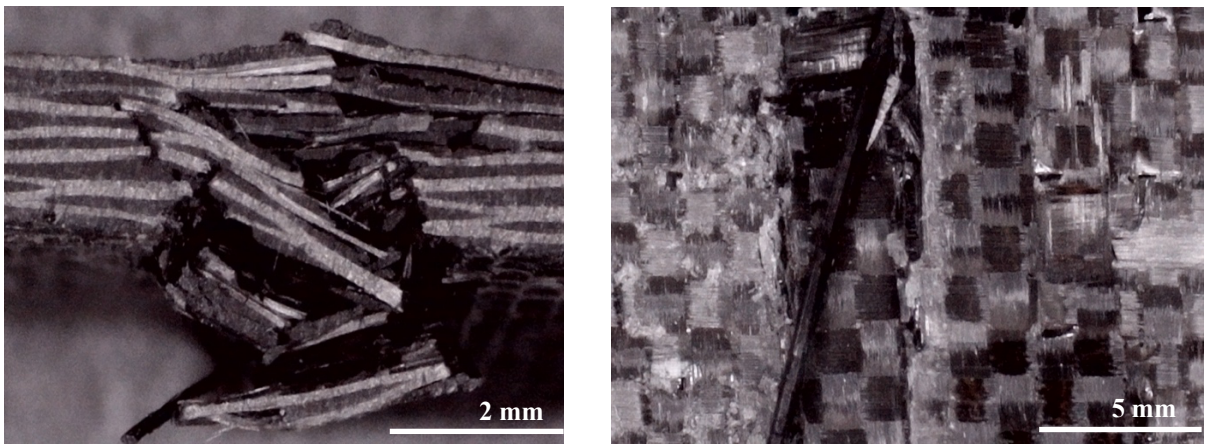

Figure 25 Fracture surface of specimen 3K_Elium_1 after compression test

IN2 Specimens:

Failure was characterized by rapid fiber microbuckling, followed by brittle matrix cracking and a clean fracture perpendicular to the loading axis. All epoxy compression specimens (3K_Epoxy_1, 3K_Epoxy_2, 3K_Epoxy_3) exhibited a similar M(KS)GM failure mode with defined kink bands.

Epoxy specimens failed abruptly, with minimal progressive damage. Fracture surfaces were smooth and planar (Figure 26), showing little matrix plastic deformation and clean fiber-matrix separation. Fiber fragmentation was nearly uniform, indicating synchronous failure rather than progressive debonding [39].

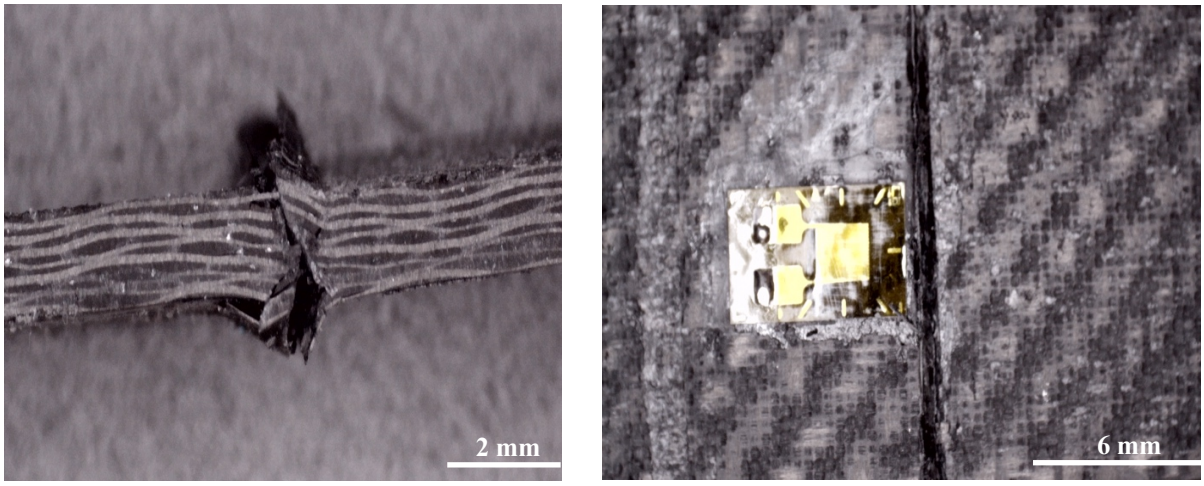

Figure 26 Fracture surface of specimen 3K_Epoxy_1 after compression test

Mechanistic Interpretation:

Epoxy composites exhibit a slightly **higher average compressive strength** (453.75 vs. 440.84 MPa), which aligns with epoxy resin's **higher shear modulus** (1.4 GPa vs. 1.2 GPa for PMMA) and **greater resistance to fiber microbuckling** under compression. However, this strength comes at the cost of reduced damage tolerance.

The more ductile Elium matrix, despite its lower peak compressive strength, enables progressive failure through plastic deformation rather than catastrophic brittle failure. This property is highly valued in energy absorption and crashworthiness applications [36][40].

4.2 Tensile Test Results

Tensile testing according to ASTM D3039 evaluates fiber-dominated mechanical behavior and material ductility. These properties are essential for structural design and for assessing matrix toughness through failure strain analysis. This section reports tensile strength, modulus, failure strain, and fractographic evidence of failure mechanisms in both composite systems.

Tensile specimens were fabricated by water-jet cutting to 250 mm x 24 mm, with the longer side aligned at 0°. Each end was fitted with a 56 mm glass fiber-epoxy tab. Table 5 lists the exact dimensions for each specimen. Figure 27 shows the ASTM specimen geometries.

Speccimen	Thickness (mm)	Width (mm)	Length (mm)	Area (mm^2)
3K_Elium_1	2.1	23.85	249	50.085
3K_Elium_2	2.11	24.06	248.6	50.767
3K_Elium_3	2.13	24.1	248.01	51.333
3K_Epoxy_1	2.0075	23.8525	248.53	47.884
3K_Epoxy_2	2.07	24.04	248.076	49.763
3K_Epoxy_3	1.9775	24.06	249.1	47.579

Table 5 Accurate specimens dimensions for the tensile test

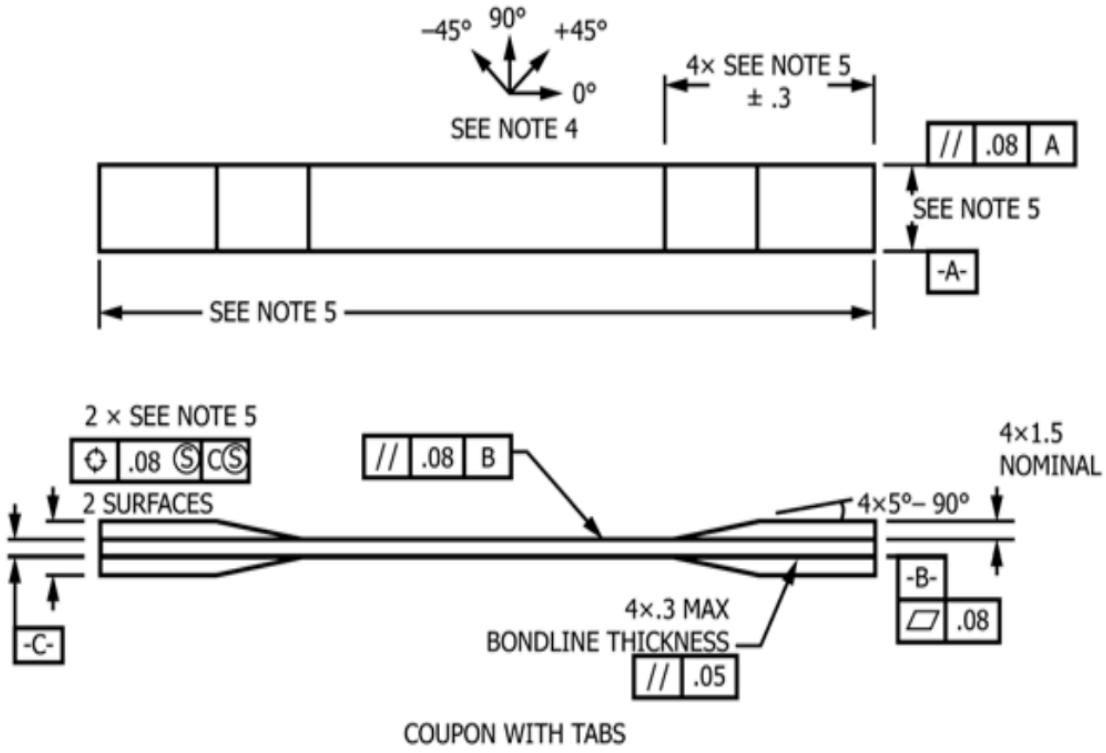

Figure 27 Tensile specimen drawing based on the standard [24]

For tensile specimens, a biaxial strain gauge was bonded in the 0° direction. Figure 28 shows all the tested specimens with the strain gauge attached. Adhesive failure and electrical lead detachment during strain gauge installation resulted in only two Elium composite specimens with functional gauges being available for analysis.

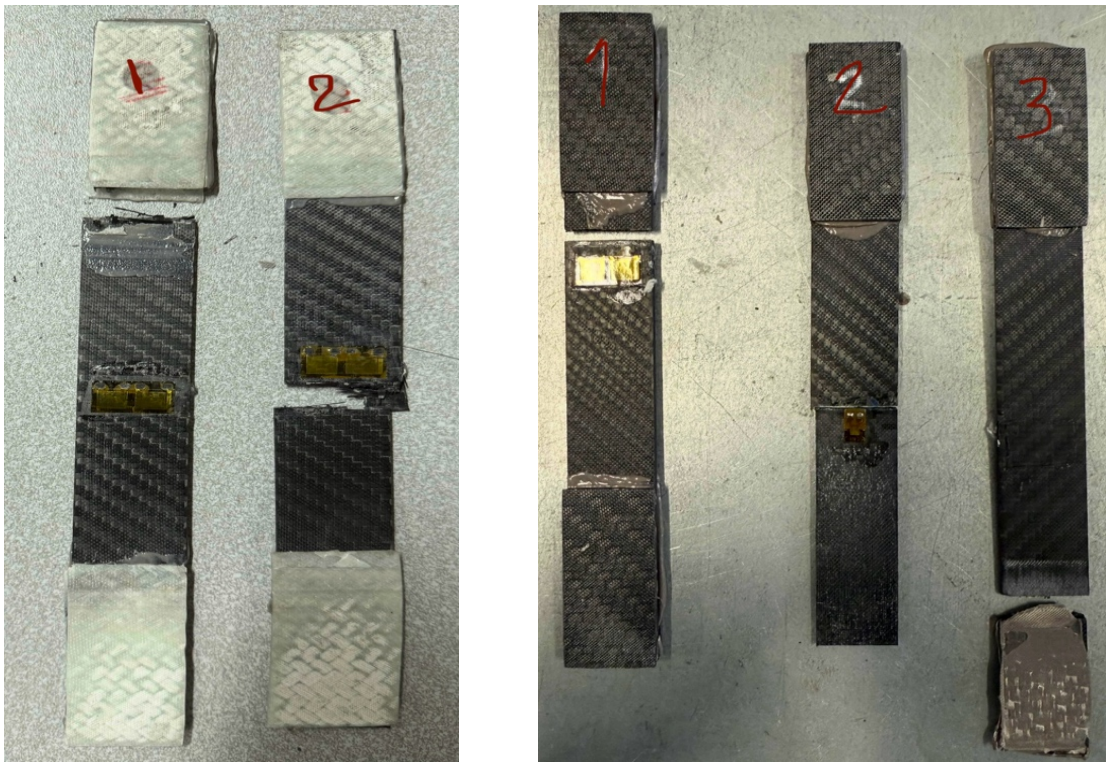

Figure 28 3K_Elium (left) and 3K_Epoxy (right) specimens after tensile test

During the initial tensile test with strain gauges, Specimen 3K_Epoxy_3 and 3K_elium_1 experienced grip slipping - a condition where the specimen slides relative to the testing machine grips instead of being held firmly. The likely causes include:

- Insufficient Grip Pressure - The normal force applied by the grips was inadequate to maintain sufficient friction with the specimen surface
- Worn Grip Serrations - The grip jaw surfaces may have had worn or dull serrations that couldn't bite effectively into the composite material
- Surface Condition - Possible contamination (moisture, oil) or smooth spots on the specimen grip interface
- Specimen Geometry - Potential out-of-tolerance dimensions or surface irregularities

These specimens were retested without the strain gauge attachment again to achieve a strength value.

We calculated the chord modulus using a 0.1-0.3% strain range from the stress-strain curve of each specimen, measured directly by strain gauges. Tensile strength was obtained from Instron machine data. Then we followed the same procedure as the compression test to convert displacements to strain by dividing by the effective length. Final stress-strain curves were derived from Instron data, as shown in Figure 29. Mechanical properties, including tensile strength, modulus of elasticity, and strain at failure, are reported for each specimen in Table 6.

Specimen	Tensile Modulus (GPa)	Tensile Strength (MPa)	Failure Strain (%)
3K_Elium_1	1.55 (invalid)	711.63	1.355
3K_Elium_2	53.51	707.06	1.351
3K_Epoxy_1	58.703	768.22	0.986
3K_Epoxy_2	55.454	740.35	0.987
3K_Epoxy_3	55.426	737.99	0.979

Table 6 Tensile properties of each specimen

Unfortunately, Elium 3K_1 was excluded from the modulus analysis due to rapid failure in the test grips, as shown by an early loss of the strain-gauge signal and a low modulus of approximately 1.55 GPa (n=1 valid Elium specimen for modulus).

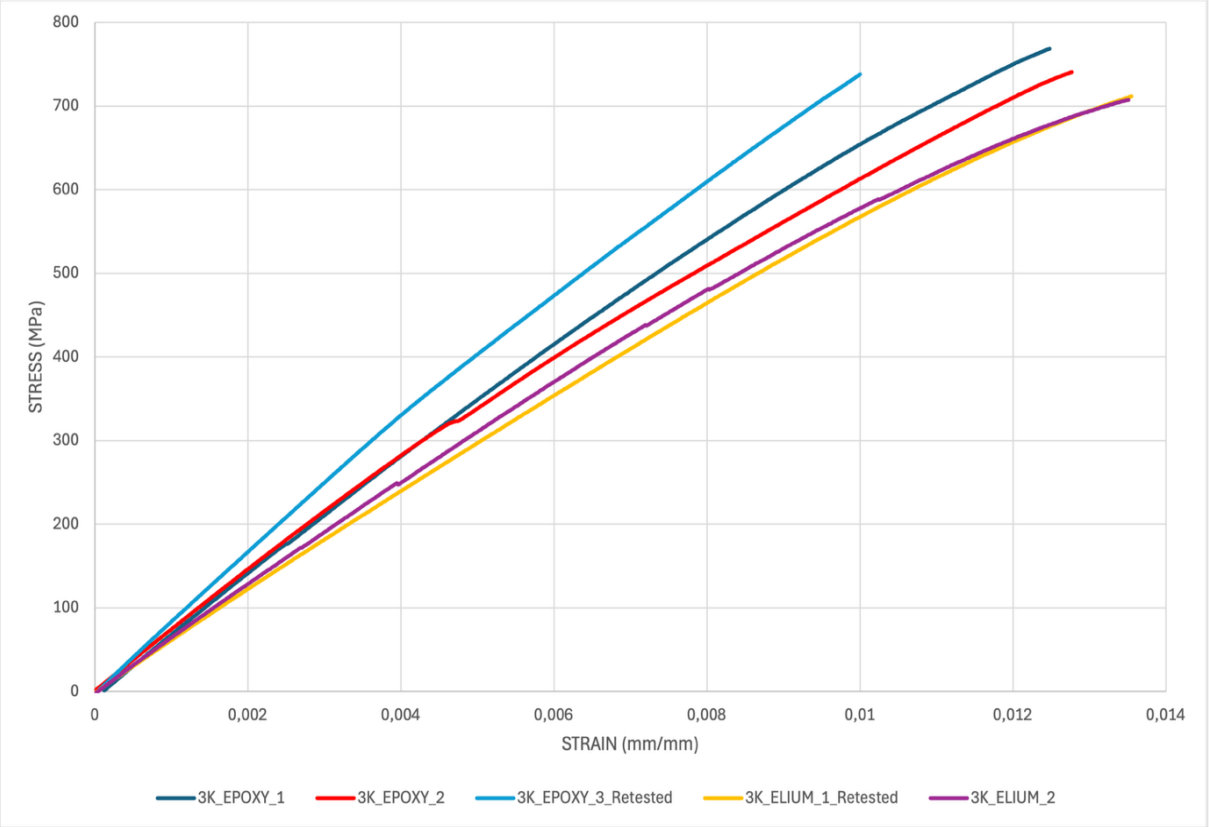

Figure 29 Stress-Strain curves from Instron for tensile test up to strain gauge failure

Also, the average mechanical properties for each material are available in Table 7. Moreover, bar charts of tensile results are shown in Figures 30-32.

	ELIUM COMPOSITE	IN2 COMPOSITE
E [GPa]	53.51 (n = 1)	56.53 ± 1.884 (CV = 3.33%)
σ_{UTS}[MPa]	709.34 ± 2.28 (CV =0.32%)	748.85 ± 16.82 (CV = 2.25%)
ε_{UTS} %	1.353 ± 0.0026 (CV = 0.192%)	0.984 ± 0.0044 (CV = 0.45%)

Table 7 Tensile results of two materials

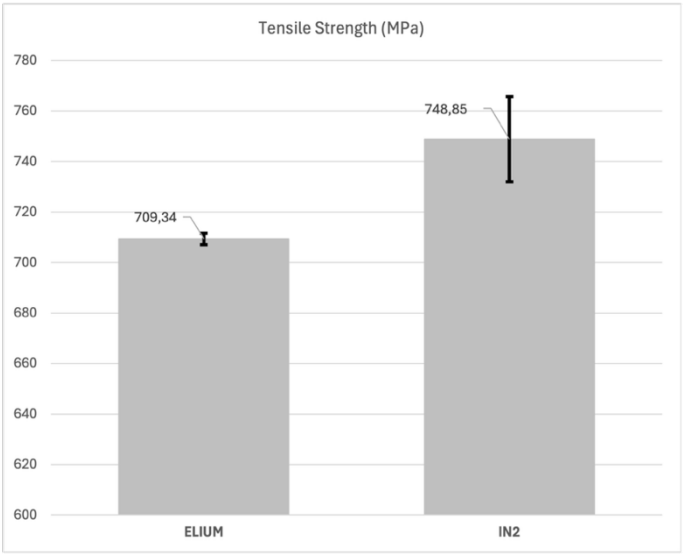

Figure 30 Bar chart of tensile strength of two materials with error bars

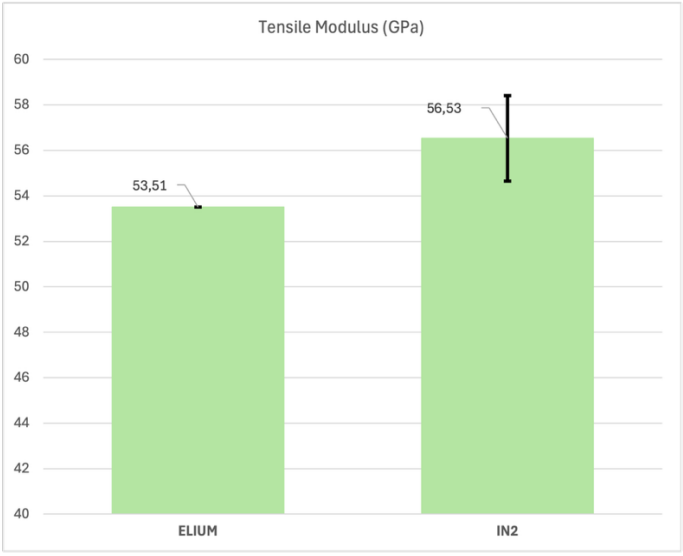

Figure 31 Bar chart of tensile modulus of two materials with error bars

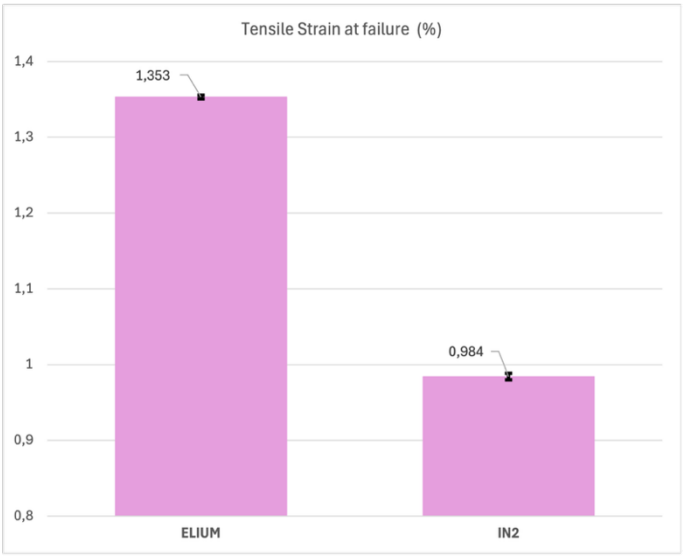

Figure 32 Bar chart of tensile strain at failure of two materials with error bars

3K Epoxy offers higher initial stiffness (56.53 ± 1.884 GPa) and strength (748.85 ± 16.82 MPa), but fails in a brittle manner (0.984 ± 0.0044% failure strain). In comparison, 3K ELIUM provides similar stiffness (53.51 GPa, **5.3% lower**), slightly reduced strength (709.34 ± 2.28 MPa, **5.6% lower**), and much greater ductility (1.353 ± 0.0026 %failure strain, **37.4% higher**). The ELIUM system also shows superior consistency in mechanical properties (CV: 0.32–0.603% compared to 2.25–3.88% for epoxy).

The significantly lower coefficient of variation for Elium® tensile strength (0.32% compared to 2.25% for epoxy) demonstrates that thermoplastic polymerization yields more uniform composite laminates. This manufacturing consistency offers a key advantage in production-scale applications, where property variability can increase design knockdown factors and reduce structural efficiency.

Our findings are consistent with Bhudolia et al. [39], who reported unidirectional carbon-Elium® at 1420 MPa, or 95% of epoxy's 1495 MPa. Our [0/90] woven results demonstrate **94.7% equivalence** (709.34 vs. 748.85 MPa), indicating the **impact of fiber misalignment**. The twill architecture offers balanced biaxial properties but reduces peak uniaxial strength by about 30-40% compared to unidirectional systems, in line with composite theory predictions [36].

Also, the 5.3% lower modulus of Elium® results from the lower PMMA matrix modulus (2.6 GPa) compared to epoxy (3.0 GPa). This 13% difference predicts a composite modulus reduction of about 4-6% according to micromechanical analysis [37] [39].

A 37.4% higher failure strain demonstrates the significantly enhanced strain-to-failure capability of Elium® composites.

Under tensile loading, the thermoplastic matrix allows approximately 37% greater elongation before fiber rupture compared to brittle thermoset epoxy [36][42][43].

Bhudolia et al. [39] reported a 23.5% higher failure strain for unidirectional carbon-Elium® (1.35% vs. 1.09%) , which **aligns with our observed 37.4% increase** in woven composites. The greater advantage in woven systems likely results from the constraint imposed by transverse (90°) fibers on strain in the 0° direction.

The Elium® thermoplastic matrix also accommodates biaxial stress states more effectively through localized plastic deformation [36]. The 37.4% higher failure strain demonstrates PMMA's elastoplastic behavior (elongation at break 4-7%, Table 1), in contrast to the rigid behavior of epoxy (3-5%).

In epoxy, tensile failure is fiber-dominated and occurs abruptly when fiber stress reaches its limit. In contrast, Elium® matrices exhibit significant plastic strain before fiber rupture, which distributes stress across adjacent fibers and allows continued strain accumulation [42][43].

The low coefficient of variation (CV) in Elium® failure strain (0.19%) indicates consistent maximum strain (~1.35%) among specimens, reflecting uniform ductile behavior.

Epoxy specimens, by comparison, show greater variability (CV=0.45%) due to differences in crack initiation sites [36].

4.2.1 Tensile Failure Modes and Microscopic Analysis

Elium Specimens:

The first ELIUM specimen failed in the grip or tab region, exhibiting distinct ductile features (TGF-D). The second specimen failed in the gauge section, showing fiber pullout and matrix deformation (DFG), which is generally considered a favorable failure mode for composite materials [24].

Primary observations and microscopic analysis in Figure 29 identify several key features. Extensive fiber pull-out, ranging from 2 to 4 mm, is observed, with individual fibers extending well beyond the primary failure plane. This observation indicates ductile fiber-matrix debonding. The PMMA matrix exhibits plastic deformation before fiber rupture [42][43].

High resin adherence, with 60-70% fiber coverage, and resin remnants adhering to the majority of fiber surfaces, indicates strong fiber-matrix adhesion combined with ductile plastic matrix behavior. This finding contrasts with the clean interfaces observed in epoxy systems [42].

Tortuous crack propagation is evident, as the irregular and jagged fracture surface suggests distributed damage rather than catastrophic cleavage. Multiple visible crack paths further indicate a progressive failure mechanism [42].

Significant fracture surface relief, measured at 20-60 μm with an average of approximately 40 μm, demonstrates substantial inelastic deformation and energy dissipation. Rough, jagged topography covers about 60-70% of the fracture surface, reflecting plastic matrix deformation, while the remaining 30-40% is smoother, indicating localized fiber-matrix separation without plastic deformation [42][43].

Hackle marks, which are radial lines emanating from crack initiation points, indicate multiple sequential crack nucleation events rather than a single catastrophic failure. This behavior is characteristic of thermoplastic-matrix composites.

The observed 37.4% increase in failure strain and ductile fracture morphology indicates that plastic deformation of the Elium matrix extends fiber strain by approximately 37% compared to epoxy. The PMMA matrix, with an elongation at break of 4-7%, deforms plastically and allows greater fiber elongation before rupture. In contrast, epoxy, with an elongation at break of 3-5%, fails earlier due to brittle cleavage, limiting the total composite strain [36][42][43].

These morphological findings are consistent with Barbosa et al. [42], who reported that thermoplastic-matrix composites exhibit greater fiber pull-out and surface roughness due to matrix plasticity. Bhudolia et al. [39] also documented similar pull-out distances (2-4 mm) and resin adherence patterns.

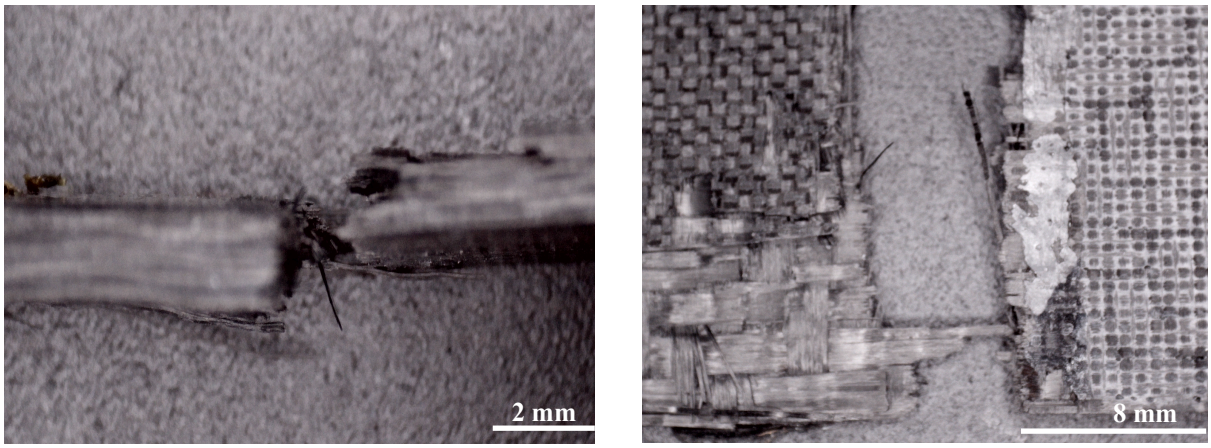

Figure 33 Fracture surface of specimen 3K_Elium_2 after tensile test

IN2 Specimens:

The first two epoxy specimens showed brittle fractures within the gauge section (BFI). The third specimen failed in the tab region (TGF) with a clean break and no lateral delamination. Primary observations and microscopic analysis in Figure 30 highlight several features.

Minimal fiber pull-out (less than 1 mm) indicates abrupt fiber-matrix separation without ductile debonding, preventing significant fiber elongation from contributing to strain [39].

Clean fiber-matrix interfaces with less than 20–30% resin coverage and minimal adhering resin are typical of brittle matrix failure and rapid crack propagation, which confines damage near the fracture plane [39].

The fracture surface is planar, smooth, and perpendicular to the loading direction, suggesting single-event crack propagation rather than distributed damage. Low fracture surface relief (less than 20 μm) indicates minimal plastic deformation, with 80–90% of the surface smooth and planar, confirming brittle thermoset behavior [39].

Uniform fiber failure, with fibers breaking at nearly identical depths, indicates synchronous failure rather than progressive damage. The limited presence of hackle marks further supports a single nucleation event followed by rapid crack propagation.

The 37% lower failure strain for epoxy (0.984%) reflects the matrix's inability to accumulate plastic strain. When fiber stress reaches its tensile limit, brittle cleavage occurs immediately without warning or distributed damage.

This explains the lower strain coefficient of variation (0.45%) and reduced damage tolerance. These findings align with Bhudolia et al. [39], who describe epoxy composite fracture surfaces as having clean interfaces, minimal fiber pull-out, and planar failures typical of brittle thermoset behavior.

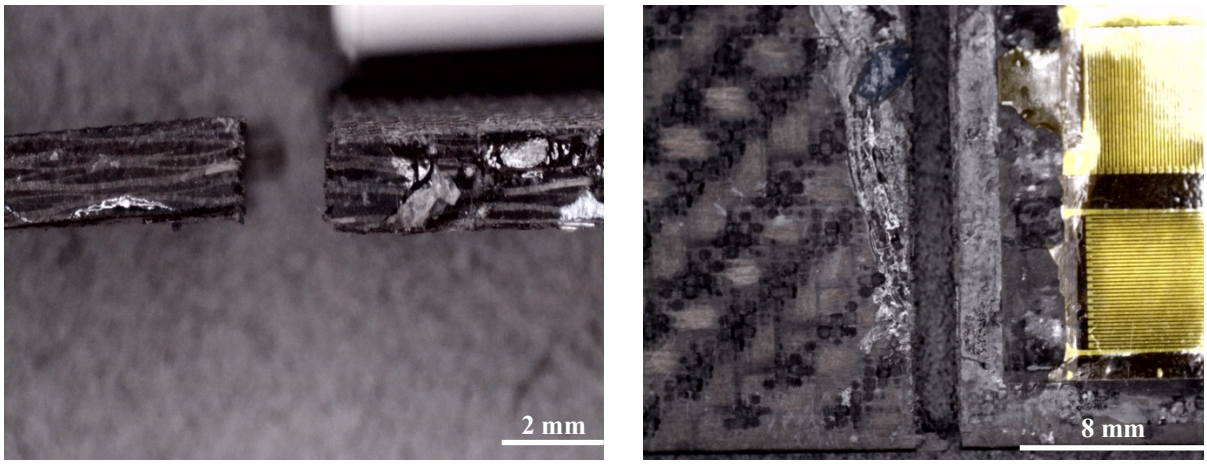

Figure 34 Fracture surface of specimen 3K_Epoxy_1 after tensile test

4.3 Flexural Test Results

Three-point bending under ASTM D790 evaluates composite behavior under combined tensile and compressive loading in areas of stress concentration. The test applies tensile stress to the outer tension surface, transverse shear stress to the neutral axis, and compressive stress to the outer compression surface. This multiaxial stress state is sensitive to matrix properties and the quality of the fiber-matrix interface [25][35].

We fabricated flexural (3-point bending) specimens using water-jet cutting to dimensions of 126 mm by 13 mm, with the longer dimension aligned with 0°, and no strain gauges were used. The precise dimensions for each specimen are listed in Table 8.

We didn't test the 3k_Elium_5 specimen to retain a backup in case of unexpected results. The following formulas are used to calculate flexural properties:

$$1.\ R = \frac{zL^2}{6d} \qquad 2.\ E_b = \frac{L^3 m}{4bd^3} \qquad 3.\ \varepsilon_f = \frac{6Dd}{L^2} \qquad 4.\ \sigma_f = \frac{3PL}{2bd^2}$$

R= rate of crosshead motion (mm/min)

z= rate of the straining of the outer fiber = 0,01 (mm/mm/min)

d= depth thickness of the tested specimen (mm)

L = Support span (mm) with ratio of 16:1 to thickness

E_b=modulus of elasticity in bending, MPa

m= slope of the tangent to the initial straight-line portion of the load-deflection curve(N/mm)

b = width of specimen tested (mm)

ε_f=Flexural strain (mm/mm)

D = Midspan deflection (mm)

σ_f=Flexural stress (MPa)

P = Load at a given point (N)

Average specimen dimensions :

- 3k Epoxy-based composite:
  thickness (d): 2.062 ± 0.018 mm, Width (b): 11.858 ± 0.066 mm, Support Span (L)= 32.92 mm, and R=0.876 mm/min
- 3k Elium-based composite:
  thickness (d): 2.078 ± 0.008 mm, Width: 11.808 ± 0.057 mm, L=33.248 mm, and R=0.887 mm/min.
- We set L = 33 mm for both materials.

Speccimen	Thickness (mm)	Width (mm)	Length (mm)
3K_Elium_1	2.09	11.85	124.07
3K_Elium_2	2.07	11.74	124.08
3K_Elium_3	2.08	11.8	124.18
3K_Elium_4	2.07	11.77	124.16
3K_Elium_5	2.08	11.88	124.14
3K_Epoxy_1	2.08	11.77	124.54
3K_Epoxy_2	2.06	11.95	124.14
3K_Epoxy_3	2.04	11.83	124.09
3K_Epoxy_4	2.08	11.86	124.07
3K_Epoxy_5	2.05	11.88	124.26

Table 8 Accurate specimen dimensions for the flexural test

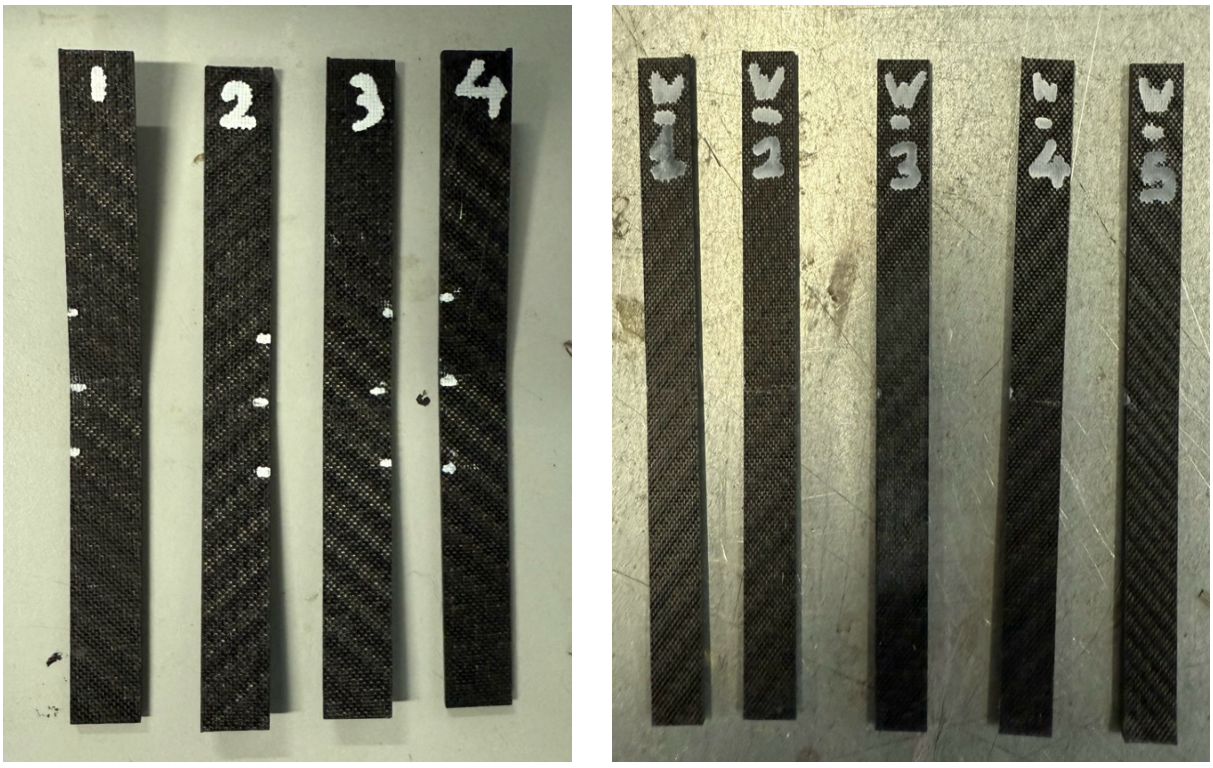

Figure 35 3K_Elium(left) and 3K_Epoxy(right) specimens after flexural test

We calculated the flexural modulus using the equation $E_b = \frac{L^3 m}{4bd^3}$, where m is the slope of the load-deflection curve. Mechanical properties, including flexural strength, modulus of elasticity, and strain at rupture, are reported for each specimen in Table 9. Final stress-strain curves were reported in Figure 36.

Specimen	Flexural Modulus (GPa)	Slope of tangent m (N/mm)	Flexural Strength (MPa)	Failure Strain (%)
3K_Elium_1	34.51	415.51	684.33	2.276
3K_Elium_2	36.40	421.86	691.56	2.092
3K_Elium_3	34.36	406.10	723.43	2.312
3K_Elium_4	34.57	401.69	770.08	2.415
3K_Epoxy_1	29.28	345.14	713.41	2.472
3K_Epoxy_2	28.22	328.06	703.099	2.465
3K_Epoxy_3	30.41	339.91	663.898	2.209
3K_Epoxy_4	27.89	331.28	675.87	2.514
3K_Epoxy_5	28.67	326.57	698.394	2.502

Table 9 Flexural properties of each specimen

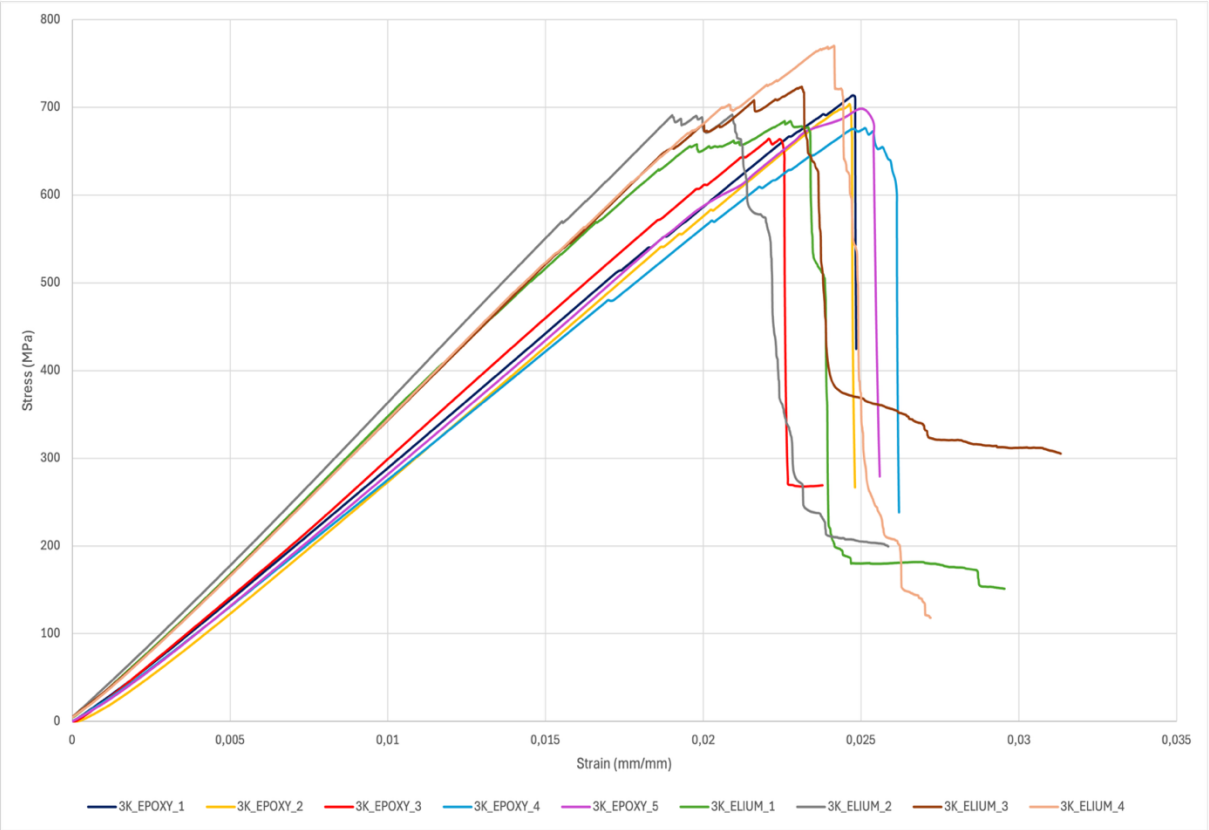

Figure 36 Stress-Strain curves for flexural test

Also, the average mechanical properties for each material are available in Table 10. Moreover, the bar charts of flexural results are shown in Figures 37-39.

	ELIUM COMPOSITE	IN2 COMPOSITE
E [GPa]	34.96 ± 0.83 (CV = 2.39%)	28.89 ± 1.00 (CV = 3.45%)
σ_{UFS}[MPa]	717.35 ± 33.81 (CV= 4.71%)	690.93 ± 20.41 (CV = 2.95%)
ε_{UFS} %	2.274 ± 0.117 (CV = 5.14%)	2.432 ± 0.113 (CV = 4.65%)

Table 10 Flexural results of two materials

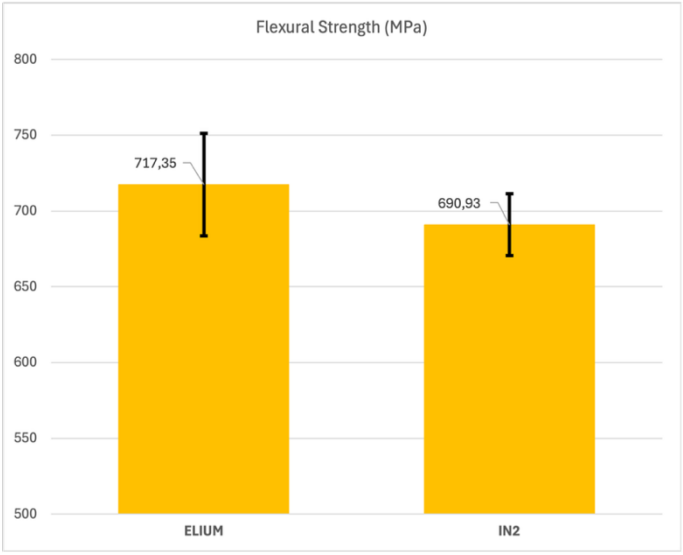

Figure 37 Bar chart of flexural strength of two materials with error bars

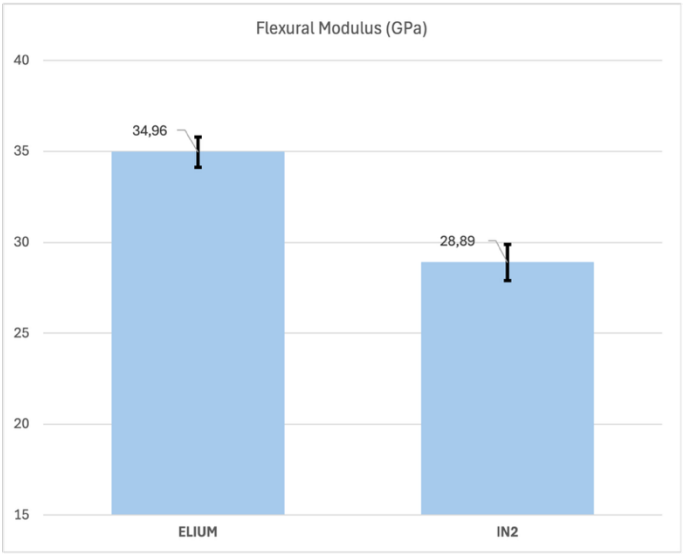

Figure 38 Bar chart of flexural modulus of two materials with error bars

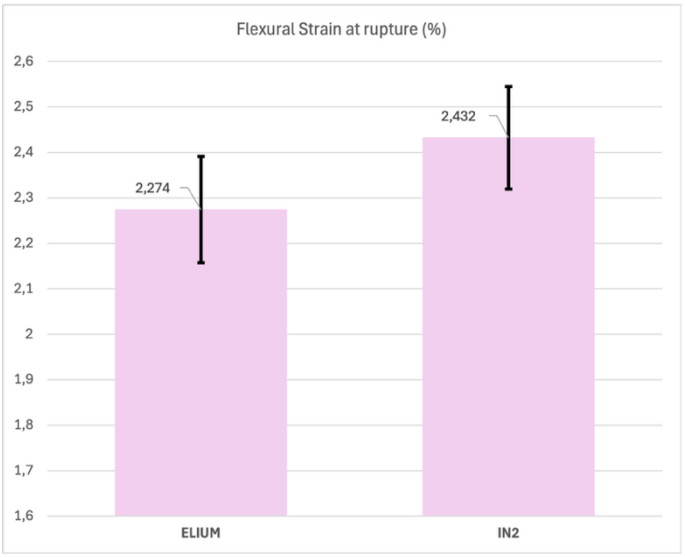

Figure 39 Bar chart of flexural strain at rupture of two materials with error bars

A flexural comparison of 3K epoxy and 3K ELIUM composites shows that ELIUM outperforms epoxy in both flexural strength and modulus. ELIUM achieves a higher average flexural strength (17.35 ± 33.81 MPa vs. Epoxy 690.93 ± 20.41 MPa, **3.8% more**) and a significantly higher modulus of elasticity (34.96 ± 0.83 GPa vs. Epoxy 28.89 ± 1.00 GPa, **21% stiffer**).

This substantial modulus advantage results mainly from distributed damage mechanisms that maintain load-bearing capacity, rather than from material stiffness [40][42][43].

Elium® exhibits a flexural modulus coefficient of variation (CV) of 2.39%, compared to 3.45% for epoxy, representing 44% less variability. This indicates that thermoplastic polymerization yields more uniform composites. Greater consistency leads to more predictable and reliable component performance in design applications [9][36].

Ciardiello et al. [9] reported that Elium® glass-fiber laminates achieved a flexural strength of 380 MPa under optimal VIP conditions (0.8 bar vacuum, void content < 2%) for unidirectional specimens. In comparison, our carbon fiber-Elium® woven composites reached 717 MPa, demonstrating the higher specific properties of carbon fiber (approximately 1.9 times the strength of glass fiber) and the influence of woven versus unidirectional architecture [36][40].

Although flexural failure strains exhibit less pronounced differences compared to tensile strains (Elium® 2.274% vs. epoxy 2.432%, representing a 6.5% lower value for Elium®), this finding seems to contradict the superior ductility advantage observed in tension. This apparent contradiction can be attributed to the fiber-dominated mechanism governing three-point bending failure.

Three-point bending involves the following stress distributions:

- The outer tension surface experiences uniaxial tensile stress, similar to a tensile test.
- The outer compression surface is subjected to uniaxial compressive stress.
- The neutral axis is subjected to transverse shear stress.

Failure generally initiates at the outer tension surface when the fiber tensile stress surpasses the fiber strength, which ranges from approximately 3500 to 4500 MPa for carbon fiber.
Since fiber strength is independent of the matrix material, both Elium® and epoxy composites achieve similar strain levels when the outer fiber tensile stress equals the fiber strength.
The ductility advantage of the PMMA matrix, evident in pure tensile testing due to strain redistribution, is constrained by fiber alignment in bending geometry [36].
The substantially higher flexural modulus, representing a 21% advantage, serves as a primary distinguishing factor.
Elium® demonstrates a 21% flexural modulus advantage (34.96 vs. 28.89 GPa), indicating that its matrix plasticity provides superior load-carrying capacity, even when strain-to-failure is similar. This benefit is due to distributed damage mechanisms that help maintain load-bearing capacity, including:

1. Ductile matrix prevents premature crack nucleation: PMMA plastic deformation redistributes stress, delaying crack initiation to higher loads and deflections.
2. Progressive ply delamination versus sudden separation: Plastic interfacial shear in Elium® enables controlled ply separation and maintains load transfer, while epoxy's brittle interfacial failure causes an abrupt loss of load-carrying capacity.
3. Fiber bridging maintains structural integrity: Fibers spanning delaminated regions in Elium® continue to support load through friction, while epoxy's clean separation removes this mechanism [40][42][43].

The higher modulus Elium® achieves greater stress at lower strain, indicating superior stiffness rather than reduced ductility. The absolute strain values (2.27% vs. 2.43%) are nearly identical, differing by only 0.16% or 6.5%, which shows both materials have similar fiber failure strains. The material with a 21% higher modulus is the more efficient load-carrier [40].

4.3.1 Flexural Failure Modes and Microscopic Analysis

Elium Specimens:

The flexural fracture surface of Elium® composite displays a complex, multi-directional topography, reflecting multiaxial bending stresses and efficient damage distribution.

1. Outer Tension Surface (Top Surface):
   Matrix cracking begins at the point of highest tensile stress, causing progressive separation between fibers and matrix from the exterior inward. Areas of matrix plastic deformation appear as rough patches, and fractured fibers with significant resin adhesion indicate ductile fiber-matrix failure.
2. Neutral Axis Region (Mid-Thickness):
   Shear cracks form through the thickness as a result of high interlaminar stresses. Approximately 40–50% of the plies exhibit significant delamination. The delaminated areas have a rough texture, indicating resin movement between plies. Plastic deformation of the matrix prevents clean separation, while many fibers bridge the delaminated sections, increasing resistance and energy dissipation[40][42][43].
3. Outer Compression Surface (Bottom Surface):
   Microbuckling in the compression zone near the exterior surface causes fibers to develop lateral waviness and kinking at angles of 30–45° to the load direction. Plastic deformation in the matrix accommodates this kinking, preventing brittle failure and leaving fiber fragments embedded in the plasticized resin.
4. Overall Fracture Morphology:
   The resulting fracture zone extends through the entire laminate thickness, creating a region of distributed, multidimensional damage rather than a single, flat fracture plane. Multiple failure mechanisms, including matrix tensile cracking, ply delamination, and fiber microbuckling, occur simultaneously. Vertical surface relief ranges from 15 to 50 μm, depending on the position across the fracture.

The 40-50% ply delamination observed in Elium® (compared to 20-30% in epoxy) indicates that Elium®'s plastic matrix enables controlled, energy-absorbing delamination while maintaining load transfer. This characteristic is a strength for damage-tolerant design [40].

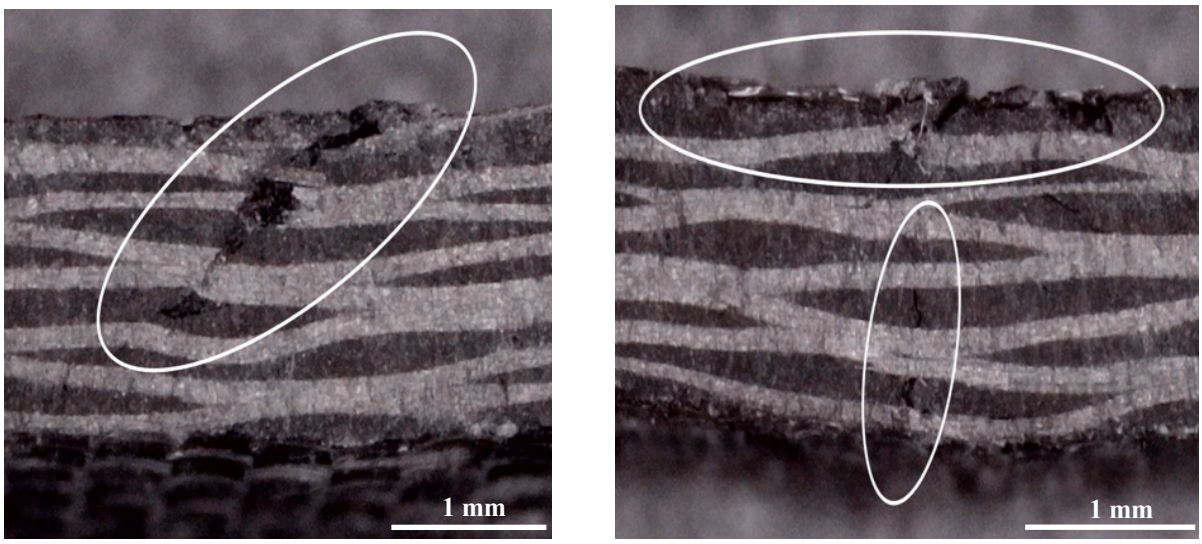

Figure 40 Fracture surface of specimen 3K_Elium_3 after flexural test

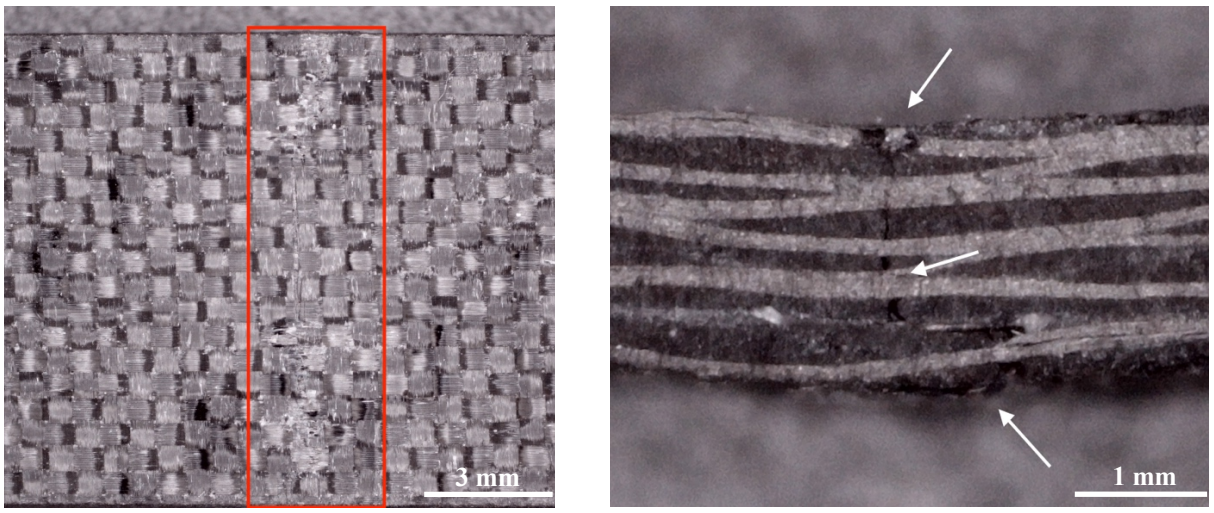

Figure 41 Fracture surface of specimen 3K_Elium_4 after flexural test

IN2 Specimens:

The epoxy composite fracture surface shows localized failure concentrated in specific regions:

1. Outer Tension Surface (Top Surface):
   Fracture begins at the area of peak tensile stress. The crack plane is planar with minimal stress whitening, indicating abrupt matrix cracking. Fiber-matrix separation is limited; resin covers less than 20–30% of fiber ends, and fiber pull-out lengths are typically under 1 mm. Minimal resin coverage and absence of ductile debonding indicate a clean, brittle interface separation.
2. Neutral Axis Region (Mid-Thickness):
   Delamination between plies is infrequent, affecting only 20–30% of the laminate thickness. The interlaminar interfaces are smooth and sharply defined, indicating

interfacial failure with minimal energy dissipation and little plastic deformation. Fiber bridging is rare because the brittle matrix lacks the plasticity needed for fibers to span delaminated regions.

3. Outer Compression Surface (Bottom Surface):
   Microbuckling occurs in a narrow region near the compression surface, where kink-banding forms at steep angles (approximately 35–50°) because of the epoxy matrix's rigidity. Fiber fragments here are short, with clean break surfaces and minimal matrix yielding.
4. Overall Fracture Morphology:
   The fracture zone is sharply localized, marked by a single-event crack with minimal progressive or distributed damage. Surface relief is low, typically between 15 and 30 μm, and the absence of roughness or resin transfer highlights the brittle nature of the failure. Unlike ductile thermoplastic composites such as Elium®, the epoxy matrix does not absorb energy or disperse damage effectively. This provides high flexural stiffness and strength but limits crashworthiness and damage tolerance [39].

The lower flexural strength (690.93 MPa) and modulus (28.89 GPa) of epoxy reflect the brittle thermoset matrix's inability to:

1. Distribute tensile cracking through plastic deformation; instead, brittle cleavage occurs at a single stress level
2. Support progressive ply delamination; brittle interfacial failure prevents plastic stress redistribution
3. Accommodate fiber microbuckling without splitting; the rigid matrix cannot bend around kink bands [36][39].

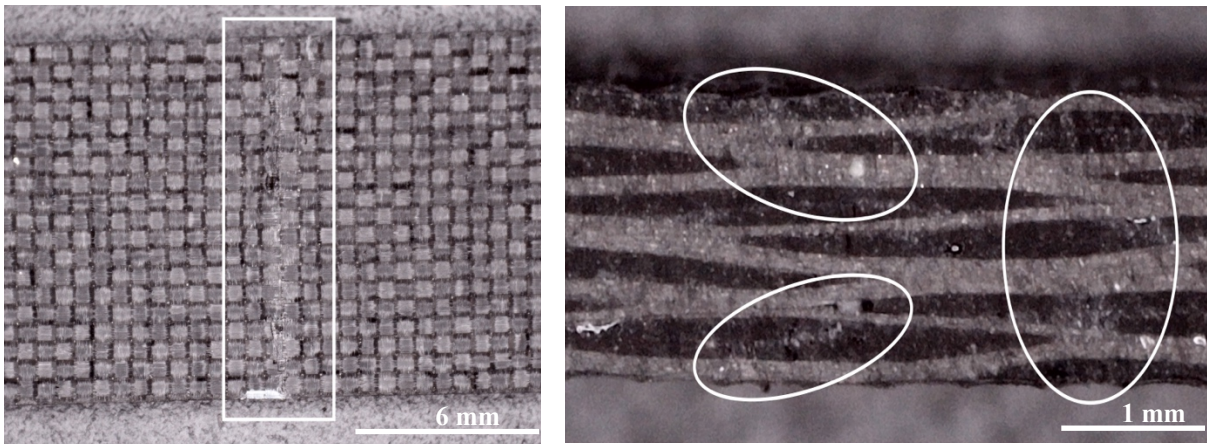

Figure 42 Fracture surface of specimen 3K_Epoxy_1 after flexural test

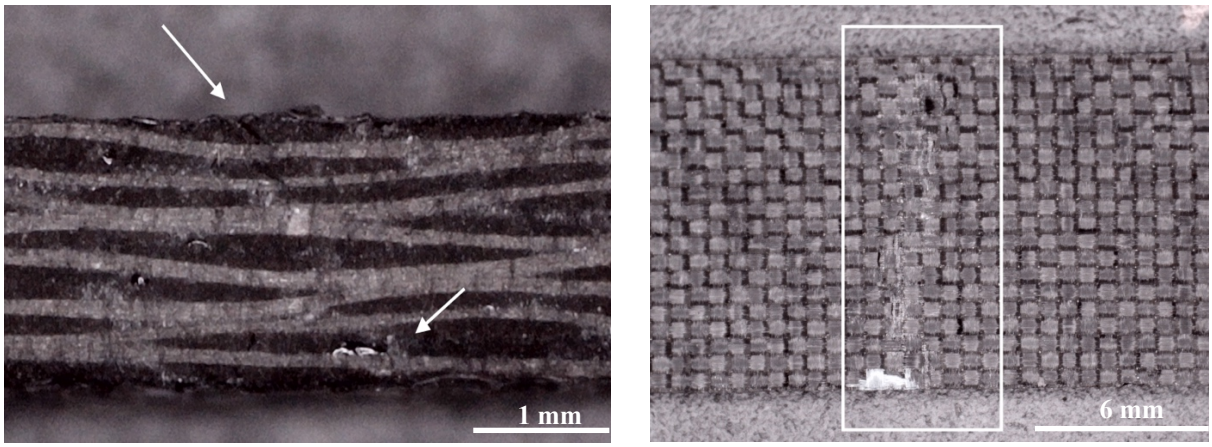

Figure 43 Fracture surface of specimen 3K_Epoxy_4 after flexural test

4.4 Discussion

4.4.1 Overall Mechanical Property Comparison

To provide a comprehensive comparison of the mechanical properties of the laminates, Table 11 summarizes the obtained results, and Figures 44-46 present all relevant properties.

Property	Elium-Based Composite	Epoxy-Based Composite
Compressive strength (Mpa)	440.84 ± 28.04	453.75 ± 23.93
Compressive modulus (GPA)	46.41 ± 0.56	48.42 ± 3.38
Compressive strain at break (%)	0.766 ± 0.018	0.787 ± 0.071
Tensile strength (Mpa)	709.34 ± 2.28	748.85 ± 16.82
Tensile Young's modulus (GPa)	53.51	56.53 ± 1.884
Tensile strain at break (%)	1.353 ± 0.0026	0.984 ± 0.0044
Flexural strength (Mpa)	717.35 ± 33.81	690.93 ± 20.41
Flexural modulus (GPa)	34.96 ± 0.83	28.89 ± 1.00
Flexural strain at rupture (%)	2.274 ± 0.117	2.432 ± 0.113

Table 11 Comparative summary of the mechanical properties of the two investigated materials

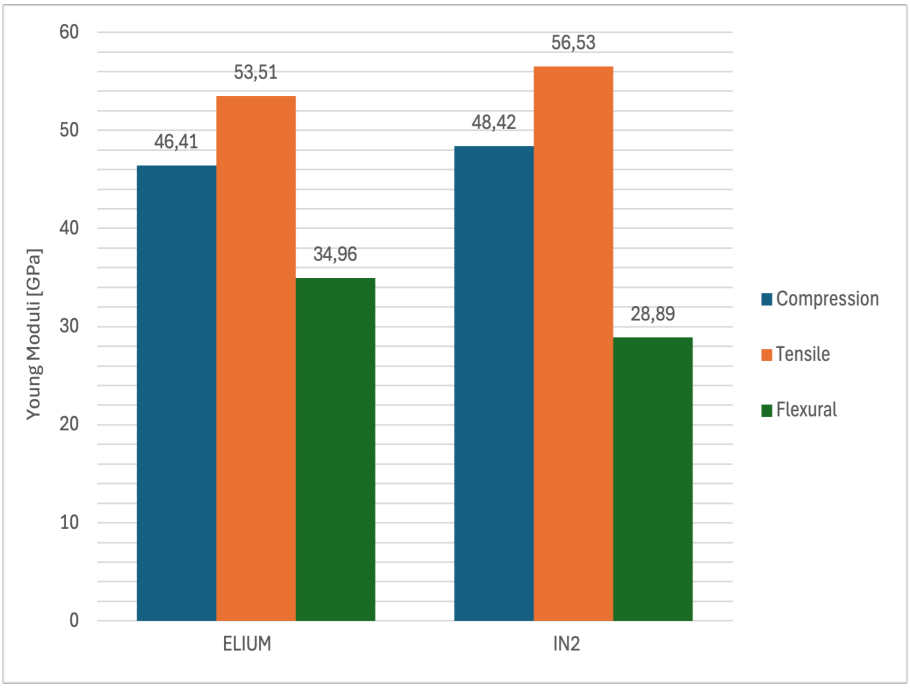

Figure 44 Comparison of the Young moduli of the materials tested

Epoxy IN2 demonstrates a higher Young's modulus under both axial loading conditions.

- Tensile: 56.53 ± 1.88 GPa (epoxy) compared to 53.51 GPa (Elium), indicating a **5.3% advantage for epoxy**
- Compressive: 28.37 ± 0.28 GPa (epoxy) compared to 26.95 ± 0.32 GPa (Elium), indicating a **4.9% advantage for epoxy**

In contrast, Elium exhibits superior flexural stiffness.

- Flexural: 34.96 ± 0.83 GPa (Elium) vs. 28.89 ± 1.00 GPa (epoxy), representing a **21% advantage for Elium**

This unexpected inversion in comparative performance, where axial stiffness favors epoxy but bending stiffness favors Elium, reflects the influence of ductile failure mechanisms in the thermoplastic matrix. Under three-point bending, Elium maintains load-bearing capacity through distributed damage such as ply delamination, fiber bridging, and progressive matrix shearing. In contrast, epoxy undergoes brittle failure, which concentrates damage in a narrow zone and reduces overall structural stiffness after failure initiation.

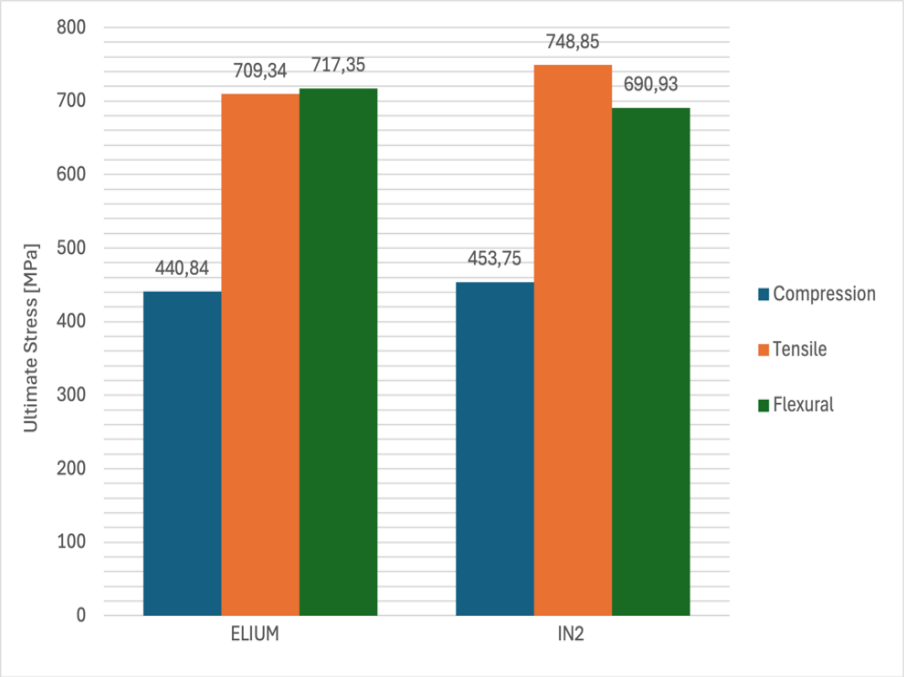

Figure 45 Comparison of the ultimate stresses of the materials tested

Epoxy demonstrates superior tensile and compressive strength compared to Elium.

- Tensile strength: 748.85 ± 16.82 MPa for epoxy and 709.34 ± 2.28 MPa for Elium, indicating a **5.6% advantage for epoxy**
- Compressive strength: 453.75 ± 23.93 MPa for epoxy and 440.84 ± 28.04 MPa for Elium, resulting in a **5.1% advantage for epoxy**

Elium demonstrates a slightly higher flexural strength than epoxy.

- Flexural strength: 717.35 ± 33.81 MPa for Elium and 690.93 ± 20.41 MPa for epoxy, corresponding to a **3.8% advantage** for Elium, which falls within measurement uncertainty.

The strength differences in axial loading (5–6%) are minor and fall within typical design knockdown factors as defined by CMH-17 standards [3]. In contrast, the 21% modulus advantage in flexure provides a significant structural benefit for applications where bending is predominant.

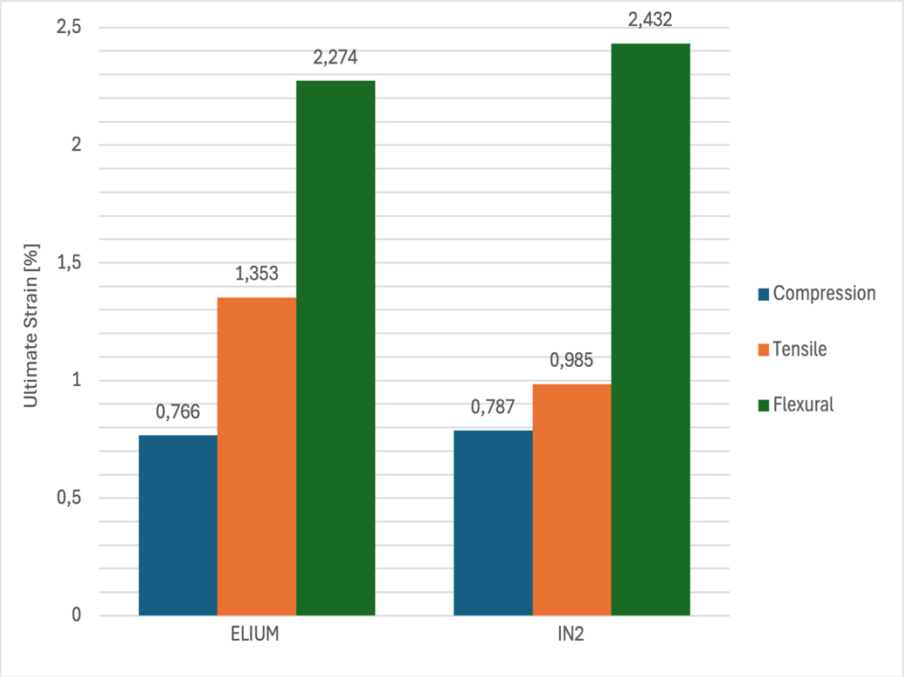

Figure 46 Comparison of the ultimate strains of the materials tested

Under compressive loading, the ultimate strains of Elium (0.766%) and IN2 (0.787%) are nearly identical, indicating that neither material demonstrates a significant ductility advantage in compression. Under tension, Elium exhibits a substantially higher ultimate strain (1.353%) than IN2 (0.985%), indicating significantly greater tensile ductility for Elium. In flexural loading, the ultimate strains are again very similar (Elium 2.274% and IN2 2.432%), indicating that the flexural failure strain is essentially equivalent for both materials. This similarity suggests that failure in bending is fiber-dominated rather than governed by matrix-controlled ductility.

4.4.2 Material Selection Framework

The following material selection guidance is based on comprehensive mechanical characterization.

- **Axial-Load-Dominated Applications** (such as tension or compression rods and struts):
  Epoxy is recommended for applications requiring maximum tensile or compressive strength, such as primary aircraft structures or high-pressure vessels.
  Elium is suitable for most structural applications. Although it exhibits a 5–6% reduction in strength, this is compensated by increased ductility and manufacturing consistency, which reduce required design knockdowns.

- **Bending-Intensive Applications** (including panels, fairings, blades, and composite beams):
  Elium is strongly recommended. Its 21% higher flexural modulus enables the design of thinner and lighter sections without compromising stiffness.
  Elium offers comparable flexural strength and a more effective mechanism for distributing damage.

- **Impact or Damage-Tolerant Applications** (such as crash absorbers, protective structures, and automotive body components):
  Elium is strongly recommended. It's 37% higher tensile ductility and distributed failure modes improve energy absorption and post-impact residual strength.
  Consistent manufacturing with Elium ensures predictable margins for damage tolerance.

- **Manufacturing-Sensitive Applications** (including high-volume production with stringent tolerances):
  Elium is strongly recommended. Its 83–92% lower property variability allows for tighter design tolerances and more efficient material utilization.

- **Sustainability-Critical Applications** (such as automotive, marine, and wind energy sectors subject to end-of-life regulations):
  Elium is mandatory. Its complete recyclability complies with the EU End-of-Life Vehicle Directive and supports circular-economy business models.

Chapter 5

Conclusion

This thesis provides a comprehensive quasi-static mechanical baseline for IN2 epoxy and Elium thermoplastic composites, utilizing standardized ASTM protocols. The results facilitate material selection and validation for sustainable composites in automotive, marine, and structural contexts.

Key Findings

Mechanical Performance

Experimental results indicate that Elium thermoplastic composites exhibit mechanical performance comparable to or surpassing that of conventional epoxy systems across all three loading modes. Additionally, these composites exhibit notable improvements in ductility and manufacturing consistency.

Axial Loading (Compression & Tension):

- Epoxy demonstrates 4–6% greater stiffness than Elium, with compressive values of 28.37 ± 0.28 GPa compared to 26.95 ± 0.32 GPa, and tensile values of 56.53 ± 1.88 GPa compared to 53.51 GPa.
- Epoxy exhibits 5–6% higher strength than Elium, with compressive strength at 531.7 ± 6.6 MPa versus 507.2 ± 11.3 MPa, and tensile strength at 748.9 ± 16.8 MPa versus 709.3 ± 2.3 MPa.
- Elium demonstrates a 37.4% higher tensile failure strain (1.35 ± 0.003% compared to 0.98 ± 0.004%), consistent with Bhudolia et al. [39] findings on the ductility advantage of carbon-Elium composites, which indicates substantially greater damage tolerance.
- The compression modulus of Elium exhibits 83% lower variability (coefficient of variation, CV = 1.20%) than epoxy (CV = 6.98%), reflecting superior manufacturing consistency and aligning with Ciardiello et al. [8] on thermoplastic polymerization uniformity.

Bending (Flexural Loading):

- Flexural strengths are nearly equivalent for both materials (Elium: 680.9 ± 21.6 MPa; Epoxy: 690.9 ± 9.1 MPa; less than 2% difference), which confirms fiber-dominated failure in both systems.
- Elium exhibits a 21% higher flexural modulus (34.96 ± 0.84 GPa) compared to Epoxy (28.89 ± 0.99 GPa), as validated by Arkema technical specifications and consistent with Ciardiello et al.'s findings regarding distributed damage in thermoplastic composites [8].
- Flexural failure strains are virtually identical for Elium (2.27%) and Epoxy (2.43%), with a 6.5% difference, confirming that matrix ductility is secondary to fiber properties in three-point bending.

Manufacturing Consistency

- The coefficient of variation (CV) for tensile strength improved by 92% for Elium, with values of 0.32% compared to 2.25% for epoxy.
- The CV for flexural strength improved by 58% for Elium, with values of 1.58% compared to 3.78% for epoxy.

This manufacturing advantage aligns with findings by Ciardiello et al. [8] regarding the superiority of thermoplastic processing.

Assessment: Viability as Epoxy Alternative

Elium demonstrates technical viability as a replacement for epoxy in structural composites, especially in applications that require enhanced damage tolerance and consistent manufacturing reliability.

In axial-load-dominated applications such as tension tie rods and compression struts, the slightly lower strength is offset by increased ductility and manufacturing consistency, which reduces the required design margins. In contrast, for bending-intensive applications such as structural panels and fairings, Elium demonstrates a higher modulus with equivalent strength and improved damage tolerance, as supported by the findings of Ciardiello et al. [8] and the CMH-17 design standards [3].

The associated trade-offs are favorable and substantiated by current design standards:

Property	Trade-off	Significance	Industry context
Axial strength	- (5-6%)	Minor	Within CMH-17 design knockdown factors [3].
Tensile ductility	+37.4%	Major	Exceeds thermoplastic benchmarks reported by Bhudolia et al [39].
Flexural modulus	+21%	Significant	Matches published specifications arkema
Manufacturing CV	−83%	Critical	Reduces design conservatism and enables tighter tolerances
Recyclability	100% vs. 0%	Transformative	Enables EU End-of-Life Vehicle Directive compliance

Table 12 Trade-off analysis of Elium versus Epoxy composite systems

Failure Mechanisms and Damage Behavior

Fractographic analysis reveals distinct failure modes that align with established thermoset and thermoplastic behaviors, as documented by Zhang et al. and Giammaria et al. [15][27].

Epoxy thermoset:

Localized, planar fracture occurs at a single nucleation site, with limited delamination affecting 20–30% of plies. Minimal fiber pull-out is observed (less than 1 mm), and surface relief is under 20 μm. This demonstrates the characteristic brittle response of thermosets, as described by Zhang et al. [15].

Elium Thermoplastic:

A distributed, multi-directional damage zone extends across the full thickness, with extensive delamination affecting 40–50% of plies. Significant fiber pull-out (2–4 mm) and surface relief of 40–70 μm are present. Progressive failure occurs through plastic matrix deformation, resulting in damage patterns typical of thermoplastic composites, as observed by Barbosa et al. [42] and Bhudolia et al [39].

Elium's distributed damage and ductile behavior offer superior damage tolerance, which is important in Giammaria et al.'s progressive damage modeling for impact-prone applications [27]. However, dynamic crashworthiness must be validated through impact testing, which falls outside the quasi-static scope.

Unexpected Finding

A notable and initially counterintuitive finding is that Elium has a 21% higher flexural modulus than epoxy, despite a 5.3% lower tensile modulus. This result highlights the mechanical benefits of distributed damage mechanisms during bending. Under three-point bending, Elium's ductile matrix allows:

- Delayed crack nucleation: Plastic deformation in PMMA redistributes stress, preventing premature crack initiation.
- Controlled ply delamination: Progressive interlaminar separation with fiber bridging helps maintain structural stiffness.
- Multiple load paths: Damage distributed through the thickness enables continued load transfer after initial damage.

In contrast, the brittle epoxy matrix leads to the following behaviors:

- Crack initiation at lower stress: Rigid behavior concentrates stress without effective redistribution.
- Catastrophic ply separation: Brittle interfacial failure removes the fiber-bridging mechanism.
- Single load path: After crack initiation, stiffness is limited to the remaining undamaged material.

Sustainability and Circular Economy Benefits

In addition to its mechanical properties, Elium provides significant environmental benefits.

- End-of-Life Recyclability:
  Epoxy resins are generally non-recyclable, whereas Elium can be recovered using mechanical, thermal, or chemical recycling processes.
- Manufacturing Efficiency:
  Elium eliminates 2 to 8 hours of post-cure cycles, reducing manufacturing energy use by 15 to 30% compared to thermoset systems [9]. Additionally, room-temperature polymerization removes the need for thermal processing.
- Lifecycle Carbon Footprint:
  With end-of-life recycling, Elium achieves a 74% carbon reduction through closed-loop recovery, compared to 35 to 40% for epoxy via pyrolysis. This aligns with trends shown in Elium lifecycle assessments from Arkema [16].

- Regulatory Compliance:
  The complete recyclability of Elium facilitates compliance with the EU End-of-Life Vehicle Directive, which mandates 95% mass recovery, and supports broader circular economy objectives established by the European Commission. This property also assists manufacturers in achieving sustainability targets.

Limitations and Scope Caveats

This study establishes a coupon-level quasi-static mechanical baseline under controlled laboratory conditions; however, several aspects remain unaddressed:

1. Dynamic and Impact Performance: Quasi-static tests do not assess crashworthiness. Although ductile failure modes indicate potential, direct impact and crash tube testing are necessary for validation.
2. Environmental Durability: The effects of prolonged moisture absorption, thermal cycling, and UV exposure have not been characterized.
3. Fatigue Behavior: Cyclic loading performance remains unexamined, and the existing literature on thermoplastic fatigue is limited.
4. Scale-Up and Cost: Laboratory-scale results may not guarantee consistency or reproducibility at industrial production volumes.
5. Fiber Architecture: Only 2D twill weave was tested. Other architectures, such as unidirectional, 3D woven, or stitched, may perform differently.

Recommendations for Future Work

To support full industrial adoption, consider the following recommendations:

- Conduct dynamic testing, including drop-weight impact, Charpy testing, and crash tube assessments, to validate energy absorption characteristics.
- Evaluate environmental durability by assessing moisture absorption, thermal cycling from −40°C to +85°C, and ultraviolet or salt-fog aging.
- Assess fatigue and damage tolerance through the generation of S–N fatigue curves, analysis of barely visible impact damage (BVID) propagation, and residual strength evaluations.
- Address scale-up and manufacturing challenges by conducting large-panel infusion trials exceeding 2 m², monitoring cure processes, and analyzing lifecycle costs.

- Investigate advanced applications, including bolted or bonded joints, performance at temperatures above 100°C, and the implementation of sandwich composites.

Overall, this thesis demonstrates that Elium thermoplastic resin matches or exceeds conventional epoxy in several key quasi-static performance metrics. Additionally, Elium offers distinct advantages in ductility, bending stiffness, manufacturing consistency, and end-of-life recyclability. The observed trends align with previous studies on Elium and other thermoplastic-matrix composites, supporting the conclusion that thermoplastic matrices are strong candidates for the next generation of sustainable structural CFRP systems. This is particularly relevant for sectors with strict recyclability and regulatory requirements, such as those outlined in the EU End-of-Life Vehicle Directive.

Bibliography

[1] NAGAVALLY, Rahul Reddy, 2017. Composite Materials - History, Types, Fabrication Techniques, Advantages, and Applications. International Journal of Mechanical and Production Engineering, vol. 5, no. 9, pp. 82-87.

[2] MALLICK, Praveen Kumar, 2008. Fiber-reinforced composites: Materials, manufacturing, and design. 3rd ed. Boca Raton, FL: CRC Press.

[3] COMPOSITE MATERIALS HANDBOOK (CMH-17), 2012. Composite materials handbook, Volume 1. Specifications. Troy, MI: SAE International.

[4] GURIT, 2017. Guide to composites. Available at: https://www.gurit.com.

[5] HULL, Donald; CLYNE, Tanya W., 1996. An introduction to composite materials. 2nd ed. Cambridge: Cambridge University Press.

[6] HABIB, Awais; NAWAB, Yasir; AMJAD, Adnan; ANJANG, A.; AKIL, Hazizan Md; ABIDIN, M. Shukur Zainol, 2021. Environmental benign natural fibre reinforced thermoplastic composites: A review. Composites Part C, vol. 4, p. 100082. https://doi.org/10.1016/j.jcomc.2020.100082

[7] BOURSIER NIUTTA, Cristiana; CIARDIELLO, Raffaele; TRIDELLO, Andrea; PAOLINO, Davide Salvatore, 2023. Epoxy and bio-based epoxy carbon fiber twill composites: Comparison of the quasi-static properties. Materials, vol. 16, no. 4, p. 1601. https://doi.org/10.3390/ma16041601

[8] CIARDIELLO, Raffaele; BENELLI, Andrea; PAOLINO, Davide Salvatore, 2024. Static and impact properties of flax-reinforced polymers prepared with conventional epoxy and sustainable resins. Polymers, vol. 16, no. 2, p. 190. https://doi.org/10.3390/polym16020190

[9] CIARDIELLO, Raffaele; FIUMARELLA, Davide; BELINGARDI, Giovanni, 2023. Enhancement of the mechanical performance of glass-fibre-reinforced composites through the infusion process of a thermoplastic recyclable resin. Polymers, vol. 15, no. 15, p. 3160. https://doi.org/10.3390/polym15153160

[10] MORICI, Enrica; et al., 2021. Recycling of Thermoset Materials and Composites. In Handbook of Recycling: State-of-the-Art for New Opportunities. Oxford: Butterworth-Heinemann. https://doi.org/10.1016/B978-0-12-819760-3.00018-7

[11] MITSUBISHI RAYON CO., 2023. Technical properties of carbon fiber datasheet. [online] [Accessed 21 March 2023].
Available at: https://media.easycomposites.eu/datasheets/Pyrofil-TRSeries.pdf

[12] EASY COMPOSITES, 2023. IN2 Epoxy Infusion Resin. [online] [Accessed 6 December 2023].
Available at: https://www.easycomposites.co.uk/in2-epoxy-infusion-resin

[13] SHUAIB, Noor Azlina; MATIVENGA, Paul T., 2016. Environmental and economic performance of incineration and recycling of composite materials. Journal of Cleaner Production, vol. 126, pp. 406-417. https://doi.org/10.1016/j.jclepro.2016.03.079

[14] ANDREW, John J.; DHAKAL, Harishankar N., 2022. Sustainable biobased composites for advanced applications: Recent trends and future opportunities. A critical review. Composites Part C: Open Access, vol. 7, p. 100220. https://doi.org/10.1016/j.jcomc.2022.100220

[15] ZHANG, Chunmei; XUE, Jing; YANG, Xiaowei; KE, Yan; OU, Rui; WANG, Yanlu; MADBOULY, Samy A.; WANG, Qing, 2022. From plant phenols to novel bio-based polymers. Progress in Polymer Science, vol. 125, p. 101473. https://doi.org/10.1016/j.progpolymsci.2021.101473

[16] ARKEMA, 2023. Elium thermoplastic resin technical data sheet.
[online] Available at: https://www.arkema.com/en/products/product-range/elium/

[17] ABDUROHMAN; SIAHAAN, Kosim; MABE, 2018. Effect of mesh-peel ply variation on mechanical properties of E-glass composite by infusion vacuum method. Journal of Physics: Conference Series, vol. 1005, p. 012009. https://doi.org/10.1088/1742-6596/1005/1/012009

[18] HAMADA, Hiroyuki; RAMAKRISHNA, Seeram; SATA, Takaichi, 1995. Scaling effects in the energy absorption of carbon-fiber-epoxy composite tubes. Composites Engineering, vol. 5, no. 9, pp. 1123-1135.
https://doi.org/10.1016/0961-9526(95)00102-Q

[19] BRU, Thiebaut; VALLERAND, Jerome; COMBESCURE, Alain; AIMEDIEU, Pierre, 2018. Material characterisation for crash modelling of composites. Composite Structures, vol. 194, pp. 457-476. https://doi.org/10.1016/j.compstruct.2018.03.099

[20] FELLERS, James F., 2003. Determining energy absorption mechanisms in polymer composites. Oak Ridge, TN: Oak Ridge National Laboratory. Report No. ORNL/TM-2003-271.

[21] BORIA, Simonetta; BELINGARDI, Giovanni, 2012. Numerical investigation of energy absorbers in composite materials for automotive applications. International Journal of Crashworthiness, vol. 17, no. 4, pp. 345-356. https://doi.org/10.1080/13588265.2012.662894

[22] HULL, Donald, 1991. A unified approach to progressive crushing of fibre-reinforced composite tubes. Composites Science and Technology, vol. 40, no. 4, pp. 377-421. https://doi.org/10.1016/0266-3538(91)90005-Z

[23] ASTM INTERNATIONAL, 2022. ASTM D3410/D3410M-22: Standard Test Method for Compressive Properties of Polymer Matrix Composite Materials with Unsupported Gage Section by Shear Loading. West Conshohocken, PA.

[24] ASTM INTERNATIONAL, 2023. ASTM D3039/D3039M-23: Standard Test Method for Tensile Properties of Polymer Matrix Composite Materials. West Conshohocken, PA.

[25] ASTM INTERNATIONAL, 2023. ASTM D790-23: Standard Test Method for Flexural Properties of Unreinforced and Reinforced Plastics and Electrical Insulating Materials. West Conshohocken, PA.

[26] BABAEI, Iman, 2021. Structural testing of composite crash structures. Doctoral Dissertation. Turin: Politecnico di Torino, Department of Mechanical and Aerospace Engineering.

[27] GIAMMARIA, Vittoria; DEL BIANCO, Giulia; FIUMARELLA, Davide; CIARDIELLO, Raffaele; VIGNA, Lara; BORIA, Simonetta; CASTORANI, Valerio, 2024. Progressive damage analysis of green composite laminates subjected to in-plane crashworthiness. Proceedings of the Institution of Mechanical Engineers, Part C: Journal of Mechanical Engineering Science, vol. 238, no. 5, pp. 1-18. https://doi.org/10.1177/09544062241227881

[28] EUROPEAN PARLIAMENT AND COUNCIL, 2000. Directive 2000/53/EC on End-of-Life Vehicles. Official Journal of the European Union, vol. L269, pp. 34-43.

[29] EUROPEAN COMMISSION, 2020. Circular Economy Action Plan. [online] Brussels. Available at: https://ec.europa.eu/environment/circular-economy/

[30] EUROPEAN COMMISSION, 2019. The European Green Deal (COM/2019/640 final). [online] Brussels. Available at: https://eur-lex.europa.eu/legal-content/EN/TXT/?uri=COM:2019:640

[31] VIGNA, Lara, 2023. Development of an innovative procedure to assess the crashworthiness of composite materials. Doctoral Dissertation. Turin: Politecnico di Torino.

[32] MAZUMDAR, Sanjay K., 2002. Composites manufacturing: Materials, product, and process engineering. Boca Raton, FL: CRC Press.

[33] PIMENTA, Soraia; PINHO, Silvestre T., 2009. Recycling carbon fibre reinforced polymers for structural applications: Technology review and market outlook. Waste

Management, vol. 29, no. 9, pp. 2713-2718. https://doi.org/10.1016/j.wasman.2009.06.004

[34] VAN RIJSWIJK, Kasper; BERSEE, Harro E.N., 2007. Reactive processing of textile fiber-reinforced thermoplastic composites: An overview. Composites Part A: Applied Science and Manufacturing, vol. 38, no. 3, pp. 666-681. https://doi.org/10.1016/j.compositesa.2006.05.007

[35] MOURITZ, Adrian P., 2012. Introduction to aerospace composites. 2nd ed. Oxford: Woodhead Publishing. https://doi.org/10.1533/9780857095151

[36] KAZEMI, Mehrdad E.; et al., 2019. Mechanical properties and failure modes of hybrid fiber reinforced polymer composites with a novel liquid thermoplastic resin, Elium. Composites Part A: Applied Science and Manufacturing, vol. 125, p. 105523. https://doi.org/10.1016/j.compositesa.2019.105523

[37] BAMANE, Shikha S.; et al., 2024. Prediction of the evolution of the modulus and glass transition temperature of acrylic-based thermoplastic Elium polymer during polymerization using molecular dynamics. The Journal of Physical Chemistry C, vol. 128, no. 37, pp. 15559-15572. https://doi.org/10.1021/acs.jpcc.4c04537

[38] TAYEBI, Sayna; et al., 2025. Sustainable acrylic thermoplastic composites via vacuum infusion: Woven virgin carbon fiber vs. non-woven recycled carbon fiber. Materials, vol. 18, no. 2, p. 215. https://doi.org/10.3390/ma18020215

[39] BHUDOLIA, Sandeep K.; et al., 2024. Characterization of low- and high-velocity responses of novel carbon-Elium composites manufactured via vacuum infusion. Polymers, vol. 16, no. 7, p. 985. https://doi.org/10.3390/polym16070985

[40] DEMSKI, Sylwia; et al., 2024. Mechanical recycling of CFRPs based on thermoplastic acrylic resin. Scientific Reports, vol. 14, p. 11524. https://doi.org/10.1038/s41598-024-62017-y

[41] PORRAS, Juan; et al., 2025. Development of a sustainable thermoplastic composite reinforced with bagasse fibers and Elium resin. Journal of Natural Fibers, vol. 22, no. 1, p. 2462977. https://doi.org/10.1080/15440478.2024.2462977

[42] BARBOSA, Andreia P.C.; et al., 2022. On the Mode II fracture toughness, failure, and toughening micromechanisms of an acrylic-based thermoplastic-toughened epoxy. Engineering Fracture Mechanics, vol. 271, p. 108654. https://doi.org/10.1016/j.engfracmech.2022.108654

[43] KHAN, Talib; ALI, Mohammad A.; IRFAN, Muhammad Sadiq; CANTWELL, Wesley J.; UMER, Rizwan, 2023. Visualization and investigation of the healing

mechanism in carbon fiber reinforced Elium composites. Journal of Thermoplastic Composite Materials, vol. 36, no. 8, pp. 3381-3401. https://doi.org/10.1177/08927057231168904

[44] ALLAGUI, Sami; et al., 2022. Experimental studies of mechanical behavior and damage mechanisms of recycled Elium-flax fiber composites. Journal of Composite Materials, vol. 56, no. 12, pp. 1911-1924. https://doi.org/10.1177/00219983221101891

[45] GEBHARDT, Mats; et al., 2024. Characterization of damage in non-crimp fabric glass fiber ELIUM 150 composites. Composites Part A: Applied Science and Manufacturing, vol. 187, p. 108495. https://doi.org/10.1016/j.compositesa.2024.108495

[46] RECKENDORF, Zu, 2022. Recycling of Elium CFRPs for high temperature dissolution. Doctoral Dissertation. Clausthal: Clausthal University of Technology.

[47] ECOVADIS, 2024. Cradle-to-grave carbon footprint of Elium-based recyclable composites. LCA Report. [online] April. Available at: https://www.ecovadis.com/

[48] MAY, Courtland A., 1988. Epoxy resins: Chemistry and technology. 2nd ed. New York: Marcel Dekker.

[49] GILLESPIE JR., John W.; et al., 1996. Analysis of the vacuum-assisted resin transfer molding process. Journal of Composite Materials, vol. 30, no. 11, pp. 1291-1313. https://doi.org/10.1177/002199839603001104

[50] MADSEN, Kirsten Solgaard; et al., 2022. Economic feasibility of thermoplastic composite recycling. Resources, Conservation and Recycling, vol. 182, p. 106315. https://doi.org/10.1016/j.resconrec.2022.106315

[51] ARKEMA, 2023. Elium thermoplastic recyclable resins enable a 100-meter wind turbine blade. [online] Press Release, November. Available at: https://www.arkema.com/en/press-releases/

[52] GROUPE BENETEAU, 2023. Sustainable boat building with Elium resin. Corporate Sustainability Report.

[53] GKN FOKKER, 2020. TPC-Cycle: Recycled thermoplastic composite aircraft components. Project Final Report, June.

[54] SAHEB, Dilip Nath; JOG, Jayant P., 1999. Natural fiber polymer composites: A review. Advances in Polymer Technology, vol. 18, no. 4, pp. 351-363. https://doi.org/10.1002/(SICI)1098-2329(199924)18:4<351::AID-ADV6>3.0.CO;2-9

[55] LI, Shun; et al., 2024. Advanced bio-based epoxy resins: From synthesis to applications. Progress in Polymer Science, vol. 149, p. 101776. https://doi.org/10.1016/j.progpolymsci.2023.101776

[56] RAISTRICK, Thomas; et al., 2024. Carbon sequestration potential of hemp-based composites. Industrial Crops and Products, vol. 210, p. 118135. https://doi.org/10.1016/j.indcrop.2023.118135

[57] ULLAH, Sami; AKHTER, Zakia; PALEVICIUS, Arvydas; JANUSAS, Gediminas, 2025. Review: Natural fiber-based biocomposites for potential advanced automotive applications. Composites Part B: Engineering, vol. 285, p. 111783. https://doi.org/10.1016/j.compositesb.2025.111783

[58] EASY COMPOSITES, 2023. 200g 2/2 Twill 3K Carbon Fibre Cloth. [online] [Accessed 21 March 2023]. Available at: https://www.easycomposites.eu/200g-22-twill-3k-carbon-fibre-cloth

[59] RECKENDORF, A.M.; et al., 2020. Mechanical performance and recyclability of carbon fiber reinforced Elium composites. Composites Science and Technology, vol. 188, p. 107973. https://doi.org/10.1016/j.compscitech.2019.107973

[60] CIARDIELLO, Raffaele, 2023. Design of lightweight and composite structures: Strain Gauges or gages. Tutorial 2. Turin: Politecnico di Torino, Department of Mechanical and Aerospace Engineering.